

# Measurements (and simulations) of plasma turbulence in toroidal magnetic confinement devices

Walter Guttenfelder

AST559/APC539

Turbulence and nonlinear processes in fluids and plasmas

Nov, 2020

# This talk is completely biased and in no way comprehensive

- I've used examples I'm familiar with and find useful for illustration
- See the following for broader reviews and thousands of useful references
- Transport & Turbulence reviews:
  - Liewer, Nuclear Fusion (1985)
  - Wootton, Phys. Fluids B (1990)
  - Carreras, IEEE Trans. Plasma Science (1997)
  - Wolf, PPCF (2003)
  - Tynan, PPCF (2009)
  - ITER Physics Basis (IPB), Nuclear Fusion (1999)
  - Progress in ITER Physics Basis (PIPB), Nuclear Fusion (2007)
- Drift wave reviews:
  - Horton, Rev. Modern Physics (1999)
  - Tang, Nuclear Fusion (1978)
- Gyrokinetic simulation review:
  - Garbet, Nuclear Fusion (2010)
- Zonal flow/GAM reviews:
  - Diamond et al., PPCF (2005)
  - Fujisawa, Nuclear Fusion (2009)
- Measurement techniques:
  - Bretz, RSI (1997)
- Special issue on gyrokinetic validation ([Plasma Phys. Control. Fusion 2017](#))
- There are many more examples in the last 10 years (*review paper expected next year on "Comparing gyrokinetic simulations with experiments"*)

## Some topics I'll try to touch on in two days

- **Refresher of tokamaks & gyrokinetics**
- **General turbulence characteristics of magnetized 2D drift waves**
- **Tokamak core turbulence measurements and gyrokinetic validation**
- **Tokamak edge turbulence\***

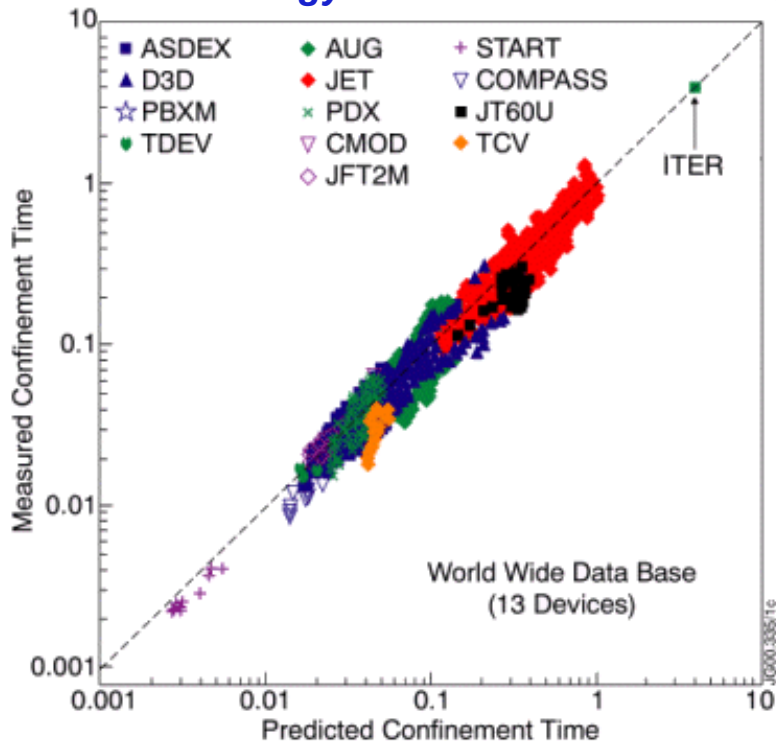
*\*Courtesy S. Zweben for some slides and videos on scrape-off-layer turbulence*

# TOKAMAKS AND CONFINEMENT

# Magnetic fusion plasmas are a possible solution for large-scale clean energy production

- Need sufficient pressure ( $p \sim 2-8$  atmospheres, at  $>100$  Million  $^{\circ}\text{C}$ ) confined for sufficiently long ( $\tau_E \sim 1-4$  s) for high gain ( $P_{\text{fusion}} \gg P_{\text{heat}}$ ) burning plasmas

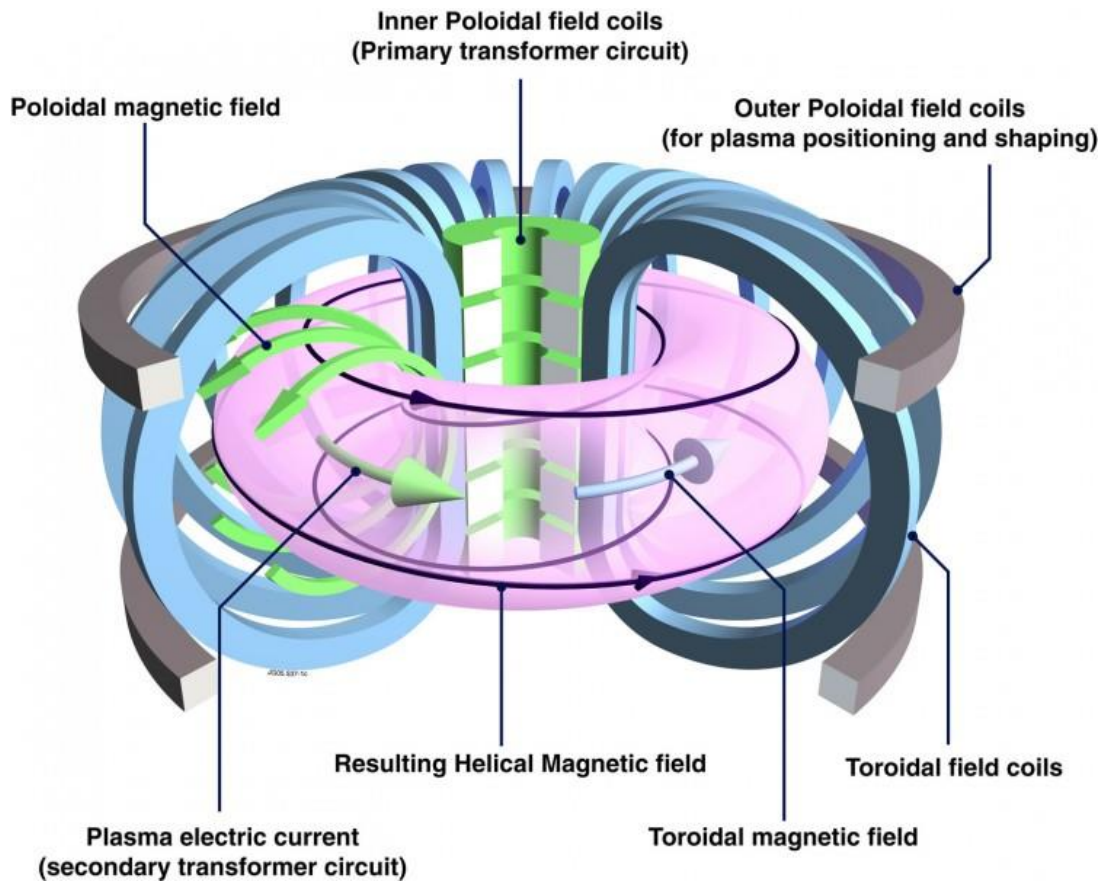
*Tokamak energy confinement time scaling*



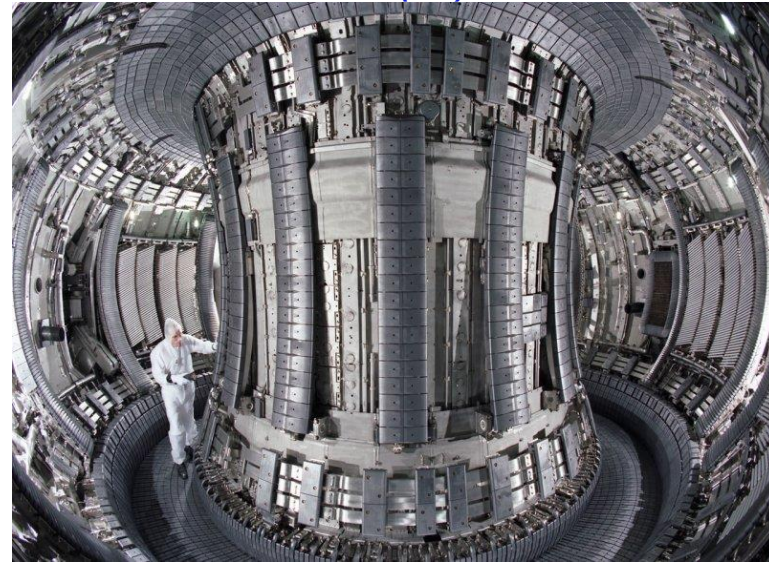
- **Confinement time set by turbulent losses**
- Can we understand turbulence and therefore reduce/optimize it?  
⇒ **Requires measurement and theory**

# Tokamaks

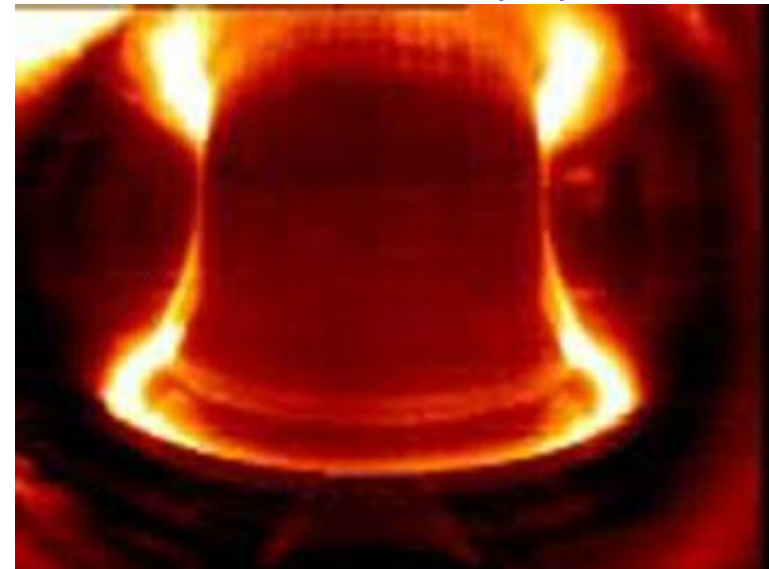
- Axisymmetric
- Helical field lines confine plasma



*JET (UK)*

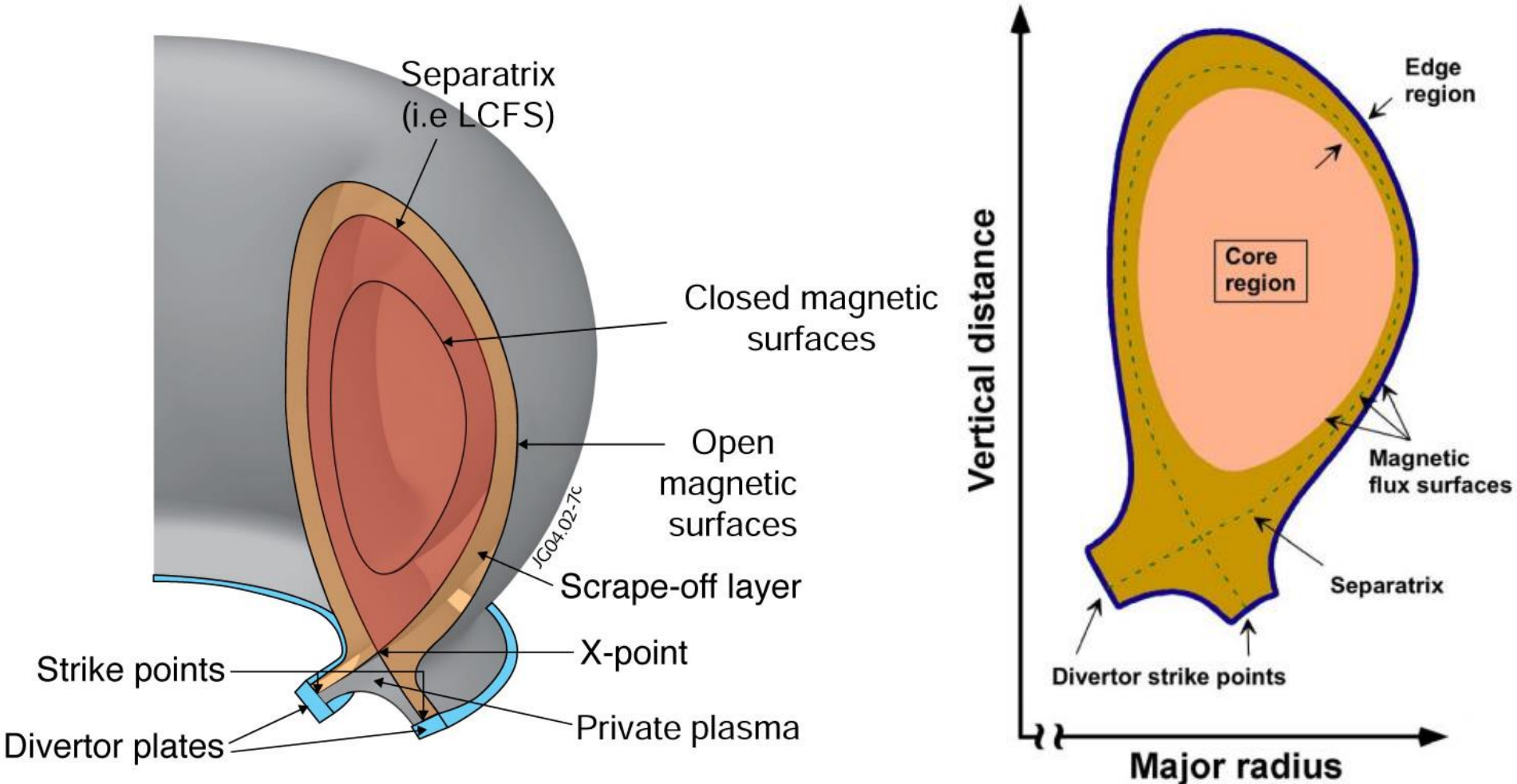


*Alcator C-Mod (MIT)*



# Going to refer to different spatial regions in the tokamaks

- Especially **core** (~100% ionized), **edge** (just inside separatrix), and **scrape-off layer** (SOL, just outside separatrix)



# Inferred experimental transport larger than collisional (neoclassical) theory – extra “anomalous” contribution

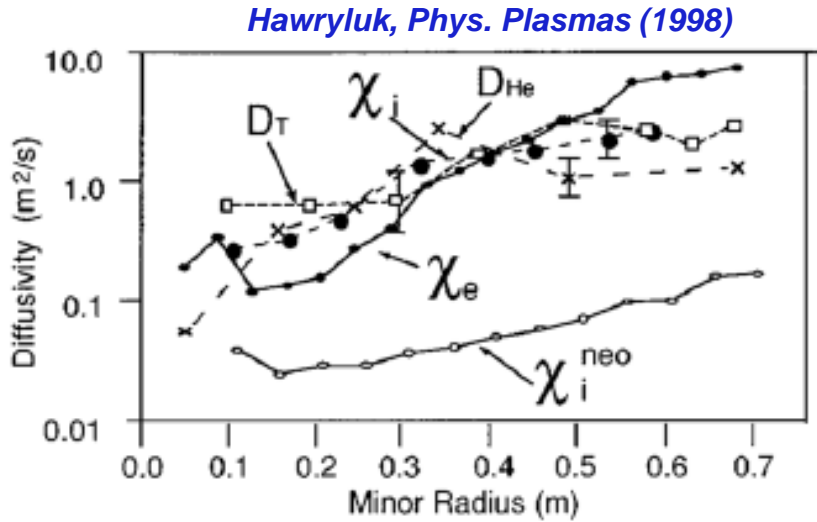
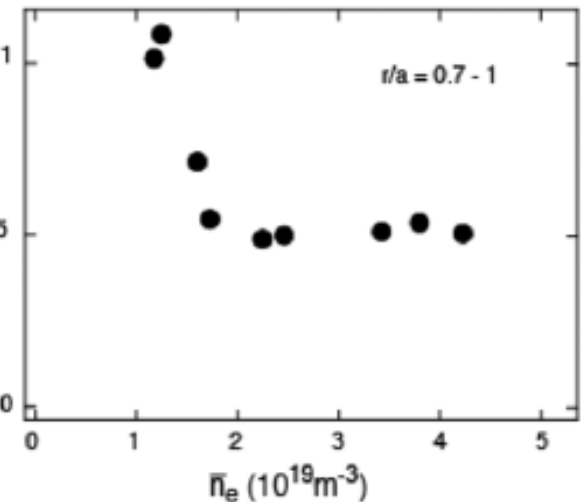
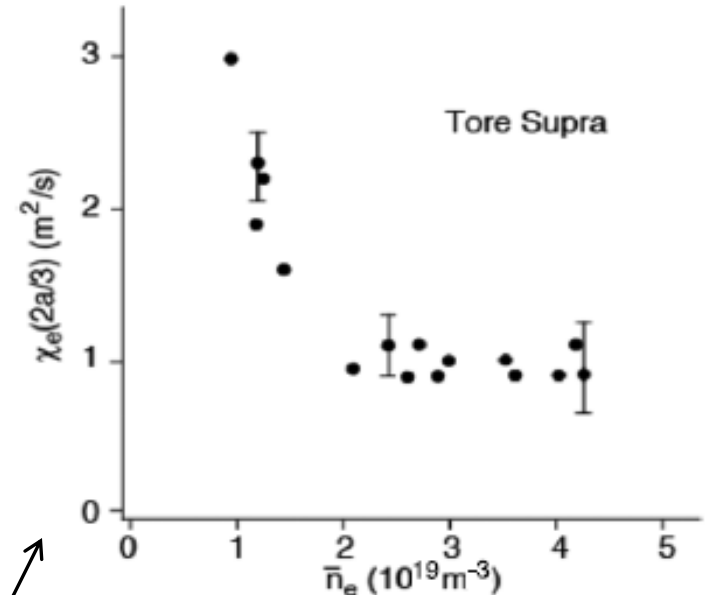


Figure 1. Results from TFTR showing ion thermal, momentum, and electron thermal diffusivities in an L-mode discharge; reprinted with permission from the American Institute of Physics.

Garbet, *Nuclear Fusion* (1992)  
Tynan, *PPCF* (2009)

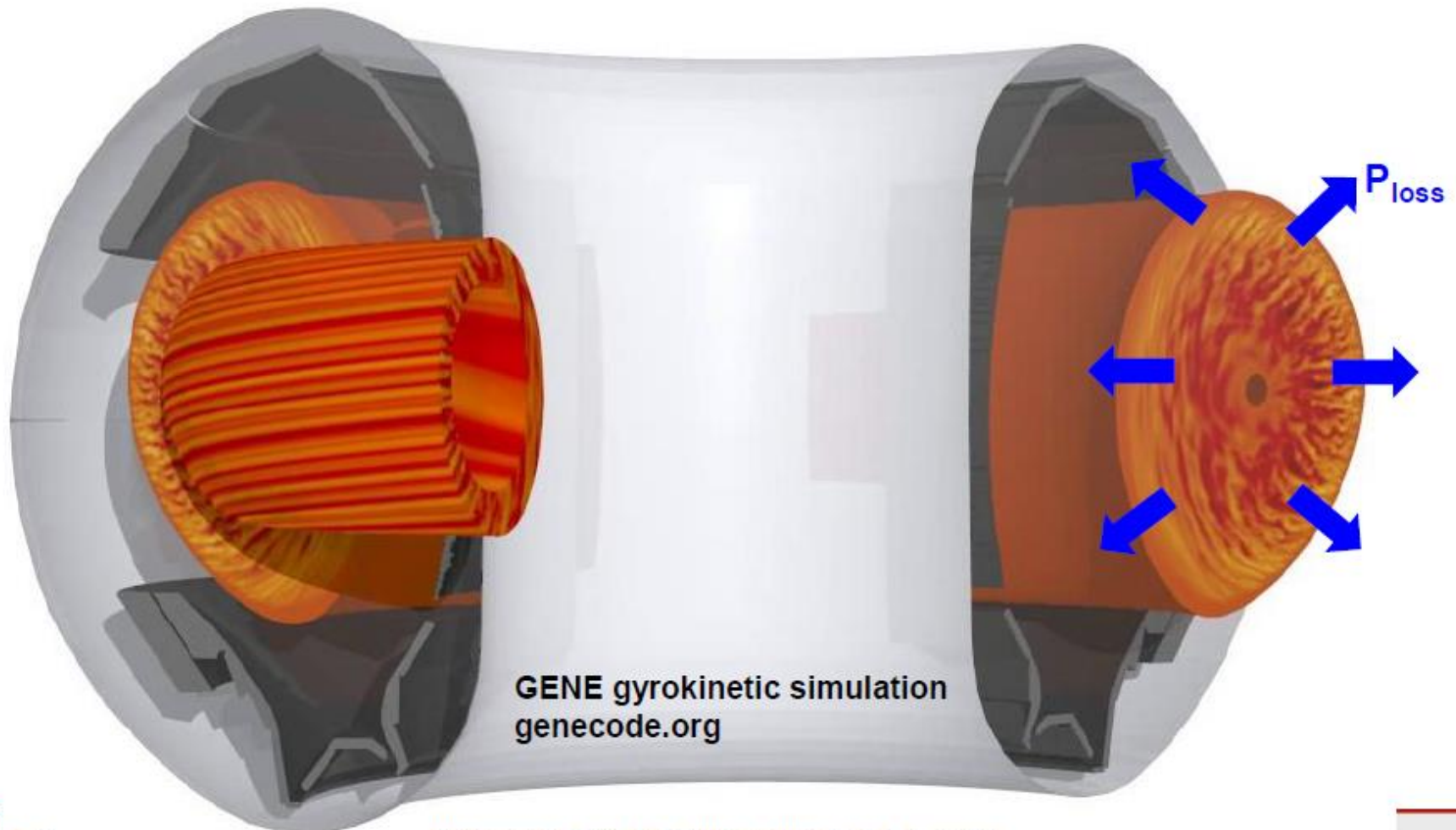


- Correlation between local transport and density fluctuations hints at turbulence



# Increasing gradients eventually cause small scale micro-instability $\rightarrow$ turbulence

- Quasi-2D dynamics: small perpendicular scales ( $L_{\perp} \sim \rho_i$ ), elongated along field lines
- Small amplitude ( $\delta n/n < 1\%$ ), **still effective at transport, limiting  $\tau_E = 3nT/P_{\text{loss}}$**



# Increasing gradients eventually cause small scale micro-instability → turbulence

- Quasi-2D dynamics: small perpendicular scales ( $L_{\perp} \sim \rho_i$ ), elongated along field lines
- Small amplitude ( $\delta n/n < 1\%$ ), **still effective at transport, limiting  $\tau_E = 3nT/P_{\text{loss}}$**

- Turbulence measurements in ~100 Million C plasma will always be challenging and incomplete
- I'm going to show a lot of results from gyrokinetic turbulence simulations, as they help develop the physics basis to explain and predict
- Such simulations are being used more frequently to predict first and guide experiments

loss



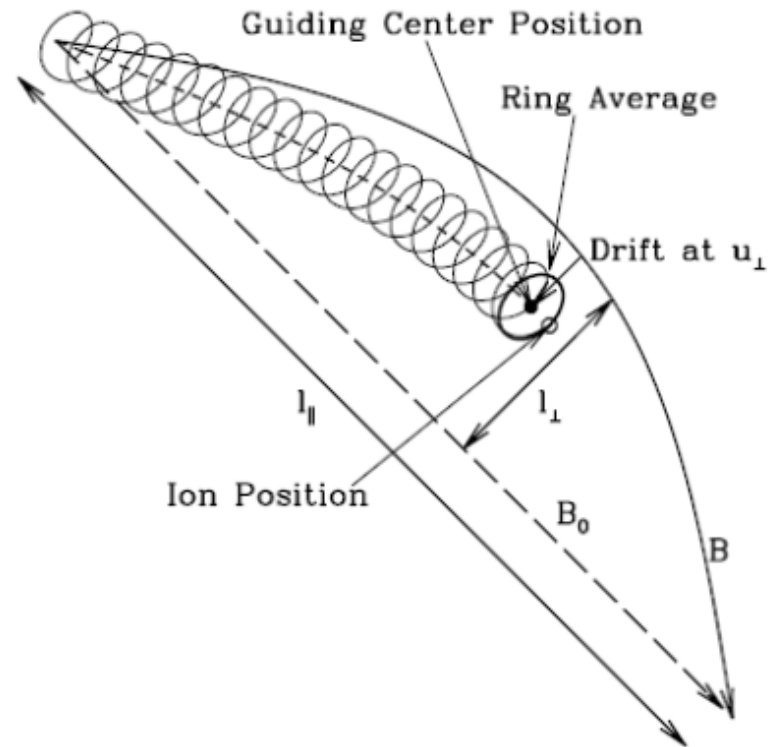
GENE gyrokinetic simulation  
genecode.org

# Gyrokinetics in brief – evolving 5D gyro-averaged distribution function

$$\frac{\omega}{\Omega} \ll 1$$

$$f(\bar{\mathbf{x}}, \bar{\mathbf{v}}, t) \xrightarrow{\text{gyroaverage}} f(\bar{\mathbf{R}}, v_{\parallel}, v_{\perp}, t)$$

- Average over fast gyro-motion  $\rightarrow$  evolve a distribution of gyro-rings



Howes et al., *Astro. J.* (2006)

# Gyrokinetics in brief – evolving 5D gyro-averaged distribution function

$$\frac{\omega}{\Omega}, \frac{\rho}{L}, \frac{\delta f}{f_0}, \frac{k_{\parallel}}{k_{\perp}} \ll 1$$

$$f(\bar{\mathbf{x}}, \bar{\mathbf{v}}, t) \xrightarrow{\text{gyroaverage}} f(\bar{\mathbf{R}}, v_{\parallel}, v_{\perp}, t) \quad f = F_M + \delta f$$

$$\frac{\partial(\delta f)}{\partial t} + \underbrace{v_{\parallel} \hat{\mathbf{b}} \cdot \nabla \delta f}_{\text{Fast parallel motion}} + \underbrace{\bar{\mathbf{v}}_d \cdot \nabla \delta f}_{\text{Slow perpendicular toroidal drifts}} + \underbrace{\delta \bar{\mathbf{v}} \cdot \nabla F_M}_{\text{Advection across equilibrium gradients}} + \underbrace{\bar{\mathbf{v}}_{E0}(\mathbf{r}) \cdot \nabla \delta f}_{\text{Dopper shift due to sheared equilibrium } E_r(r)} + \underbrace{\delta \bar{\mathbf{v}} \cdot \nabla \delta f}_{\text{Perpendicular non-linearity}} = C(\delta f)$$

Fast parallel motion

Slow perpendicular toroidal drifts

Advection across equilibrium gradients ( $\nabla T_0, \nabla n_0, \nabla V_0$ )

Dopper shift due to sheared equilibrium  $E_r(r)$

Perpendicular non-linearity

Collisions

$$\bar{\mathbf{v}}_{\kappa} = m v_{\parallel}^2 \frac{\hat{\mathbf{b}} \times \bar{\boldsymbol{\kappa}}}{qB}$$

$$\bar{\mathbf{v}}_{\nabla B} = \frac{m v_{\perp}^2}{2} \frac{\hat{\mathbf{b}} \times \nabla B / B}{qB}$$

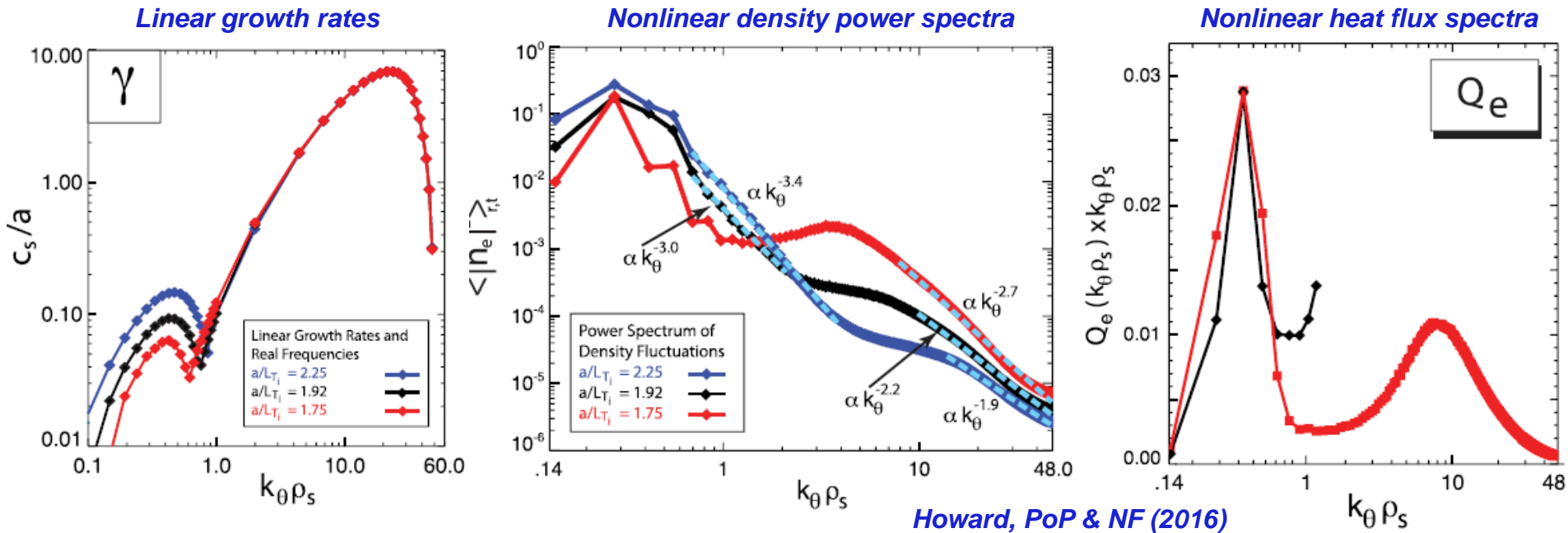
$$\delta \mathbf{v}_a \doteq \frac{c}{B} \mathbf{b} \times \nabla \Psi_a$$

$$\Psi_a(\mathbf{R}) \doteq \left\langle \delta \phi(\mathbf{R} + \rho) - \frac{1}{c} (\mathbf{V}_0 + \mathbf{v}) \cdot \delta \mathbf{A}(\mathbf{R} + \rho) \right\rangle_{\mathbf{R}}$$

- Must also solve gyrokinetic Maxwell equations self-consistently to obtain  $\delta \phi, \delta B$

Note to self: add  $d(\delta \phi)/dt$  term

# Example of state-of-the-art in multi-scale ( $\rho_i$ to $\rho_e$ ) nonlinear gyrokinetic simulations (for the core)



- Energy drive can occur across large range of scales, but turbulent spectra still exhibit decay
- Energy and enstrophy conserved in 2D
  - **Inverse** energy cascade  $E(k) \sim k^{-5/3}$
  - Forward enstrophy  $[\omega^2 \sim (\nabla \times v)^2]$  cascade  $E(k) \sim k^{-3}$
  - Non-local wavenumber interactions can couple over larger range in  $k$ -space (e.g. to zonal flows)
- Nonlinear spectra often downshifted in  $k_\theta$  (w.r.t. linear growth rates)
- Both drive and damping can overlap over wide range of  $k_\perp$ 
  - Very distinct from neutral fluid turbulence with large-scale drive + small scale dissipation

# Turbulence advects/mixes/transport energy, particles and momentum

- Turbulence provides a highly nonlinear flux-gradient relationship due to sources of free energy

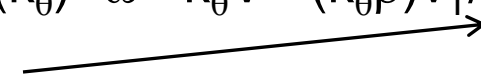
$$\begin{bmatrix} \Gamma \\ \Pi_\phi \\ Q_i \\ Q_e \end{bmatrix} = - \begin{bmatrix} \text{flux - gradient} \\ \text{relationship} \\ \text{matrix} \end{bmatrix} \cdot \begin{bmatrix} \nabla n \\ R\nabla\Omega \\ \nabla T_i \\ \nabla T_e \end{bmatrix}$$

- I realize I'm largely focusing on energy transport ( $\rightarrow$ fusion gain), but just as important for a self-consistent reactor solution is:
  - Particle transport  $\rightarrow$  need to fuel D & T in reactors
  - Impurity transport  $\rightarrow$  expelling He ash; avoiding impurity accumulation from e.g. sputtering high-Z (e.g. tungsten) walls
  - Momentum transport  $\rightarrow$  rotation is critical to macrostability (RWM/NTM) and part of self-consistent turbulence solution via  $E \times B$  sheared flows (*more later*)

# GENERAL **CORE** TURBULENCE CHARACTERISTICS

# 40+ years of theory predicts turbulence in magnetized plasma should often be drift wave in nature

## General predicted drift wave characteristics:

- Finite-frequency drifting waves,  $\omega(k_\theta) \sim \omega_* \sim k_\theta V_* \sim (k_\theta \rho) v_T / L_n$ 
  - Driven by  $\nabla n, \nabla T$  ( $1/L_n = -1/n \cdot \nabla n$ ) 
- Quasi-2D, elongated along the field lines ( $L_{\parallel} \gg L_{\perp}, k_{\parallel} \ll k_{\perp}$ )
  - Particles can rapidly move along field lines to smooth out perturbations
  - Perpendicular sizes linked to local gyroradius,  $L_{\perp} \sim \rho_{i,e}$  or  $k_{\perp} \rho_{i,e} \sim 1$
- In a tokamak, often expected to be “ballooning”, i.e. stronger on outboard side
  - Due to “bad curvature”/“effective gravity” pointing outwards from symmetry axis
- Transport has gyrobohm scaling,  $\chi_{GB} = \rho_i^2 v_{Ti} / R$ 
  - But other factors important like threshold and stiffness:  $\chi_{turb} \sim \chi_{GB} \cdot F(\dots) \cdot [R/L_T - R/L_{T,crit}]$



# Microwave & far-infrared (FIR) scattering used extensively for density fluctuation measurements

Park, RSI (1985)

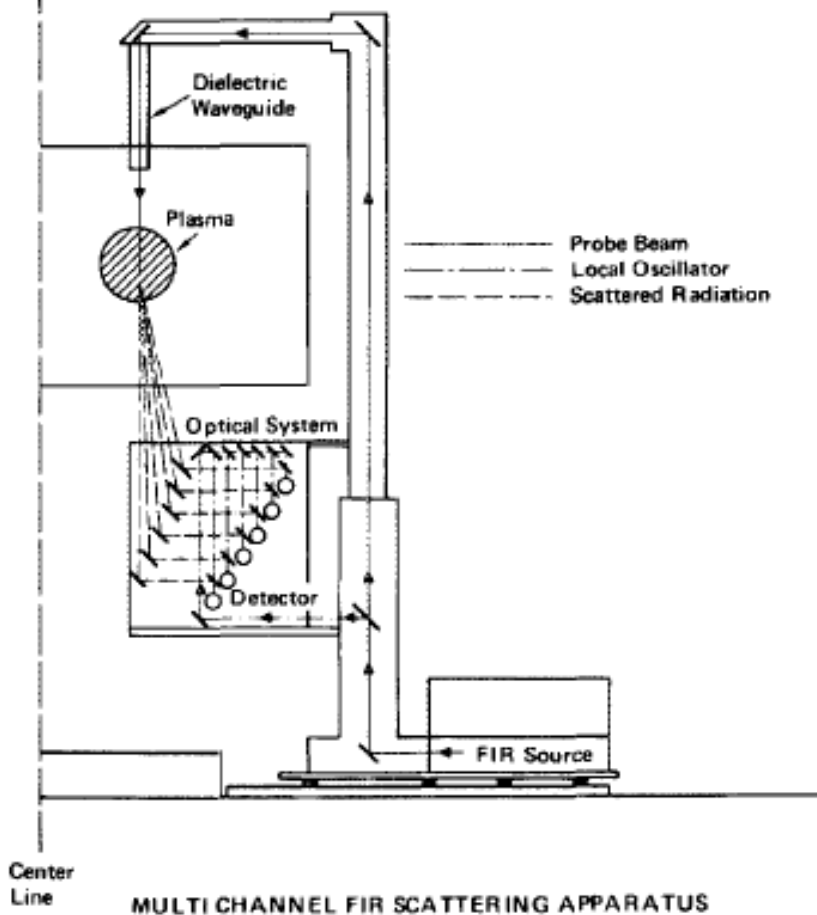


FIG. 1. Scannable multichannel FIR scattering apparatus employed on the TEXT tokamak.

- Geometry and frequency determine measurable  $\omega$ ,  $k$

$$\omega_{\text{meas}} = \omega_{\text{scat}} - \omega_{\text{incident}}$$

$$k_{\text{meas}} = k_{\text{scat}} - k_{\text{incident}}$$

- Can be configured for forward scattering, backscattering, reflectometry, ...

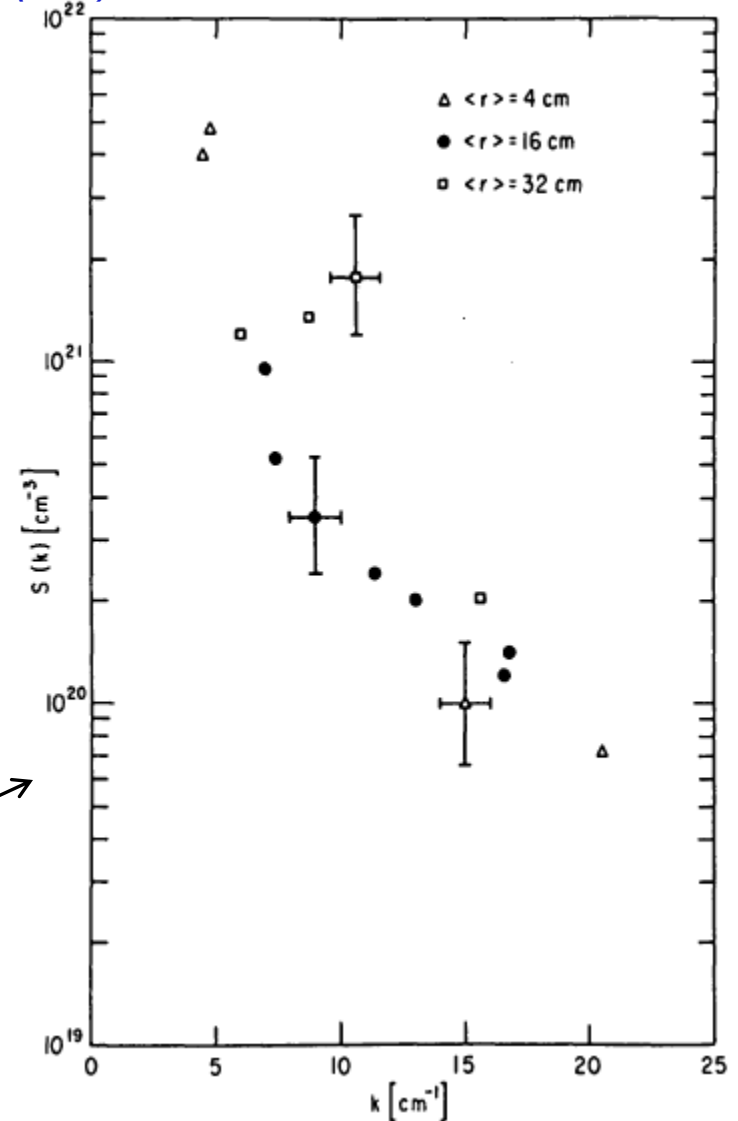
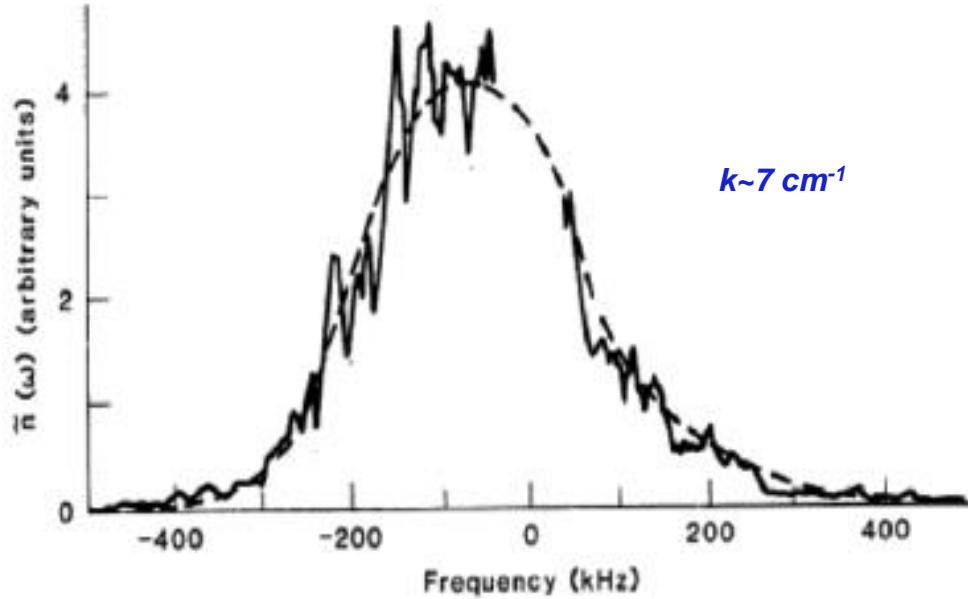
# Broad frequency spectra measured for given scattering wavenumber

Mazzucato, PRL (1982)

Surko & Slusher, Science (1983)

Princeton Large Torus (PLT)

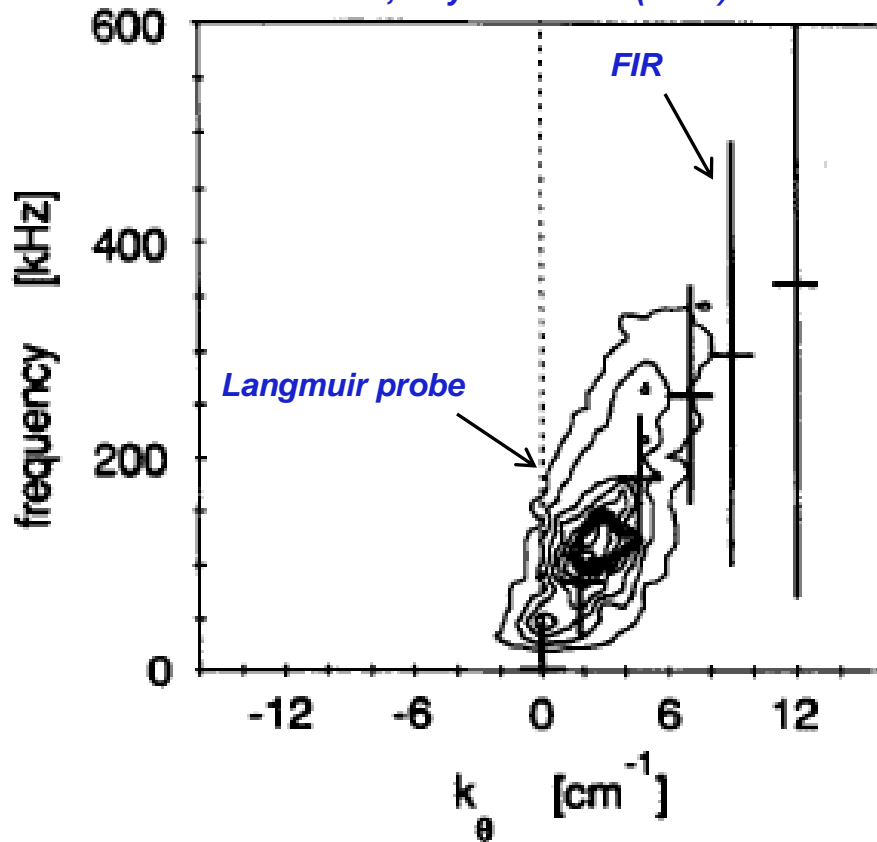
$k \sim 7 \text{ cm}^{-1}$



- Different scattering angles measure different  $k$ , observe spectral decay in wavenumber

# Broad drift wave turbulent spectrum verified simultaneously with Langmuir probes and FIR scattering

TEXT, Ritz, Nuclear Fusion (1987)  
Wooton, Phys. Fluids B (1990)



- Illustrates drift wave dispersion
- However, real frequency almost always dominated by Doppler shift

$$\omega_{\text{lab}} = \omega_{\text{mode}}(k_\theta) + k_\theta v_{\text{doppler}}$$

- Often challenging to determine mode frequency (in plasma frame) within uncertainties

FIG. 1. The  $S(k_\theta, \omega)$  spectrum at  $r = 0.255$  m in TEXT, from Langmuir probes (contours) and FIR scattering (bars indicate FWHM).

# Small normalized fluctuations in core ( $\leq 1\%$ ) increasing to the edge

- Combination of diagnostics used to measure fluctuation amplitudes

*ATF stellarator, Hanson, Nuclear Fusion (1992)*

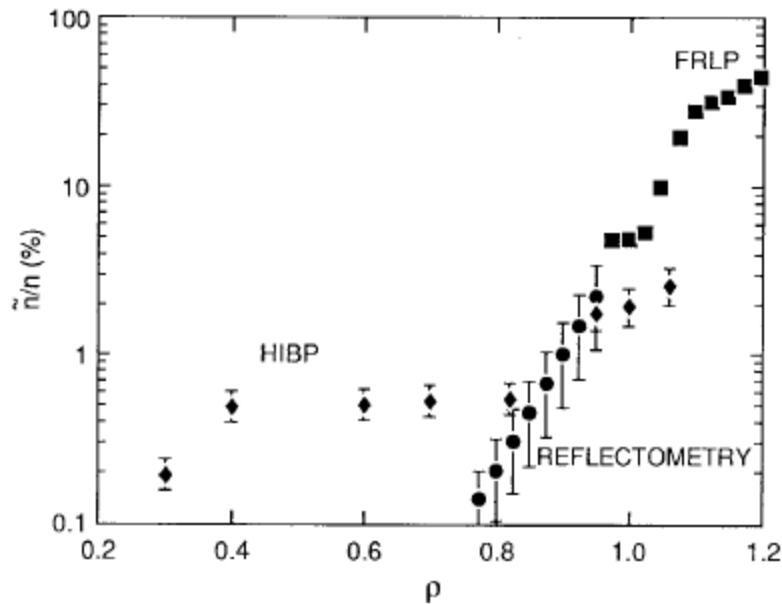


Fig. 4. Radial profile of density fluctuations (in %) in ATF stellarator obtained by combining results from different diagnostics [177].

- Measurements also often show  $\delta n/n_0 \sim \delta\phi/T_0$  (within factor  $\sim 2$ ), expected for

*TEXT tokamak, Wooton, PoFB (1990)*

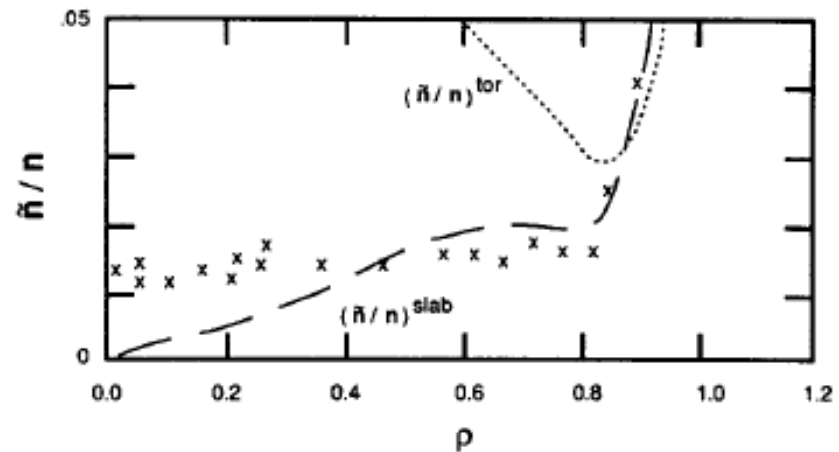


FIG. 6. The spatial variation of  $\bar{n}/n$  from TEXT ( $B_0 = 2$  T,  $I_p = 200$  kA,  $\bar{n}_e = 2$  to  $3 \times 10^{19} \text{ m}^{-3}$ ,  $\text{H}^+$ ), shown as crosses (HIBP). Also shown are the predictions of two mixing length estimates,  $(\bar{n}/n)^{\text{tor}}$  and  $(\bar{n}/n)^{\text{slab}}$ . Both electron feature  $\bar{n}/n$  and  $k_\theta$  ( $\bar{k}_\theta \rho_e = 0.1$ ) are interpreted assuming no ion feature is present.

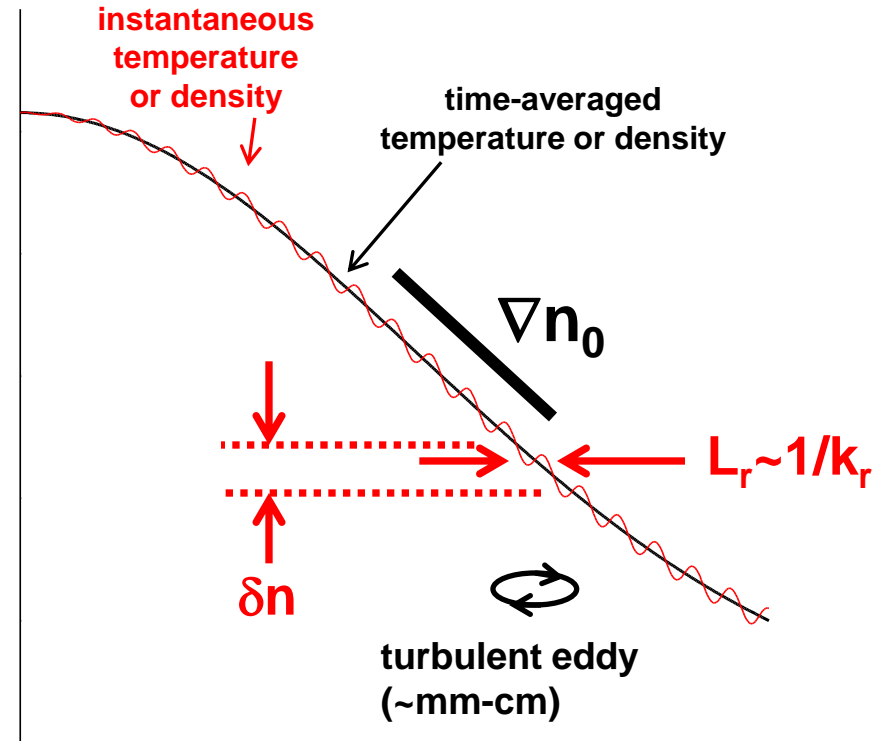
# Mixing length estimate for fluctuation amplitude

- In the presence of an equilibrium gradient,  $\nabla n_0$ , turbulence with radial correlation  $L_r$  will mix regions of high and low density
- Leads to fluctuation  $\delta n$

$$\delta n \approx \nabla n_0 \cdot L_r$$

$$\frac{\delta n}{n_0} \approx \frac{\nabla n_0}{n_0} \cdot L_r \approx \frac{L_r}{L_n} \quad (1/L_n = \nabla n_0 / n_0)$$

$$\frac{\delta n}{n_0} \sim \frac{1}{k_{\perp} L_n} \sim \frac{\rho_s}{L_n} \quad (k_{\perp}^{-1} \sim L_r; k_{\perp} \rho_s \sim \text{constant})$$



core

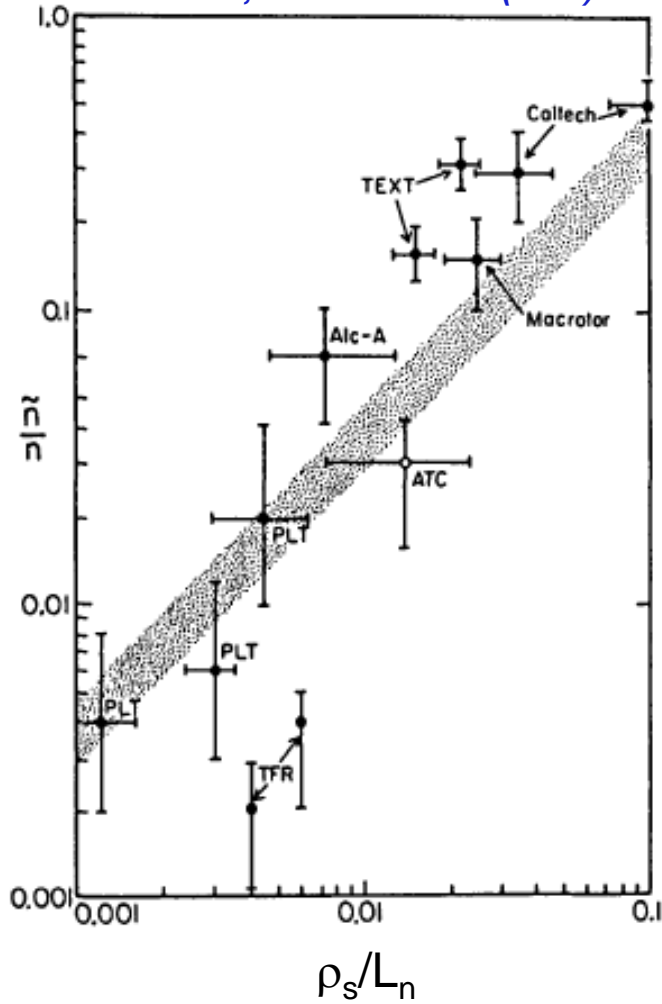
boundary

1-2 m

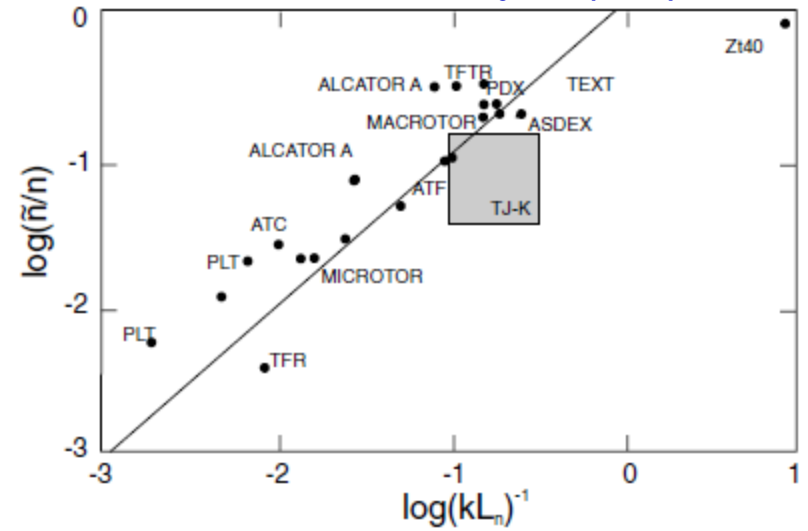
**IF turbulence scale length linked to  $\rho_s$ ,  
would loosely expect  $\delta n/n_0 \sim \rho_s/L_n$**

# Fluctuation intensity across machines loosely scales with mixing length estimate, reinforces local $\rho_s$ drift nature

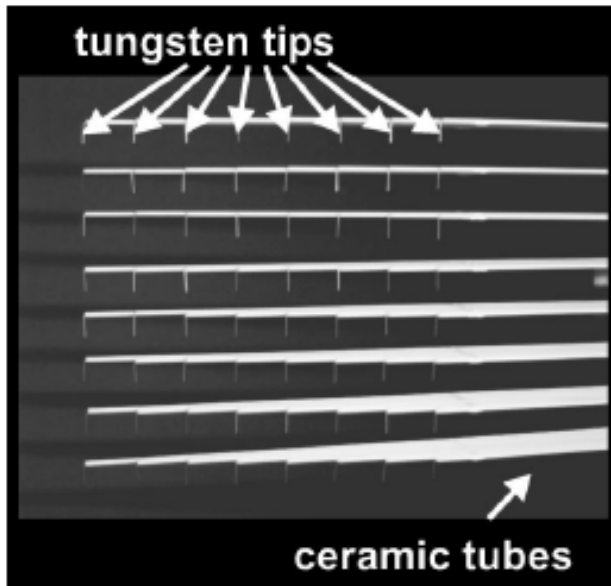
Liewer, Nuclear Fusion (1985)



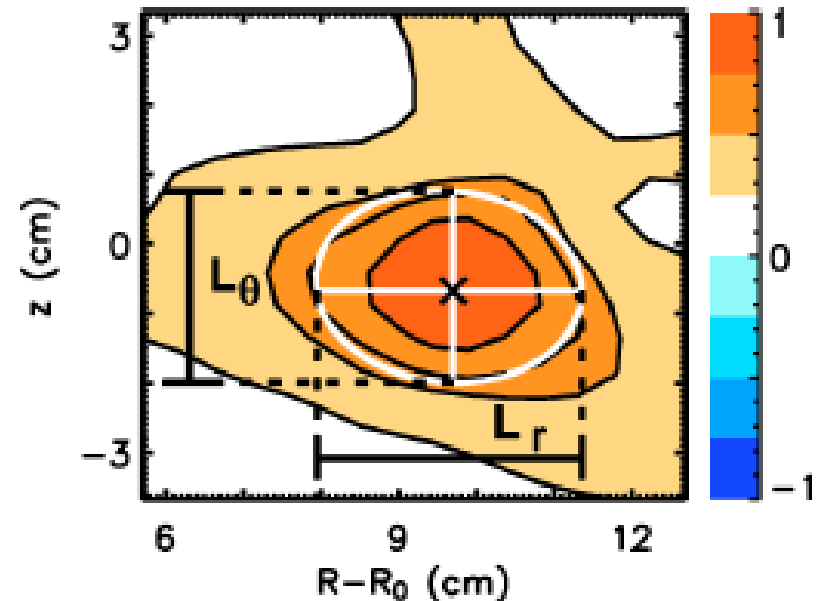
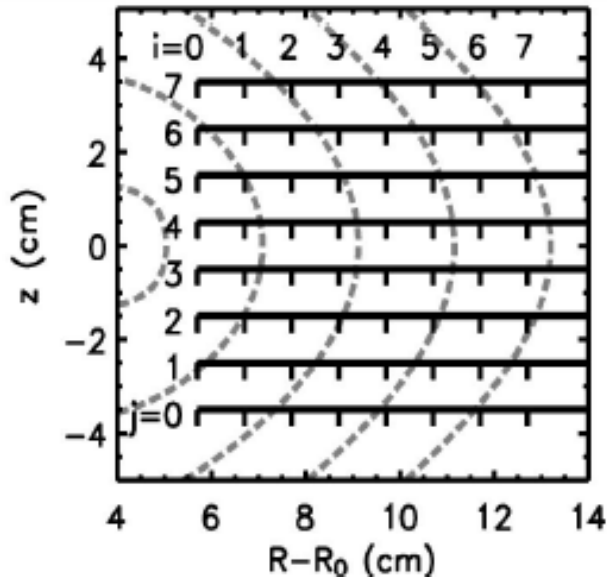
Lechte, New J. of Physics (2002)



# 2D Langmuir probe array in TJ-K stellarator used to directly measure spatial and temporal structures



- Simultaneously acquiring 64 time signals – can directly calculate 2D correlation, with time
- Caveat – relatively cool ( $T \sim 10$  eV) compared to fusion performance plasmas ( $T \sim 10$  keV)



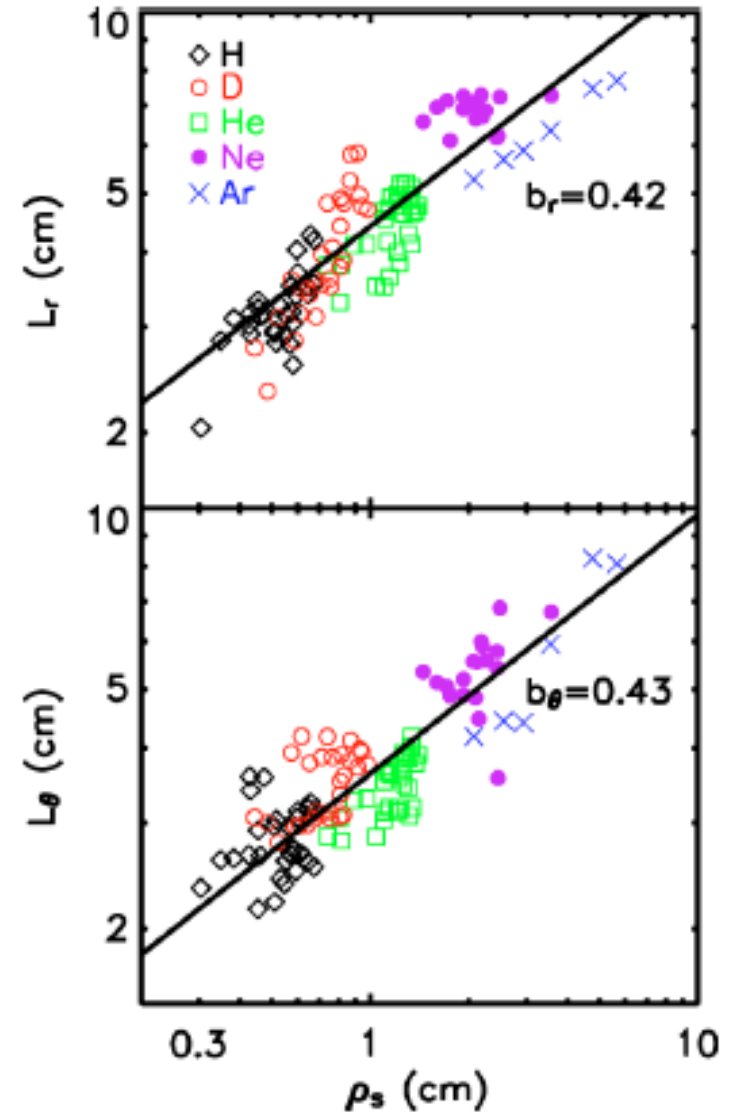
TJ-K [Ramisch, PoP (2005)]

# Radial and poloidal correlation lengths scale with $\rho_s$ reinforcing drift wave nature

TJ-K [Ramisch, PoP (2005)]

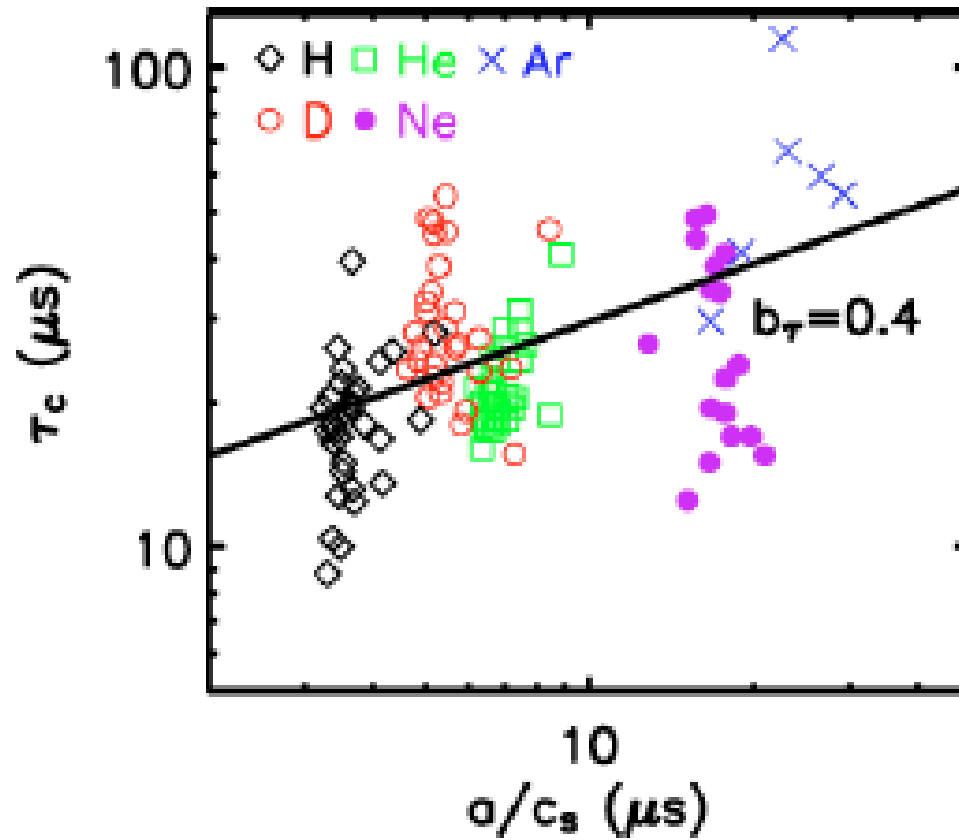
- Turbulence close to isotropic

$$L_r \sim L_\theta$$



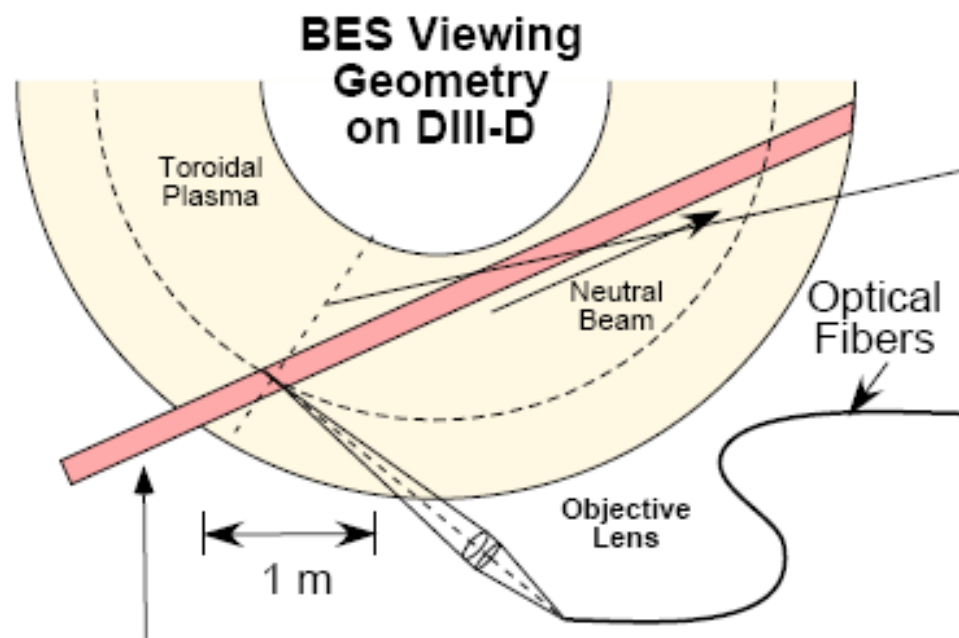
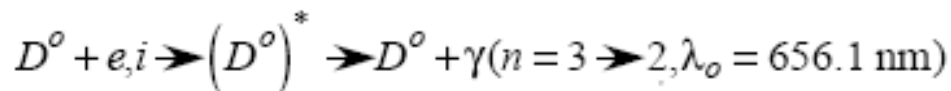


# Temporal scales loosely correlated with acoustic times $c_s/a$



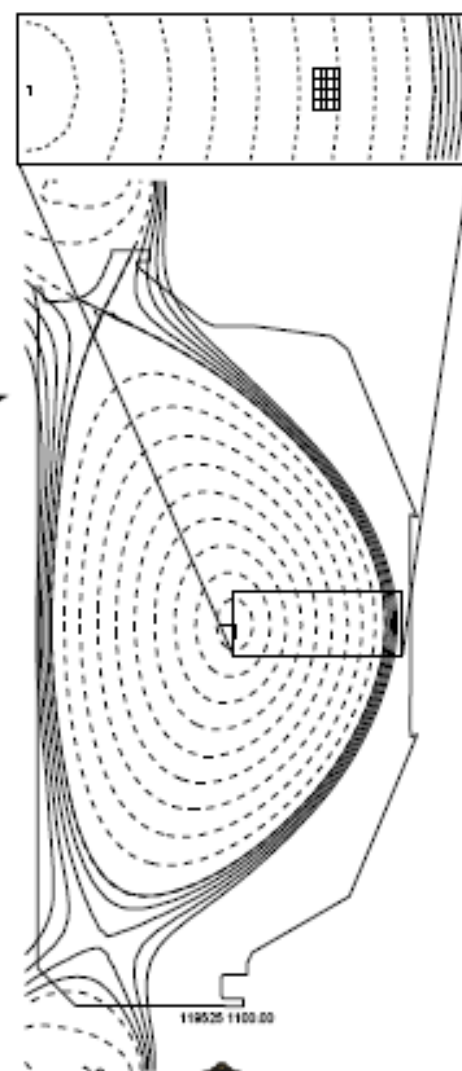
# BEAM EMISSION SPECTROSCOPY MEASUREMENT OF LOCALIZED, LONG-WAVELENGTH ( $k_{\perp}\rho_i < 1$ ) DENSITY FLUCTUATIONS

Collisionally-excited, Doppler-shifted neutral beam fluorescence



75 KeV  $D^0$  Neutral Beam  
(150 L (R))

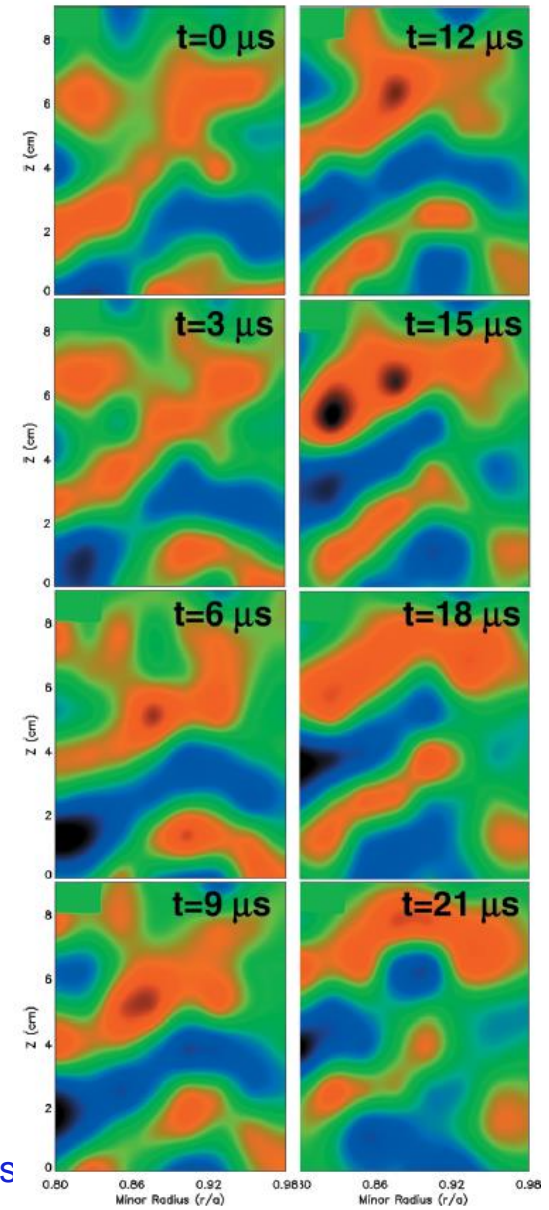
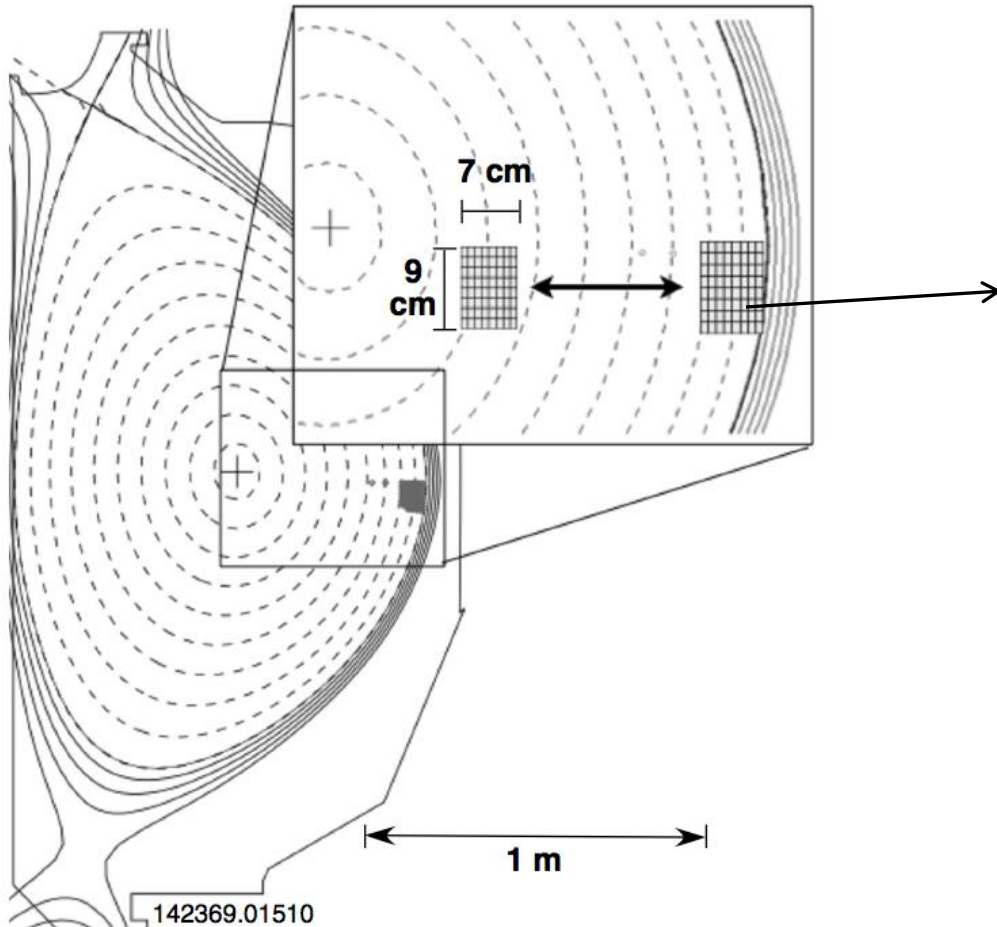
$$\frac{\tilde{I}}{I} \mu \frac{\tilde{n}}{n}$$



# Spectroscopic imaging provides a 2D picture of turbulence in hot tokamak core: cm spatial scales, $\mu\text{s}$ time scales

- Utilize interaction of neutral atoms with charged particles to measure density

DIII-D tokamak (General Atomics)



Movies at: <https://fusion.gat.com/global/BESMovies>

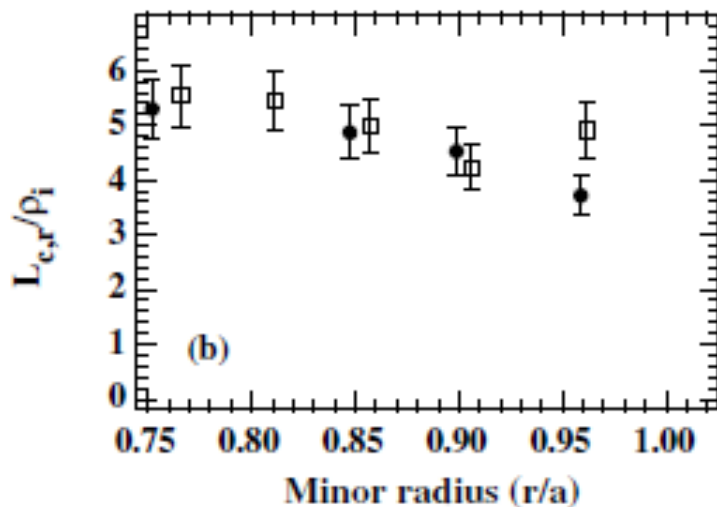
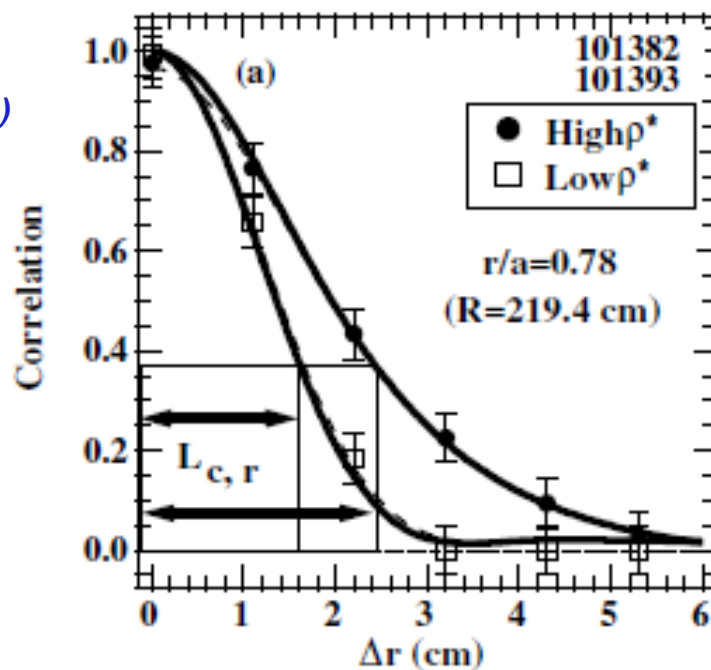
## BES videos

<https://fusion.gat.com/global/BESMovies>

(University of Wisconsin; General Atomics)

# Radial and poloidal correlation lengths scale with $\rho_s$ in core imaging, reinforcing local drift wave nature

DIII-D  
Mckee, Nucl. Fusion (2001)



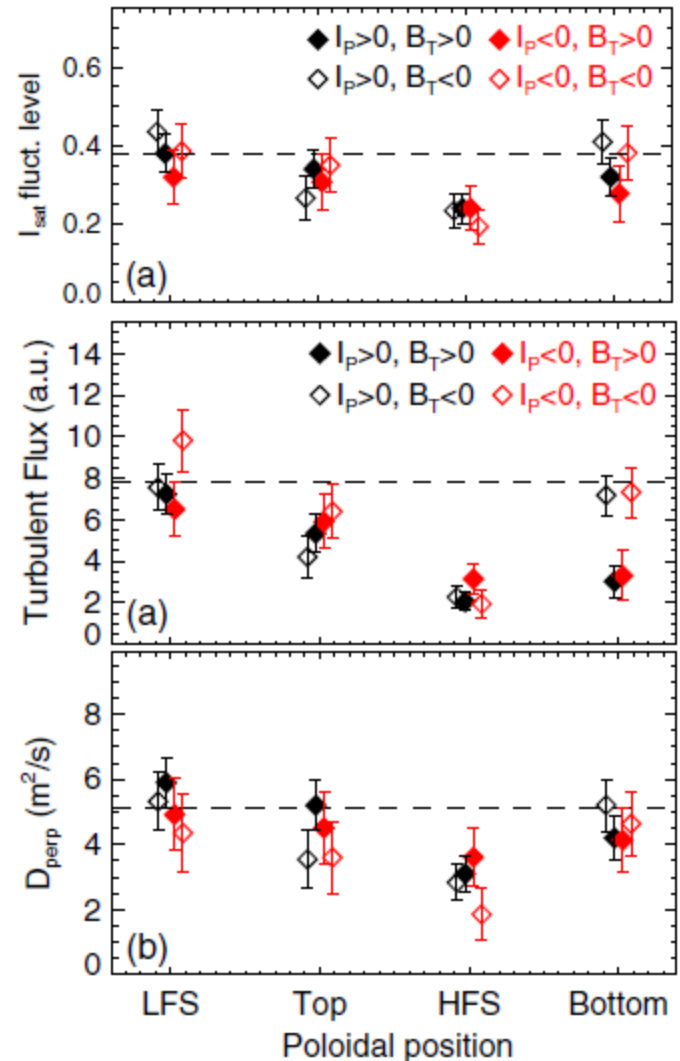
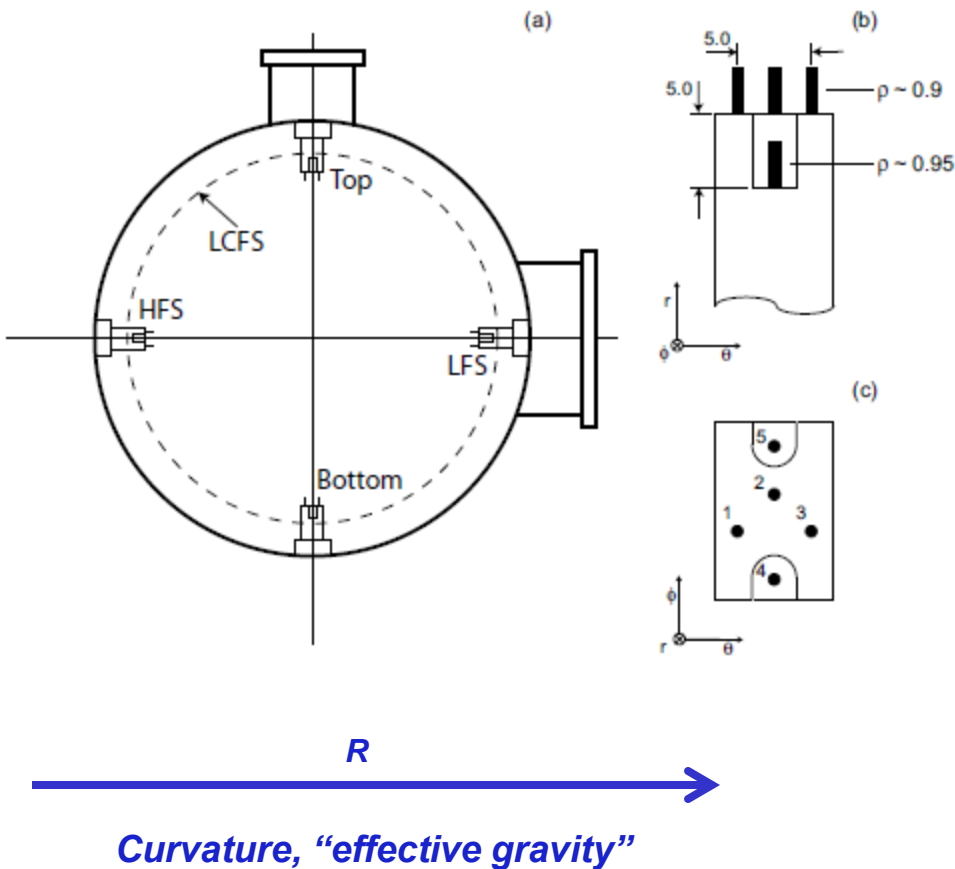
- Correlation length increases with local gyroradius  $\rho$  ( $\rho_* = \rho/a$ )

- Ratio of  $L_r/\rho$  relatively constant in radius, for the two different  $\rho_*$  discharges

# Example of stronger turbulence measured on outboard side, “ballooning” in nature

- Consistent with bad curvature drive

ISSTOK [Silva, PPCF (2011)]



## Evidence for quasi-2D ( $L_{\parallel} \gg L_{\perp}$ )

- Assume an exponential or Gaussian correlation function  

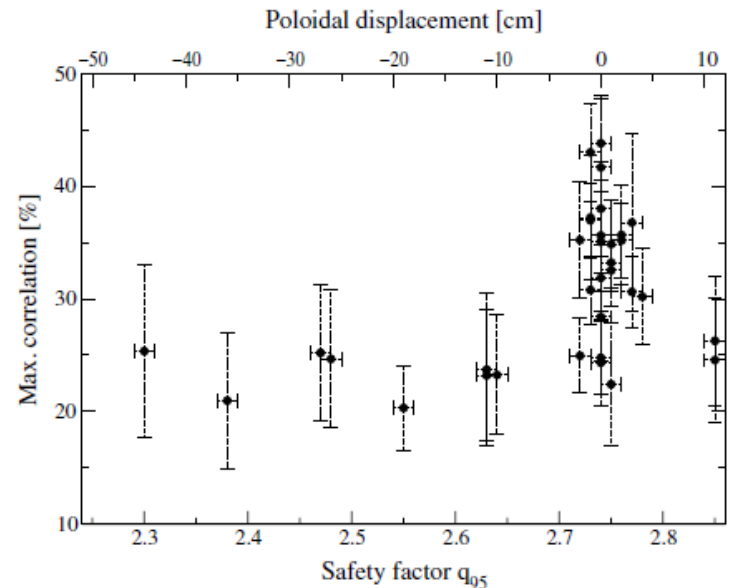
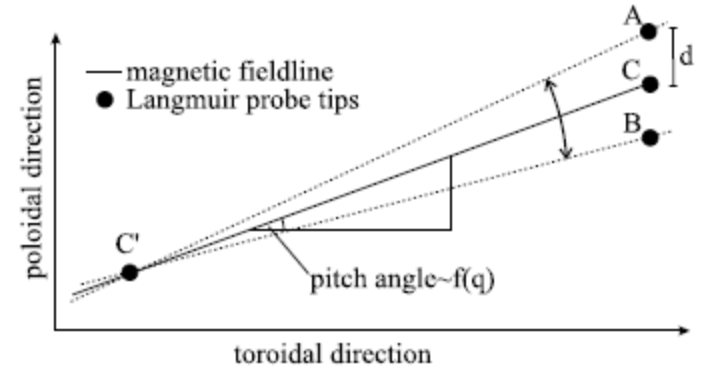
$$C(\Delta_{\perp}, \Delta_{\parallel}) \approx \exp(-\Delta_{\perp} / L_{\perp}) \exp(-\Delta_{\parallel} / L_{\parallel})$$
- Measure correlation between two probes “on the same field line” ( $\Delta_{\perp} \approx 0$ ) separated a large distance  $\Delta_{\parallel} \gg 0$

JET edge plasma

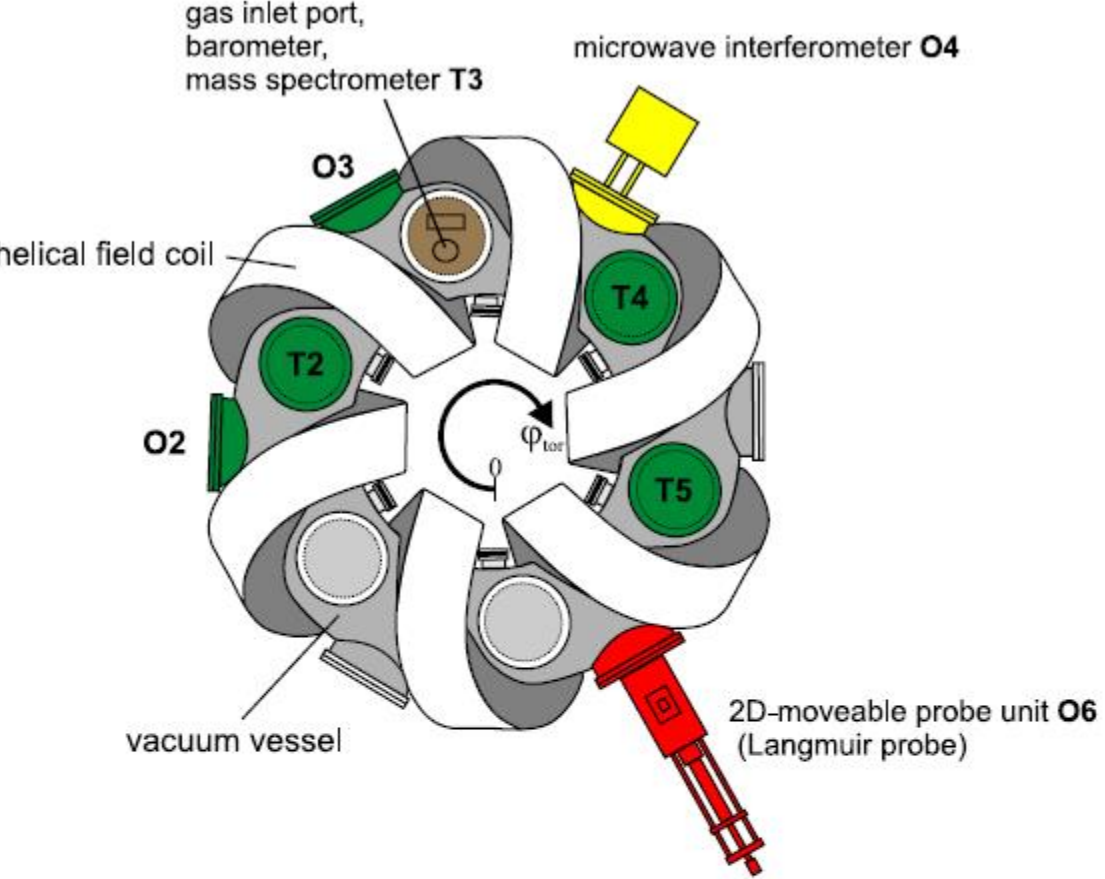
$L_{\parallel} \sim$  many meters

$L_{\perp} \sim$  mm-cm

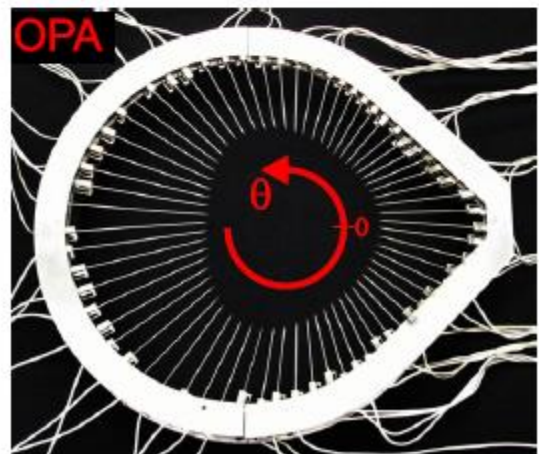
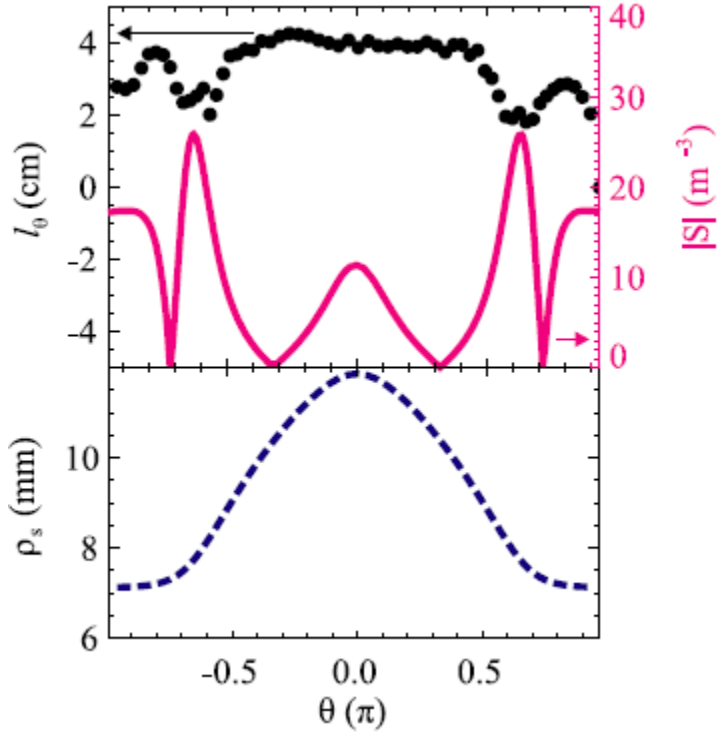
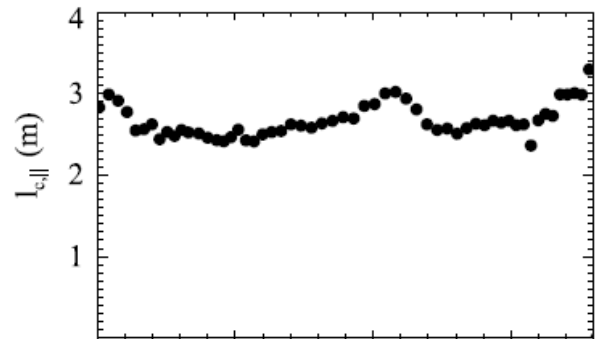
JET edge [Thomsen, Contrib. Plasma Phys. (2001)]



# More direct measurement in TJ-K plasmas



TJ-K [Birkenmeier, PPCF (2012)]





# General turbulence characteristics are useful for testing theory predictions, but we mostly care about transport

- Transport a result of finite average correlation between perturbed drift velocity ( $\delta v$ ) and perturbed fluid moments ( $\delta n$ ,  $\delta T$ ,  $\delta v$ )
  - Particle flux,  $\Gamma = \langle \delta v \delta n \rangle$
  - Heat flux,  $Q = 3/2 n_0 \langle \delta v \delta T \rangle + 3/2 T_0 \langle \delta v \delta n \rangle$
  - Momentum flux,  $\Pi \sim \langle \delta v \delta v \rangle$  (Reynolds stress, just like Navier Stokes)
- Electrostatic turbulence often most relevant  $\rightarrow E \times B$  drift from potential perturbations:  $\delta v_E = \mathbf{B} \times \nabla (\delta \phi) / B^2 \sim k_\theta (\delta \phi) / B$
- Can also have magnetic contributions at high beta,  $\delta v_B \sim v_{||} (\delta B_r / B)$  (magnetic “flutter” transport – more later)

# Measuring turbulent particle and heat fluxes using Langmuir probes

- Illustrates that turbulent transport can account for inferred anomalous transport (only possible in edge region)

TEXT, Wooton, PoFB (1990)

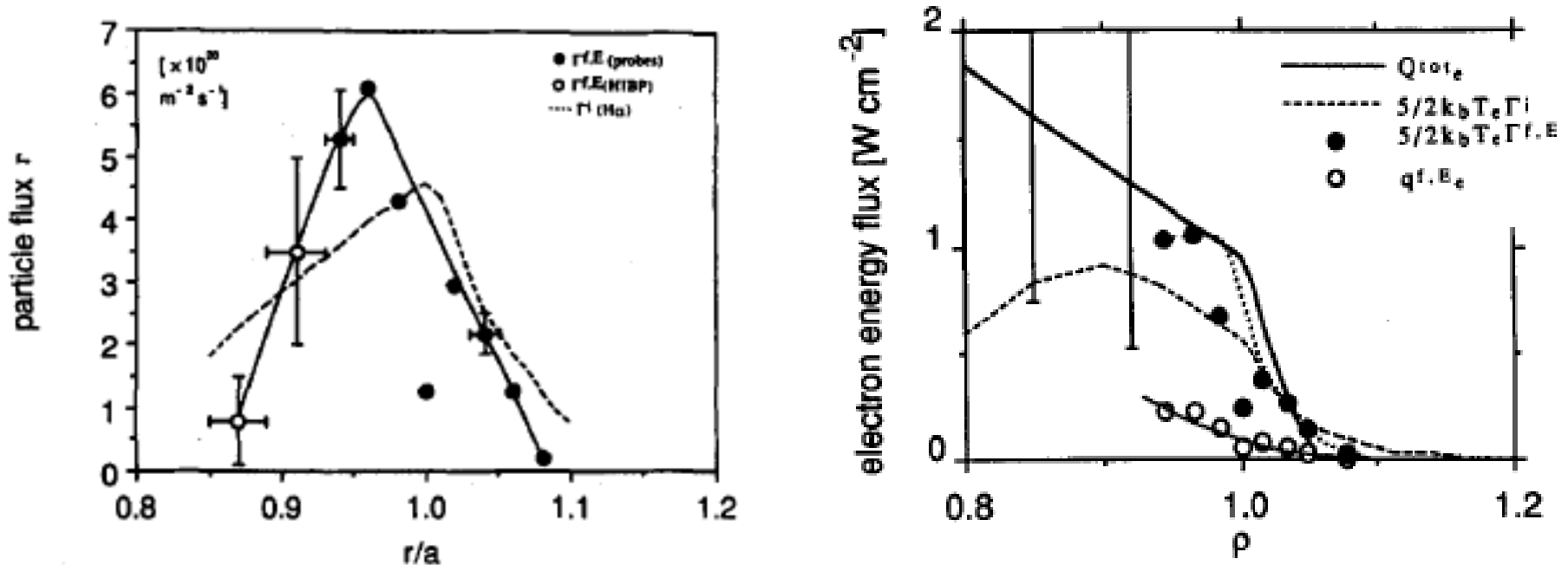


FIG. 3. A comparison of working particle fluxes in TEXT ( $B_0 = 2 \text{ T}$ ,  $I_p = 200 \text{ kA}$ ,  $\bar{n}_e = 3 \times 10^{19} \text{ m}^{-3}$ ,  $\text{H}^+$ ), the total  $\Gamma^i$  (from  $\text{H}\alpha$ ), and  $\Gamma^{f,E}$  driven by electrostatic turbulence.  $\Gamma^{f,E}$  is measured with Langmuir probes (solid line, solid points) and the HIBP (open points).

## Useful to Fourier decompose transport contributions, especially for theory comparisons

- E.g. particle flux from electrostatic perturbations:

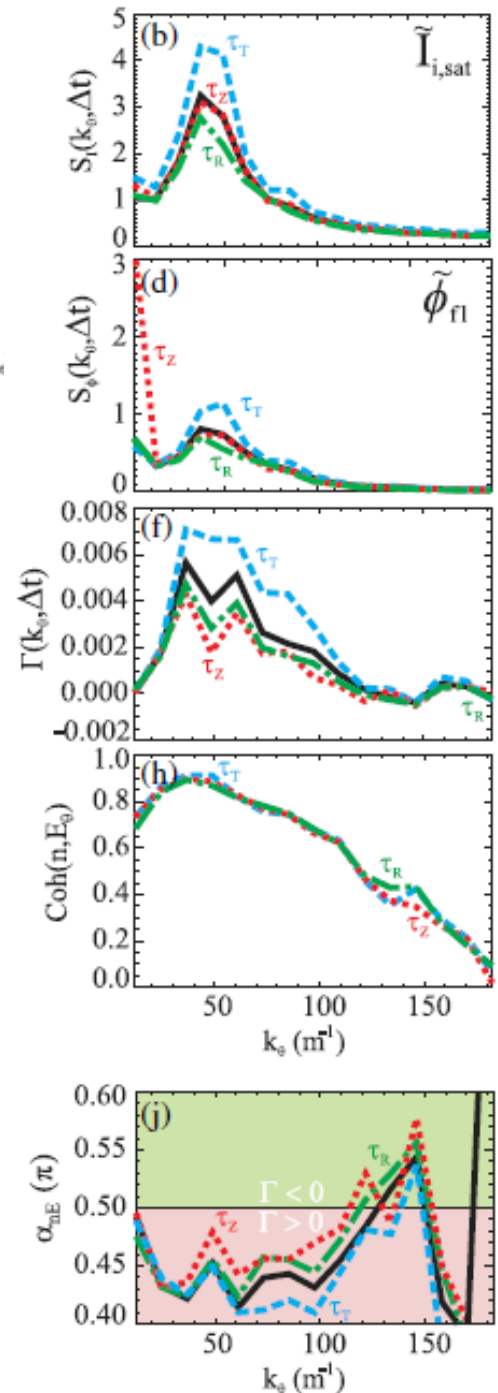
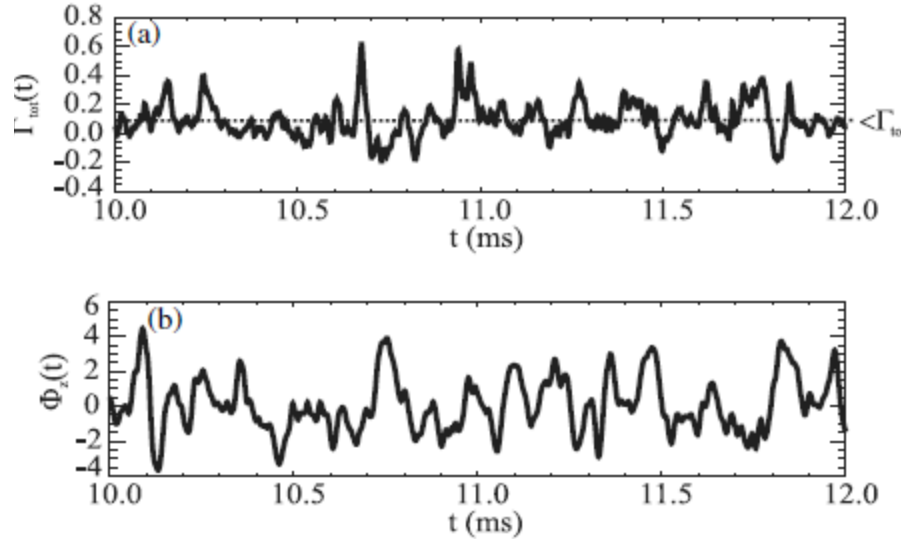
$$\Gamma(k_\theta) = \frac{nT}{B} \sum_{k_\theta} k_\theta \left| \frac{\delta n(k_\theta)}{n_e} \right| \left\| \frac{\delta \varphi(k_\theta)}{T_e} \right\| \gamma_{n\varphi}(k_\theta) \sin \alpha_{n\varphi}(k_\theta)$$

*Amplitude spectra*      *coherence*      *Cross phase*

- Everything is a function of wavenumber

# Edge Langmuir probe arrays used to decompose turbulent fluxes in $k_\theta$

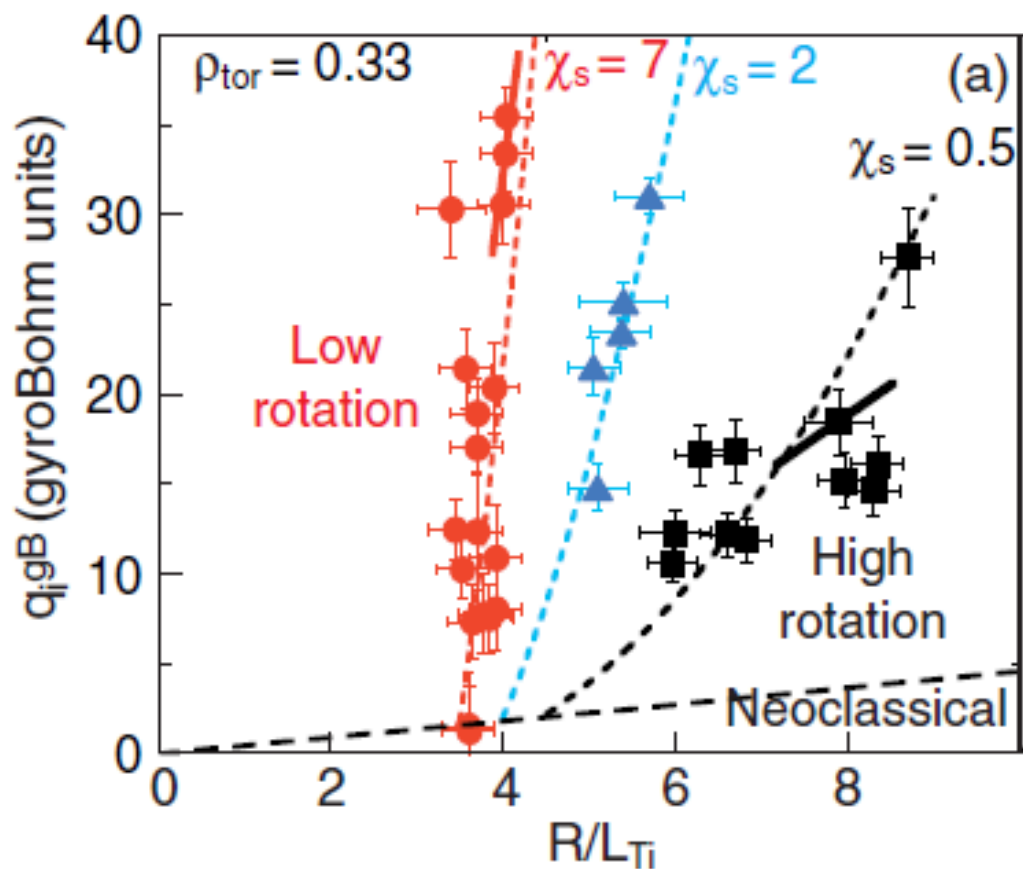
TJ-K [Birkenmeier, PPCF (2012)]



- Very rare to measure this comprehensively!
- Useful for challenging theory calculations
- Yet to be done this thoroughly for hot tokamak core, where comprehensive gyrokinetic simulations available for comparison

# Threshold-like transport behavior observed experimentally

- Vary location of heating source to locally change heat flux, map out  $Q$  vs.  $\nabla T$ 
  - Experimentally inferred threshold varies with equilibrium, plasma rotation, ...
  - Stiffness ( $\sim dQ/d\nabla T$  above threshold) also varies
  - $\chi = -Q/n\nabla T$  highly nonlinear (also use perturbative experiments to probe stiffness)

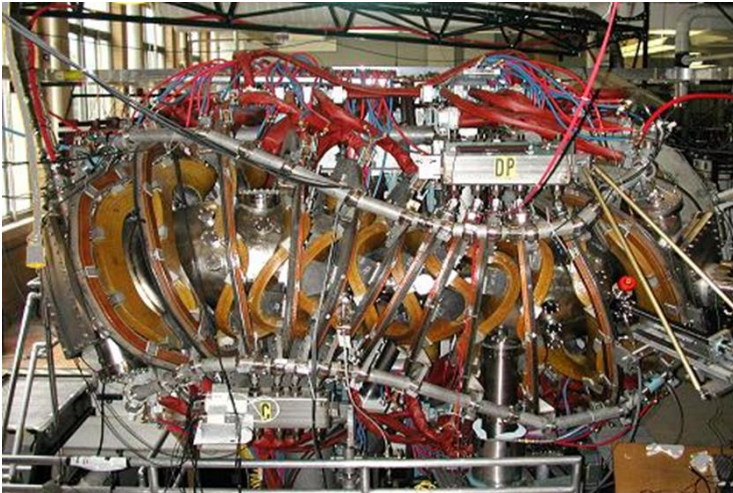


JET  
Mantica, PRL (2011)

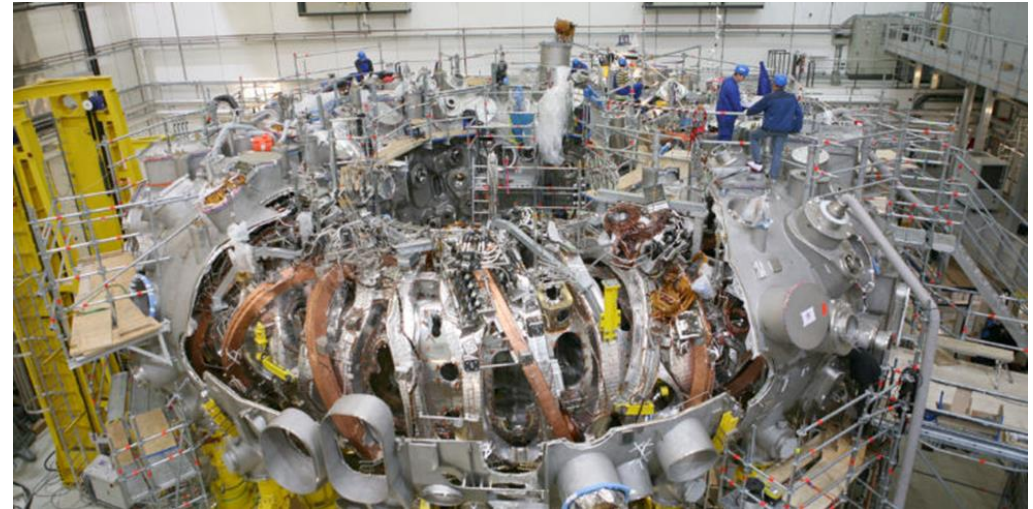
# Stellarators exhibit anomalous energy losses and similar broad spectrum of fluctuations as in tokamaks and

- No direction of true symmetry, but can optimize to be quasi-symmetric (symmetry direction in  $|B|$ ) or quasi-omnigenous / quasi-isodynamic (closed drift orbits), both which reduce traditionally poor 3D neoclassical transport
  - Validated in HSX [Gerhardt, 2004; Canik, 2006] and W7-X [Helander, APS-DPP 2020 and references therein]

HSX (UW-Madison)



W7-X (IPP-Greifswald, Germany)



- Generally, theory indicates drift wave dynamics should be similar to tokamaks, but 3D variation (of curvature, grad-B drifts, diamagnetic “drifts”, parallel streaming, zonal flows) makes a quantitative impact
- A little more challenging to solve numerically, **BUT more degrees of freedom for optimization** [Mynick; Hegna; Helander]

# Beyond general characteristics, there are many theoretical “flavors” of drift waves possible in tokamak core & edge

- Often useful to think of drift waves as gradient driven ( $\nabla T_i$ ,  $\nabla T_e$ ,  $\nabla n$ )
  - Drift waves exhibit thresholds in one or more of these parameters
- Different theoretical “flavors” of microturbulence
  - Electrostatic, ion scale ( $k_\theta \rho_i \leq 1$ )
    - Ion temperature gradient (ITG) – driven by  $\nabla T_i$ , weakened by  $\nabla n$
    - Trapped electron mode (TEM) – driven by  $\nabla T_e$  &  $\nabla n_e$ , weakened by  $v_e$
  - Electrostatic, electron scale ( $k_\theta \rho_e \leq 1$ )
    - Electron temperature gradient (ETG) - driven by  $\nabla T_e$ , weakened by  $\nabla n$
  - Electromagnetic, ion scale ( $k_\theta \rho_i \leq 1$ )
    - Kinetic ballooning mode (KBM) - driven by  $\nabla \beta_{pol}$
    - Microtearing mode (MTM) – driven by  $\nabla T_e$ , at sufficient  $\beta_e$
- Each *theoretical* instability is distinguished by:
  - Scaling with parameters ( $a/L_T$ ,  $a/L_n$ ,  $\beta$ ,  $\nu$ ,  $\alpha$ ,  $s$ ,  $q$ , ...)
  - Mode frequency (ion, electron diamagnetic direction)
  - Spatial structure (ballooning, tearing; ES, EM)
  - Partition of transport ( $\Gamma$ ,  $\Pi$ ,  $Q \rightarrow D/\chi$ ,  $\chi_\phi/\chi$ ) [“transport fingerprint”, Kotschenreuther, 2019]

# Challenging to definitively identify a particular theoretical turbulent transport mechanism

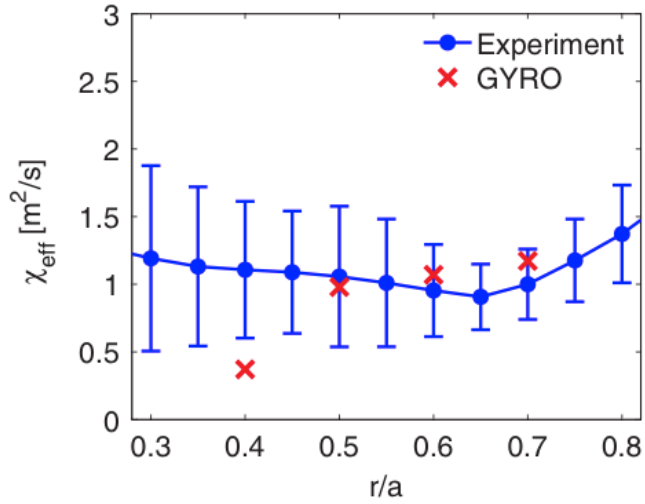
- Best we can do:
  - Measure as many transport and turbulence quantities as possible (amplitude spectra, cross-phases)
  - Scale equilibrium parameters to investigate trends, key dependencies
  - Compare with theory & simulation to (in)validate the predictions with experimental data
    - Use “synthetic diagnostics” to ensure apples-to-apples comparison
    - Quantify uncertainties and sensitivities
  - Reformulate the theory & simulation as needed
  - Make a testable prediction
  - Repeat
- A.K.A. apply the Scientific Method



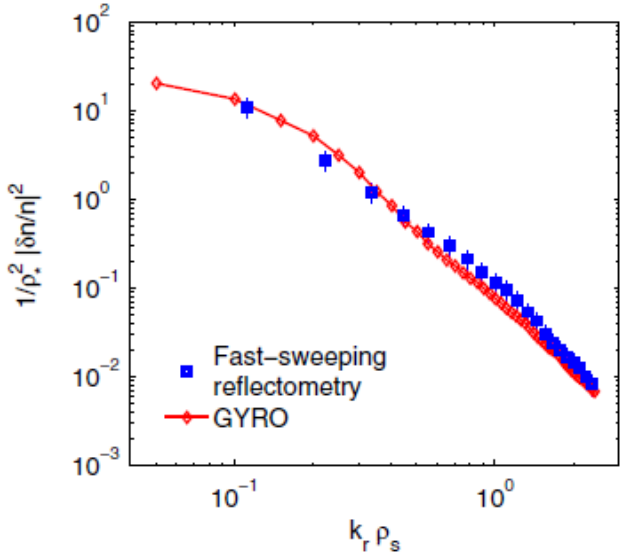
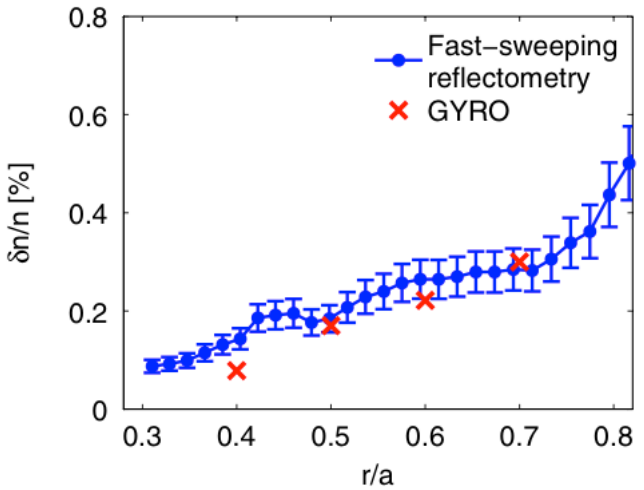
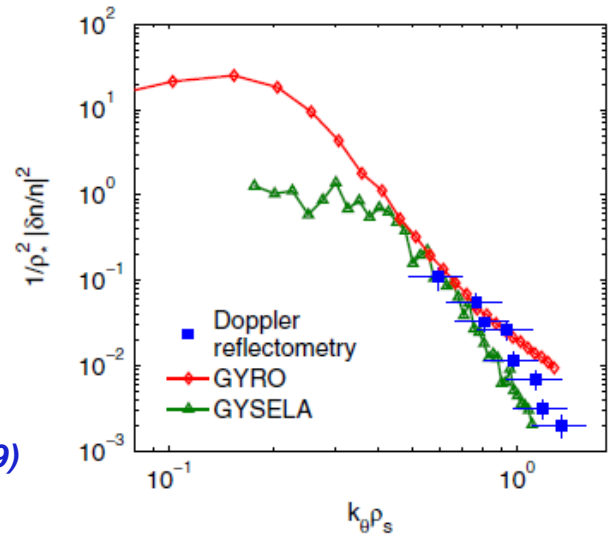
# **Example validation of core gyrokinetic theory/simulation predictions**

# Transport, density fluctuation amplitude (from reflectometry) and spectral characteristics all consistent with nonlinear ITG simulations in Tore Supra

- Provides confidence in interpretation of transport in conditions when ITG instability/turbulence predicted to be most important



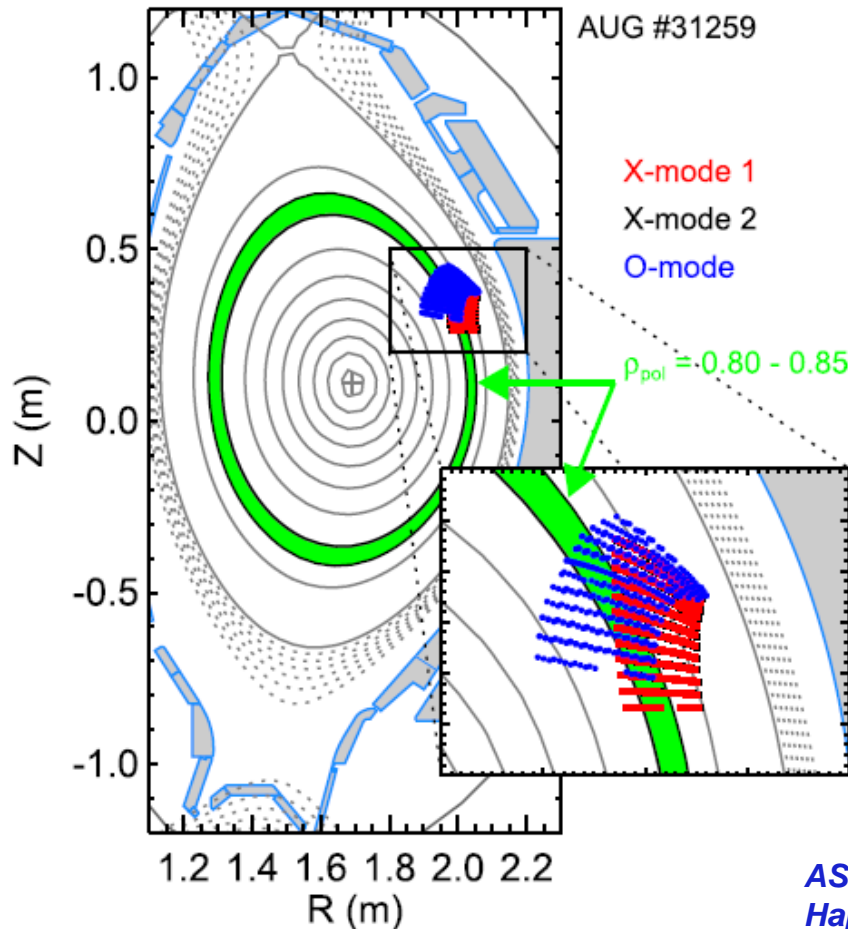
Casati, PRL (2009)



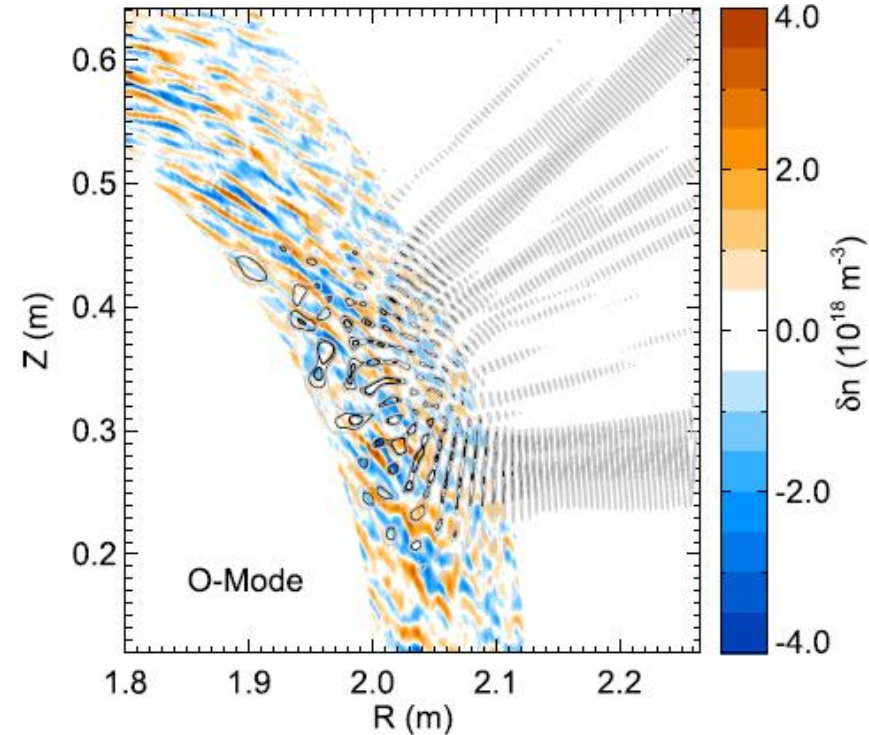
# Important to consider the impact of the diagnostic instrument response when comparing to experiment (“synthetic diagnostic”)

- E.g. using FDTD full wave simulations of EM wave propagation into predicted  $\delta n$  by nonlinear GK simulation to predict X-mode and O-mode Doppler reflectometry signal

## Doppler reflectometry scattering locations



## $\delta n$ from (flux-matched) GK turbulence simulation + wave E-field from full wave simulation

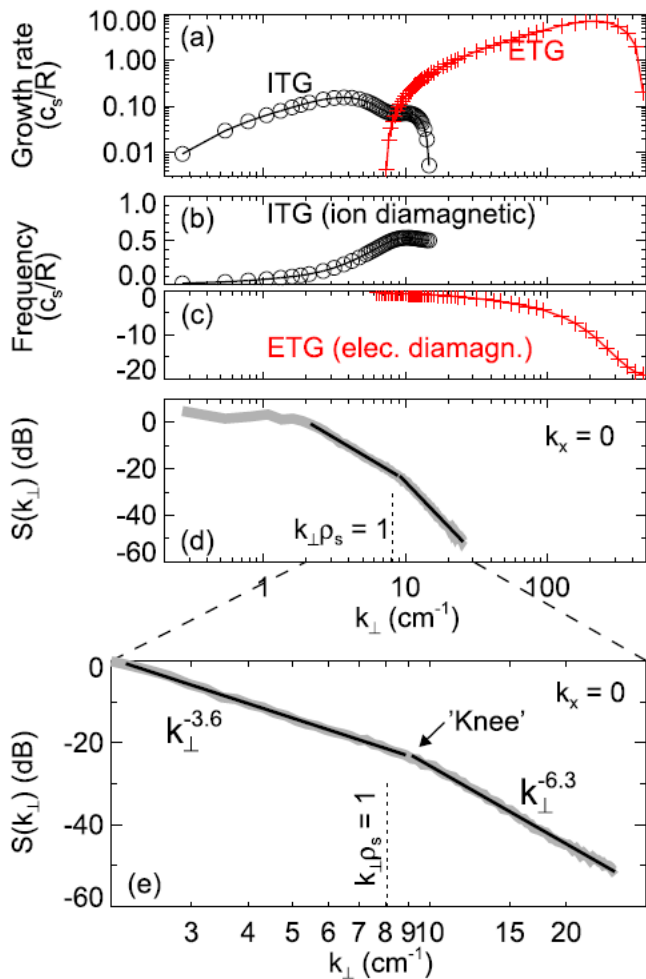


ASDEX-Upgrade  
Happel, PPCF (2017)

# Synthetic diagnostic captures significant difference seen with scattering polarization (X-mode vs. O-mode, ASDEX-Upgrade)

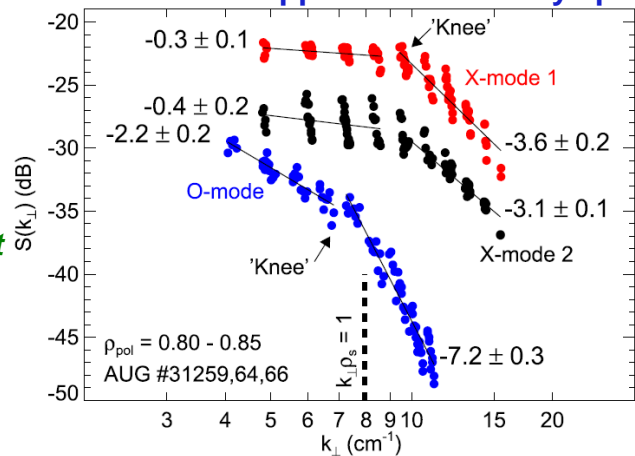
- Synthetic diagnostic also changes predicted location of “knee” in spectra & spectral decay

**GK linear frequencies & growth rates + nonlinear spectra**

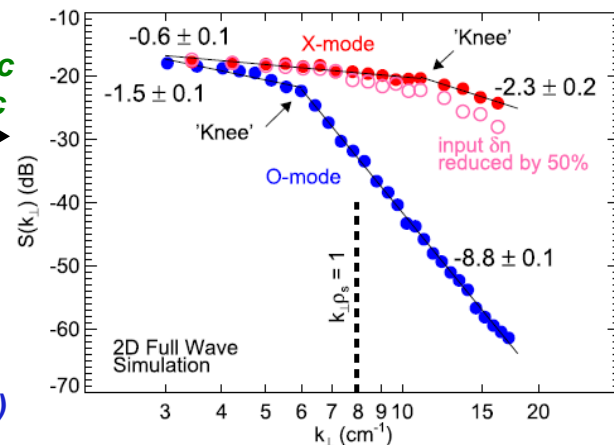


measurement  
 simulation  
 + synthetic diagnostic

**Raw measured Doppler reflectometry spectra**



**Doppler reflectometry spectra from GK sims + synthetic diagnostic (full-wave simulation)**

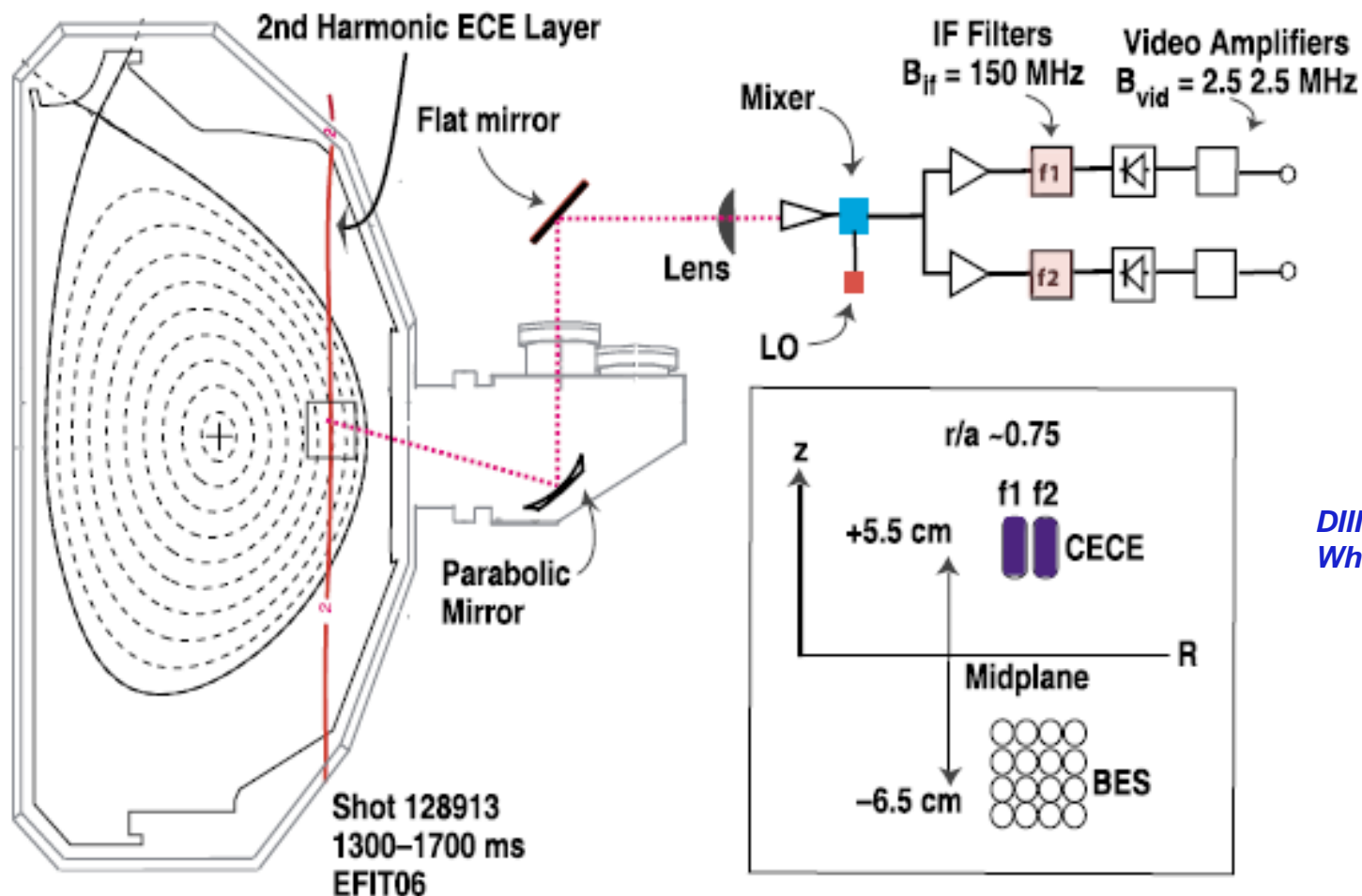


ASDEX-Upgrade  
 Happel, PPCF (2017)

# **Validation using multi-field turbulence measurements**

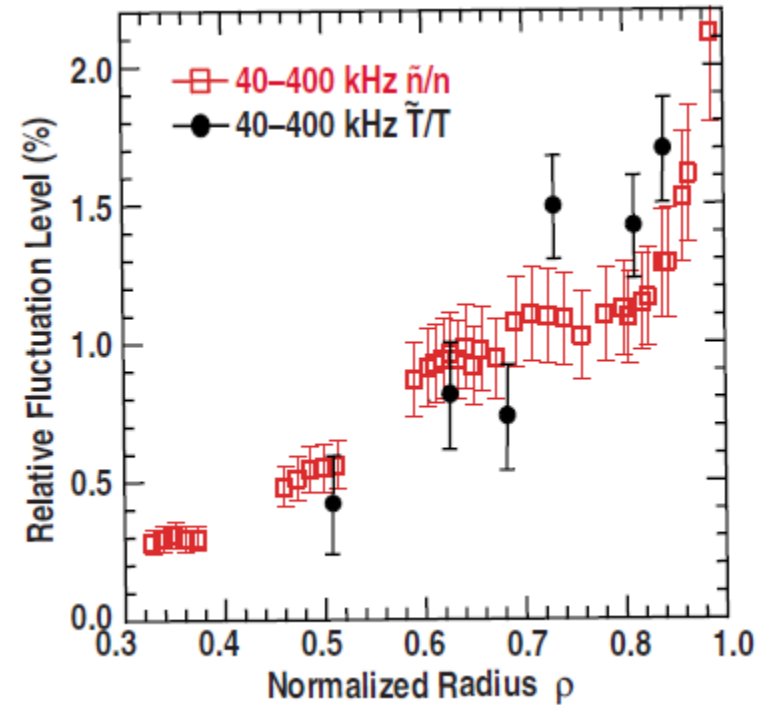
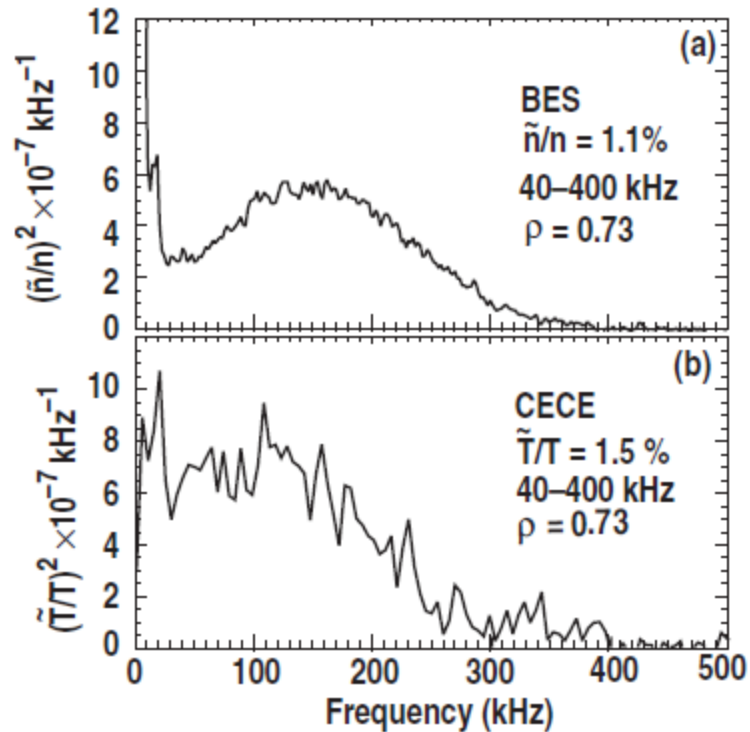
# Multi-field measurement of both electron density and temperature fluctuations at overlapping locations (DIII-D)

- Using electron cyclotron emission (ECE) to measure  $\delta T_e$



DIII-D  
White, PoP (2008)

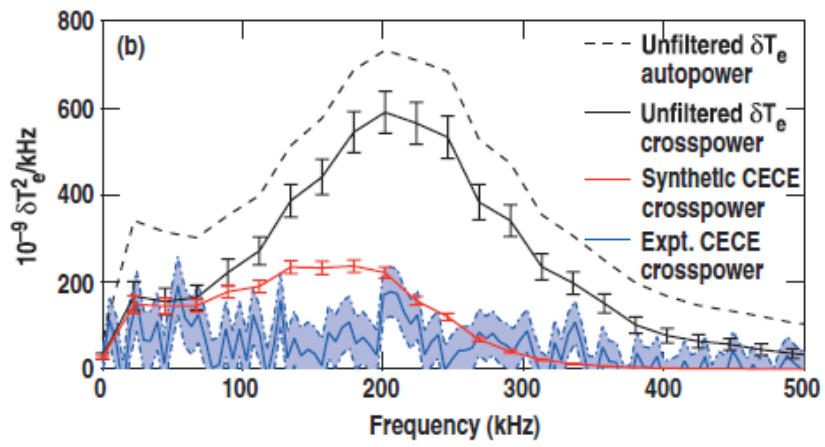
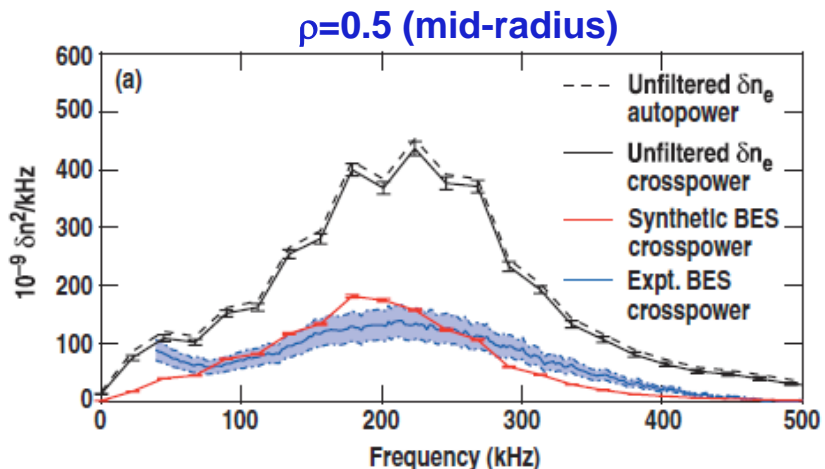
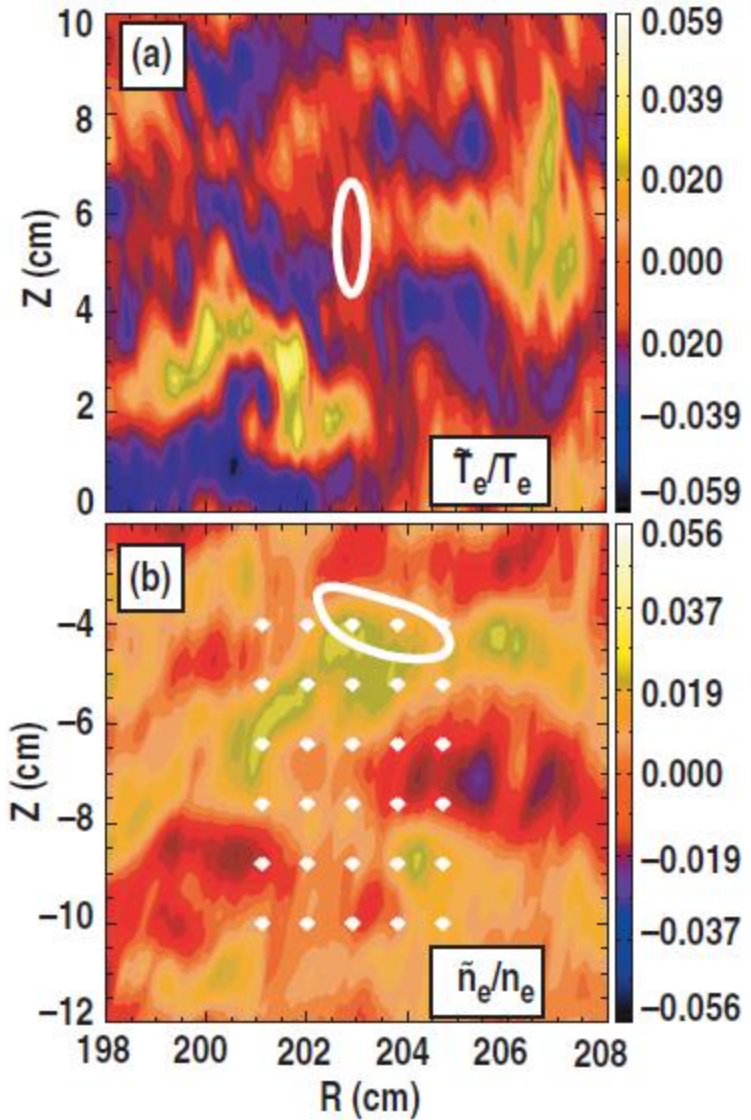
# Normalized density and temperature fluctuations are very similar in amplitude



DIII-D  
White, PoP (2008)

# Comparing $\delta n_e$ , $\delta T_e$ fluctuation spectra with simulations using synthetic diagnostic

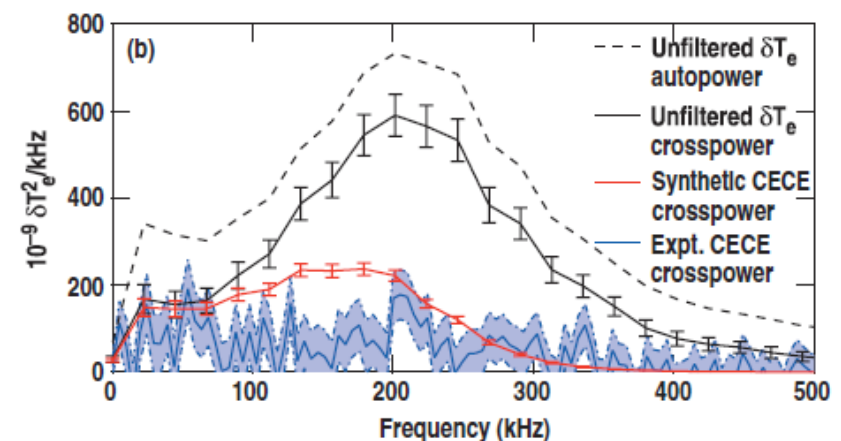
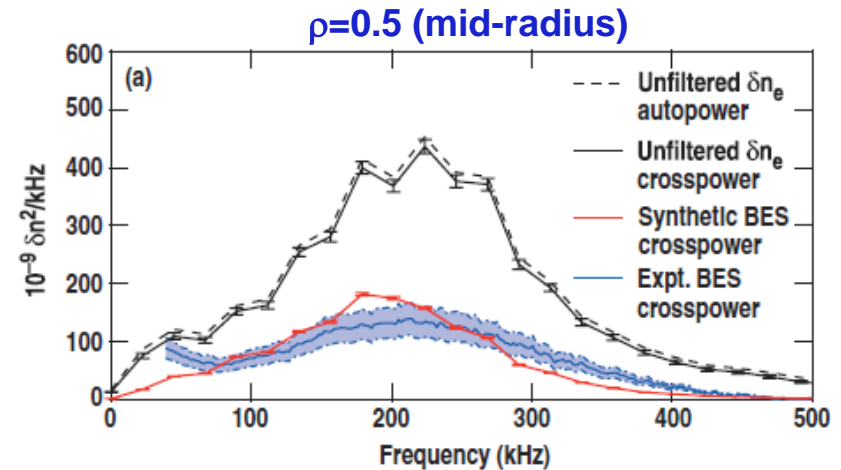
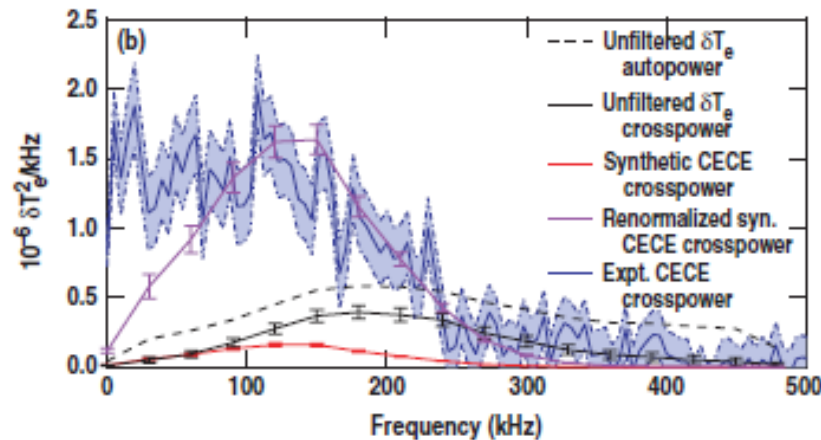
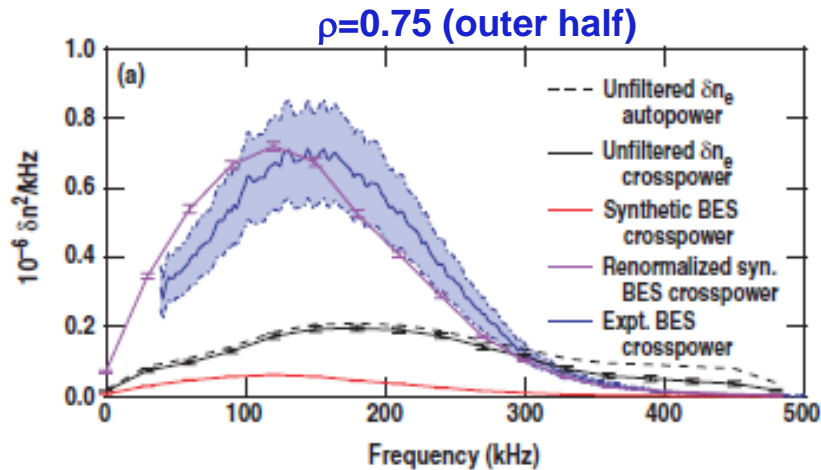
- Level of agreement sensitive to accounting for realistic instrument function





## Agreement worse further out ( $\rho=0.75$ )

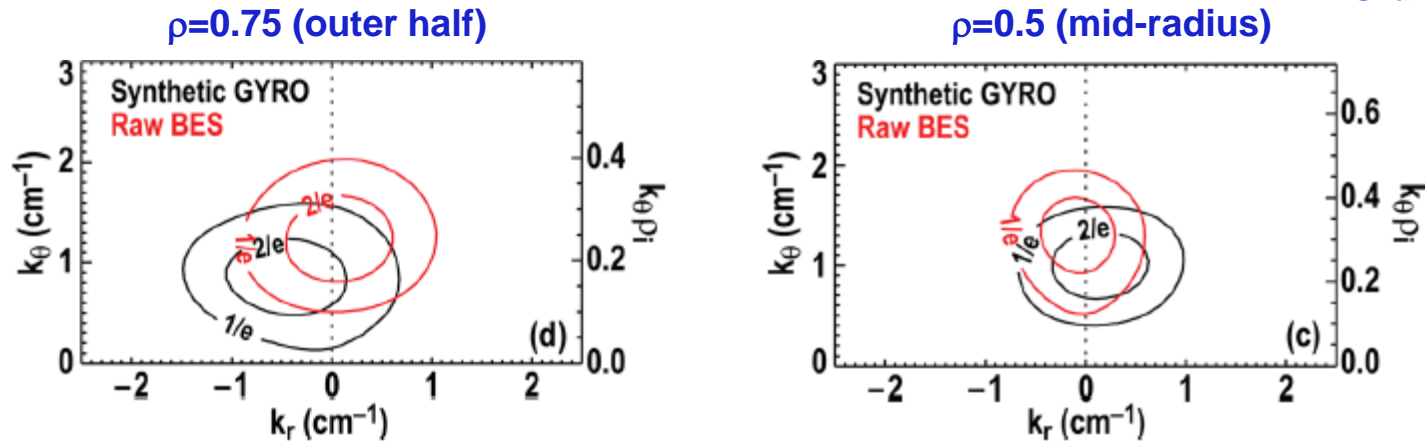
- Measured intensity larger than simulations (as is transport), so called **“edge shortfall”** problem challenging gyrokinetic simulations



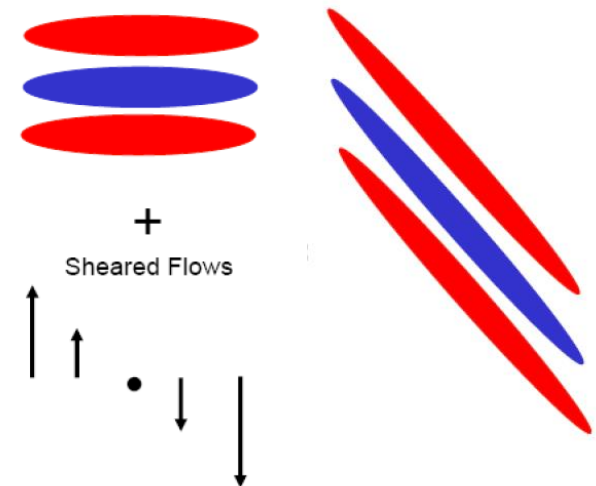
# Can also compare 2D correlation functions for additional validation, try to understand “shortfall” discrepancy

- Comparing 2D correlation/spectra reveals that simulated  $\langle k_r \rangle$  is larger than **experiment** at  $\rho=0.75$

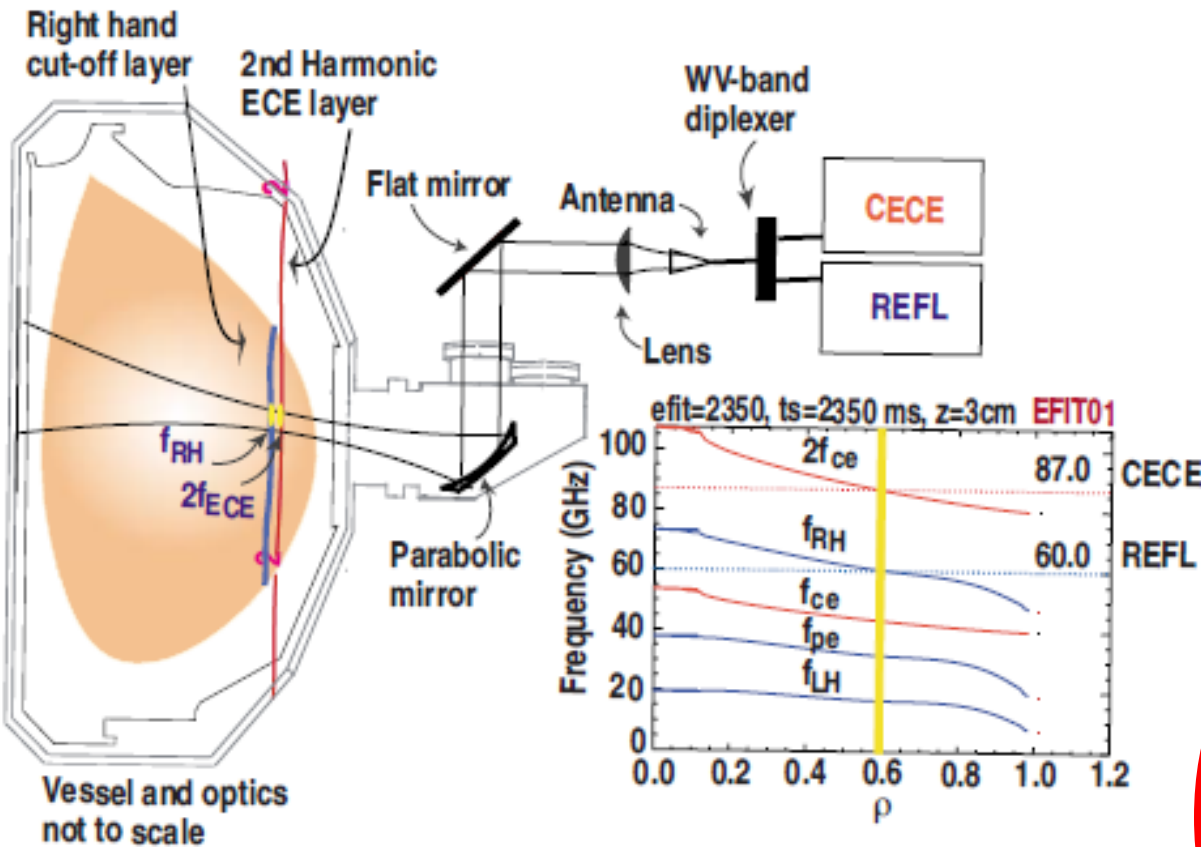
Shafer, PoP (2012)



- Larger  $\langle k_r \rangle$  in simulations possibly from tilting due to sheared equilibrium  $E \times B$  flows being too strongly represented  $\rightarrow$  also consistent with small predicted transport (more later)
- Has sparked a huge international code benchmarking & validation effort

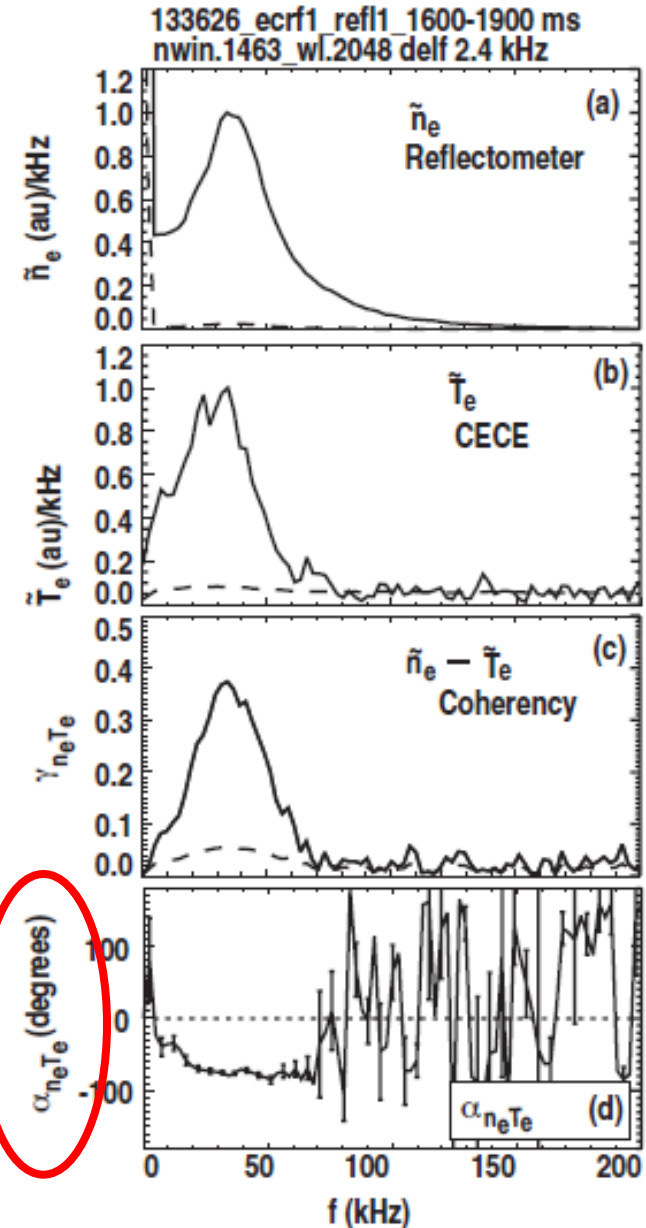


# Simultaneous measurement of $n_e$ and $T_e$ using same beam path allows for cross-phase measurement



$$\gamma_{n_e T_e}(f) = \frac{|\langle S_{\tilde{n}_e}^* S_{\tilde{T}_e} \rangle|}{|\langle S_{\tilde{n}_e} \rangle|^2 |\langle S_{\tilde{T}_e} \rangle|^2}$$

DIII-D  
White, PoP (2010)

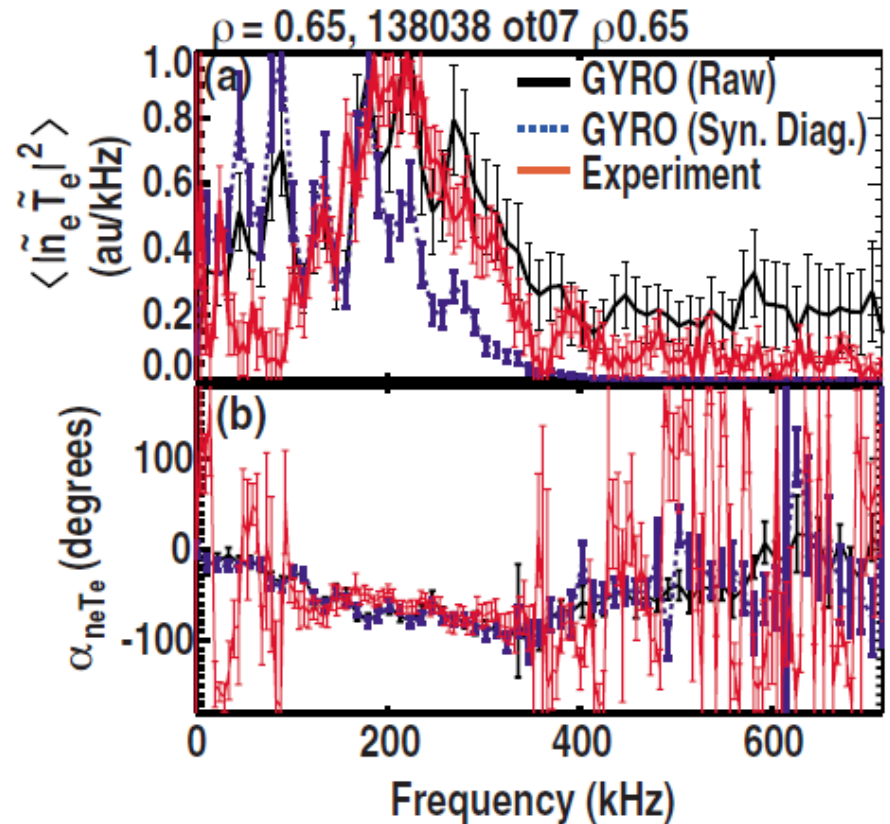


# ne-Te cross phases agree well with simulations

- Amplitude spectra and transport fluxes still off by 2-3

TABLE IV. Postexperiment GYRO simulations from 138 038,  $\rho=0.65$ ,  $t=1525$  ms. Turbulence amplitudes and cross phase are compared with synthetic diagnostic results.

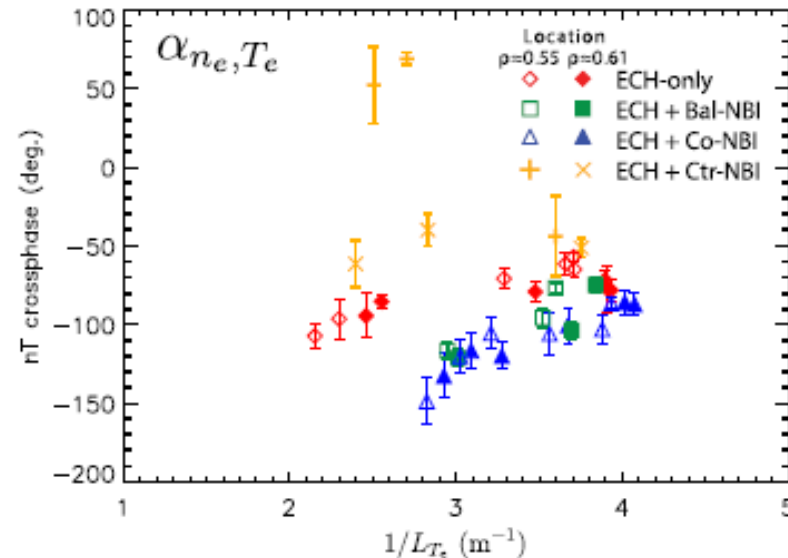
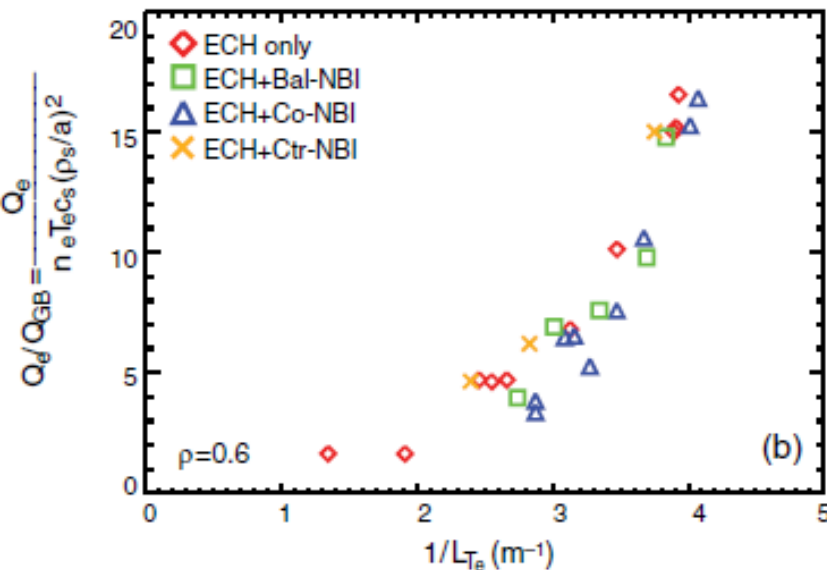
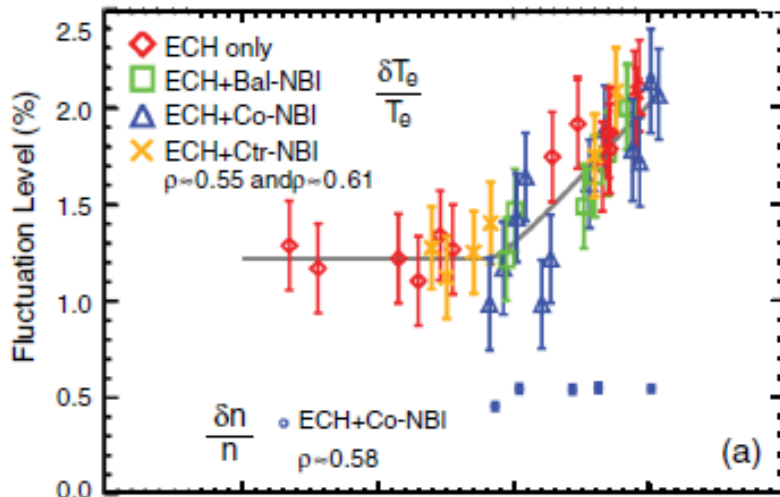
Parameter	GYRO	Experiment
$Q_e$ (MW)	$3.77 \pm 0.06$	$2.43 \pm 0.02$
$Q_i$ (MW)	$0.34 \pm 0.01$	$1.32 \pm 0.02$
$\bar{T}_e/T_e$ (%)	$1.07 \pm 0.10$	$0.95 \pm 0.05$
$\bar{n}/n$ (%)	$0.25 \pm 0.01$	$0.57 \pm 0.06$
$\alpha_{n_e T_e}$ (degrees)	$71 \pm 1$	$61 \pm 12$



# Measured changes of $\delta T_e$ , $n_e$ - $T_e$ crossphase and transport with increasing $\nabla T_e$ provides constraint for simulations

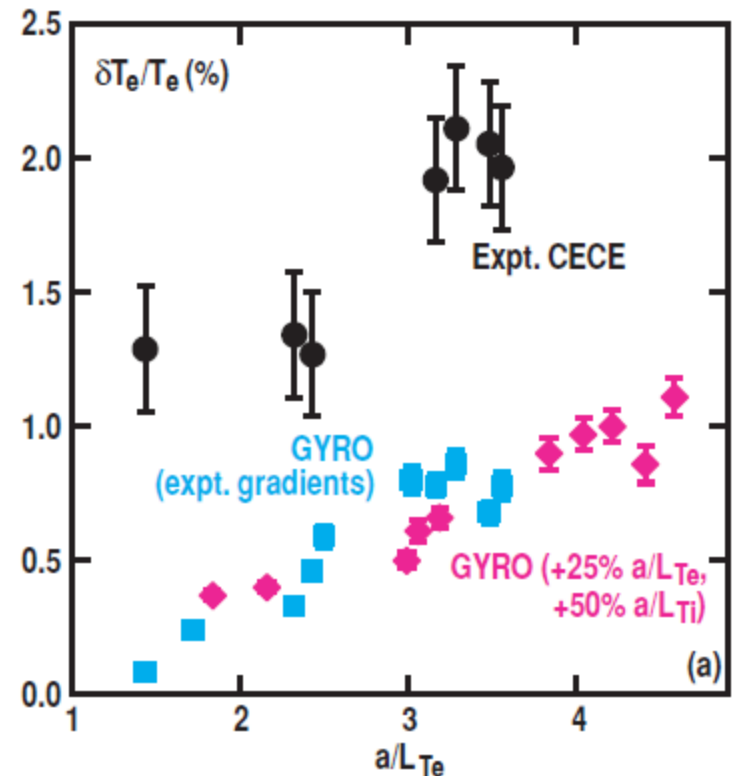
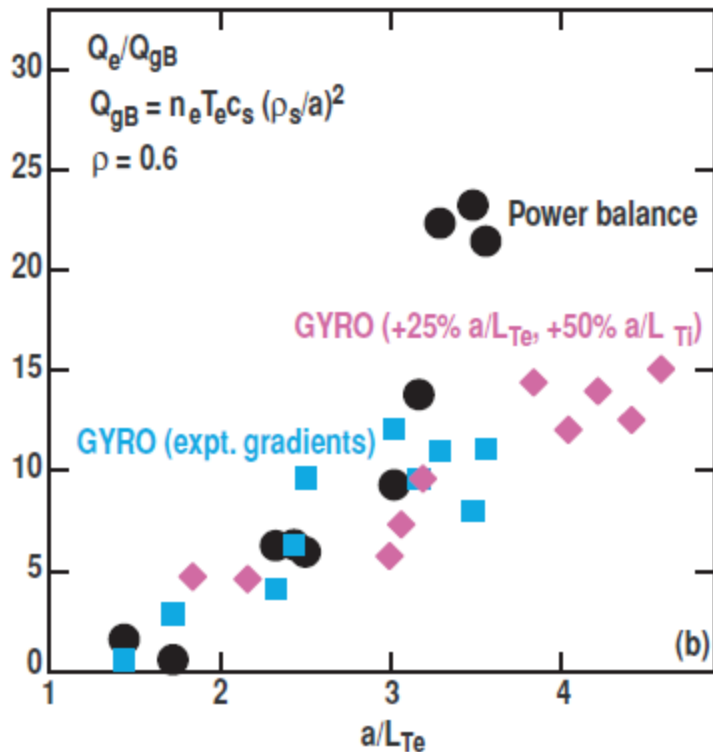
- Increasing fluctuations and transport with  $a/L_{T_e}$  consistent with enhanced TEM turbulence ( $\nabla T_e$  driven TEM)

DIII-D  
Hillesheim, PRL, PoP (2013)



# Simulations can reproduce transport... for some observations

- Predicted turbulence levels always too small, even when accounting for sensitivity to  $\nabla T_e$
- Discrepancies point to missing physics in theory/simulation



Holland, PoP (2013)

# ZONAL FLOWS, GAMs

(important elements of 2D turbulence nonlinear saturation)

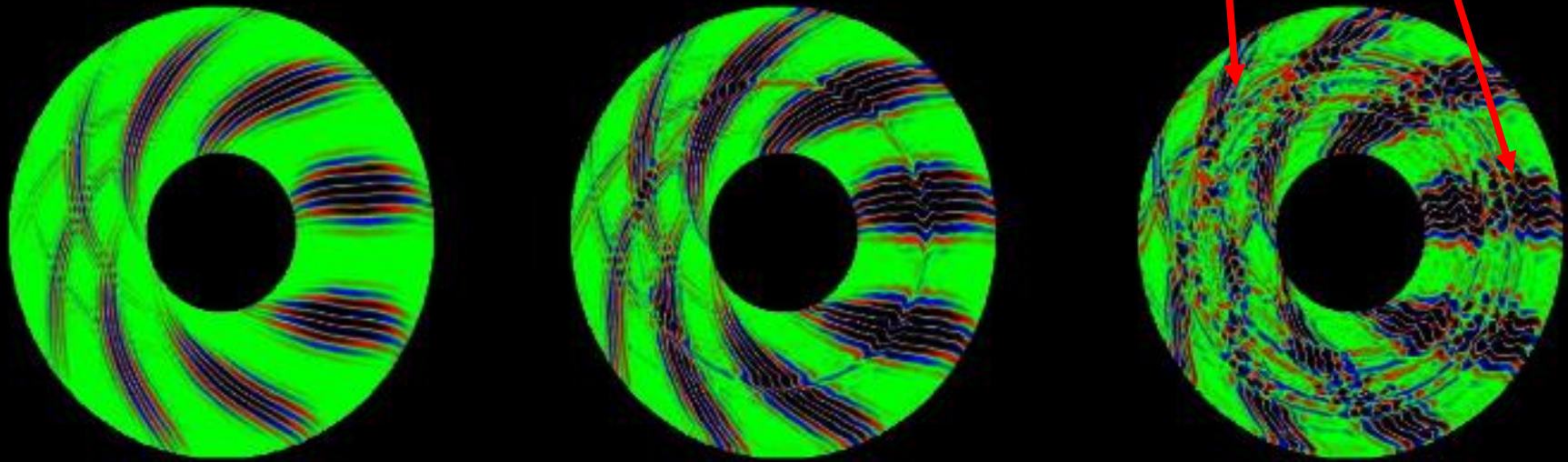
# Nonlinearly-generated “zonal flows” also impact saturation

- Potential perturbations uniform on flux surfaces ( $k_y=0$ )  $\rightarrow$  marginally stable, do not cause transport
- Turbulence can condense to system size  $\rightarrow$  ZF driven largely by non-local (in  $k$ ) NL interactions ( $k \gg k_{ZF}$ )

Linear instability stage demonstrates structure of fastest growing modes

Large flow shear from instability cause perpendicular “zonal flows”

Zonal flows help moderate the turbulence



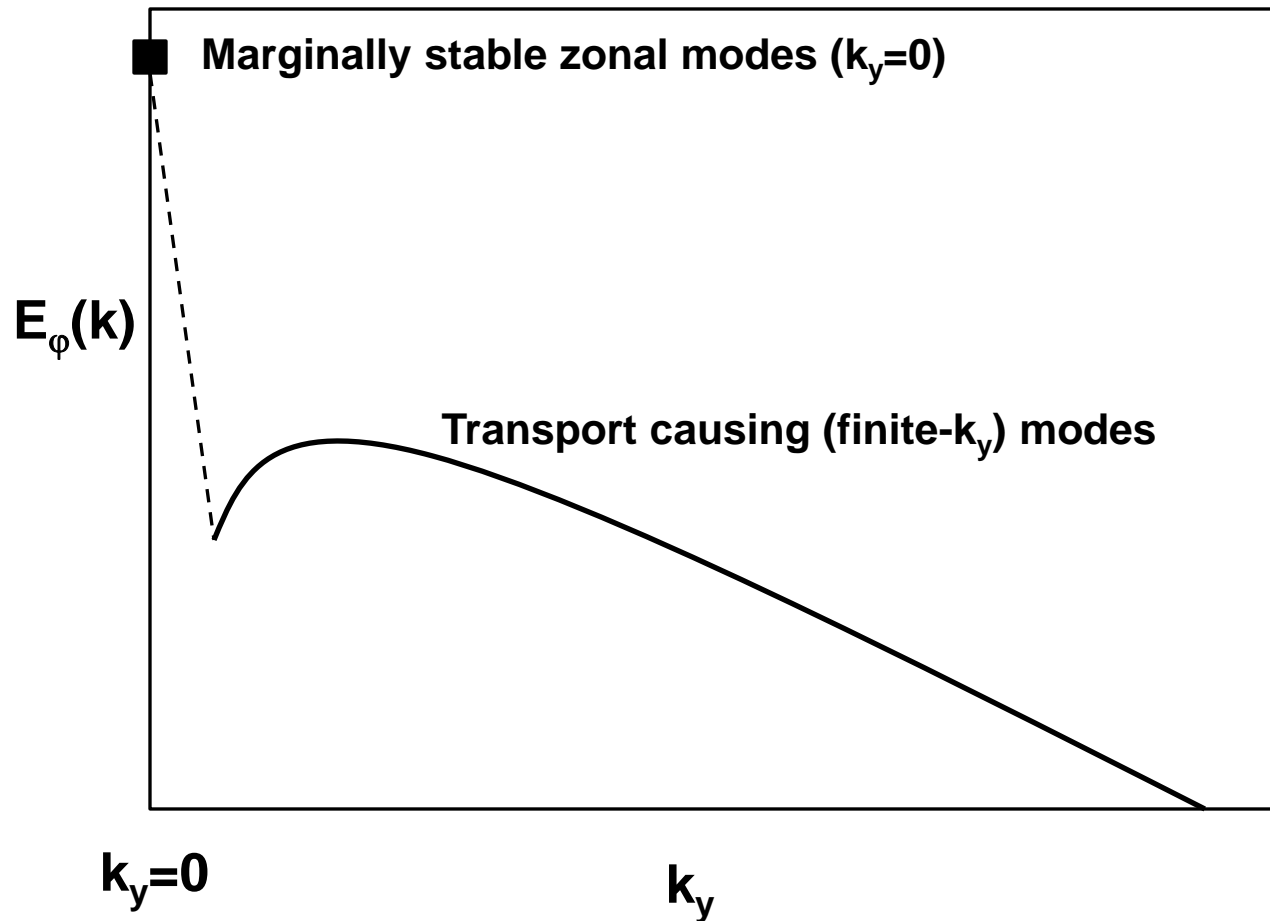
(potential contours  $\rightarrow$  stream functions)

Rayleigh-Taylor like instability driving Kelvin-Helmholtz-like instability



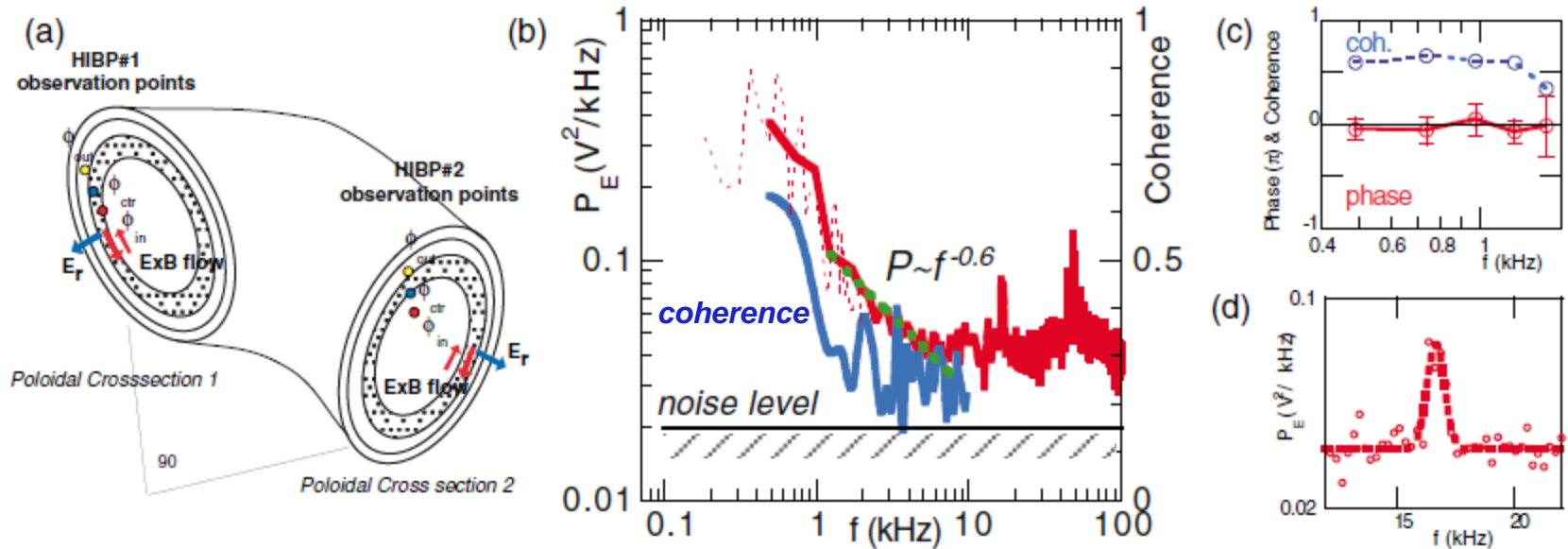
# Zonal flows can saturate at relatively large amplitude for toroidal ITG turbulence

- Regulates saturation via (i) shear decorrelation of eddies, (ii) energy sink into marginal (non-transport-causing) modes
- Typically have distinct  $k_x$  spectra (overall 2D spectra anisotropic in  $k_x, k_y$ )



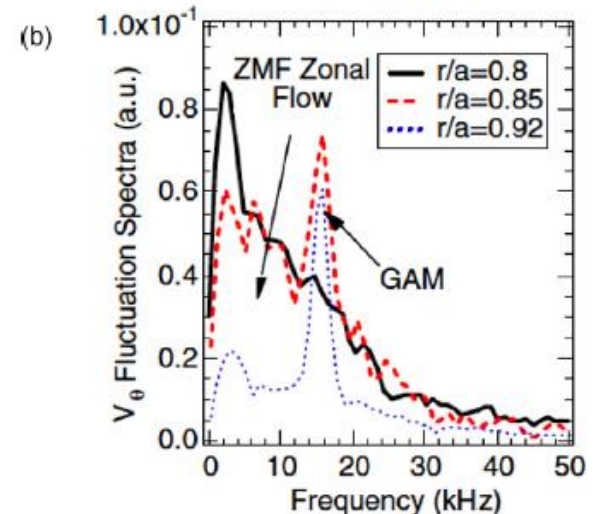
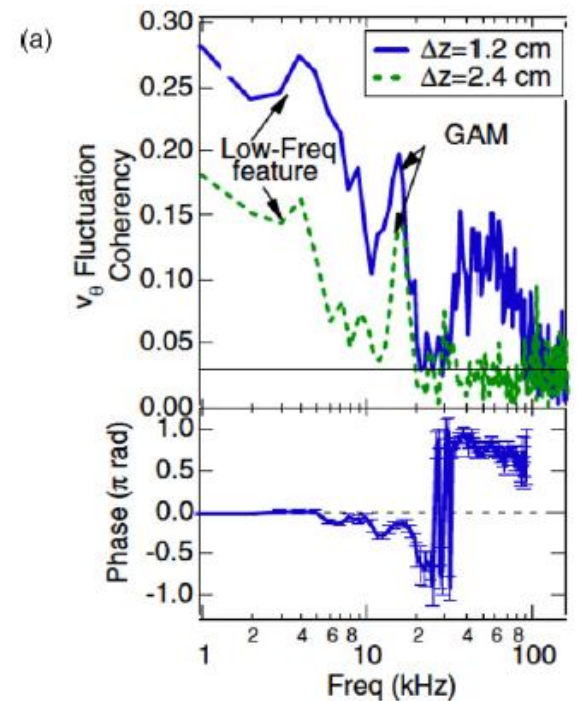
# Evidence of zonal flows from measuring potential on same flux surface at two different toroidal locations

- High coherency at very low frequency with zero phase shift suggests uniform zonal perturbation
- Also evidence of a coherent mode around 17 kHz - geodesic acoustic mode ( $\omega_{\text{GAM}} \approx c_s/R$ ) from associated  $n=0, m=1$  pressure perturbation



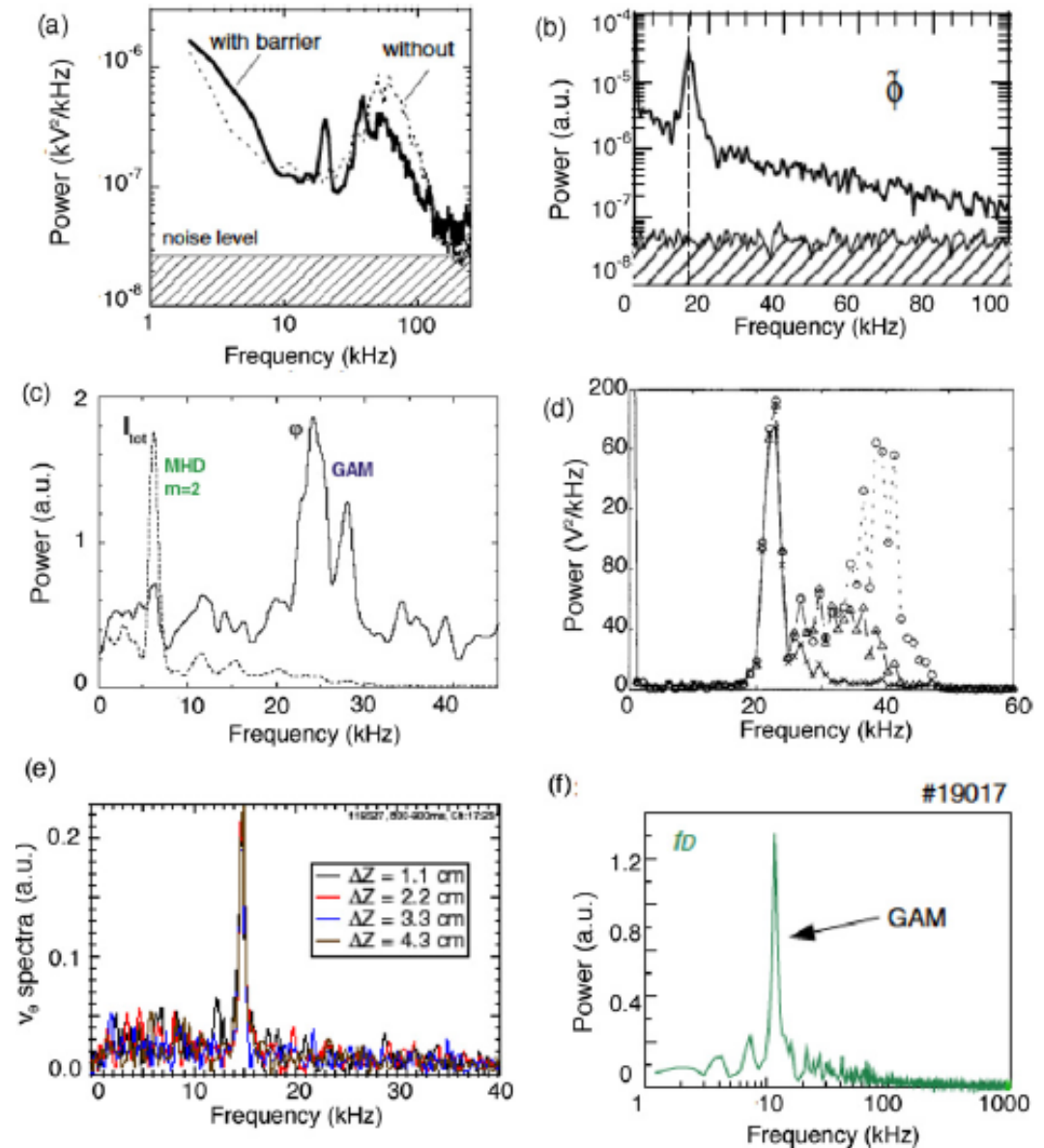
# Also found using poloidal flow measurements from BES on DIII-D

- Poloidal flow determined from time delay estimation of poloidally separated BES channels
- High coherency at low frequency, zero phase shift
- Evidence of GAM oscillation
- Relative strength of each varies with radius



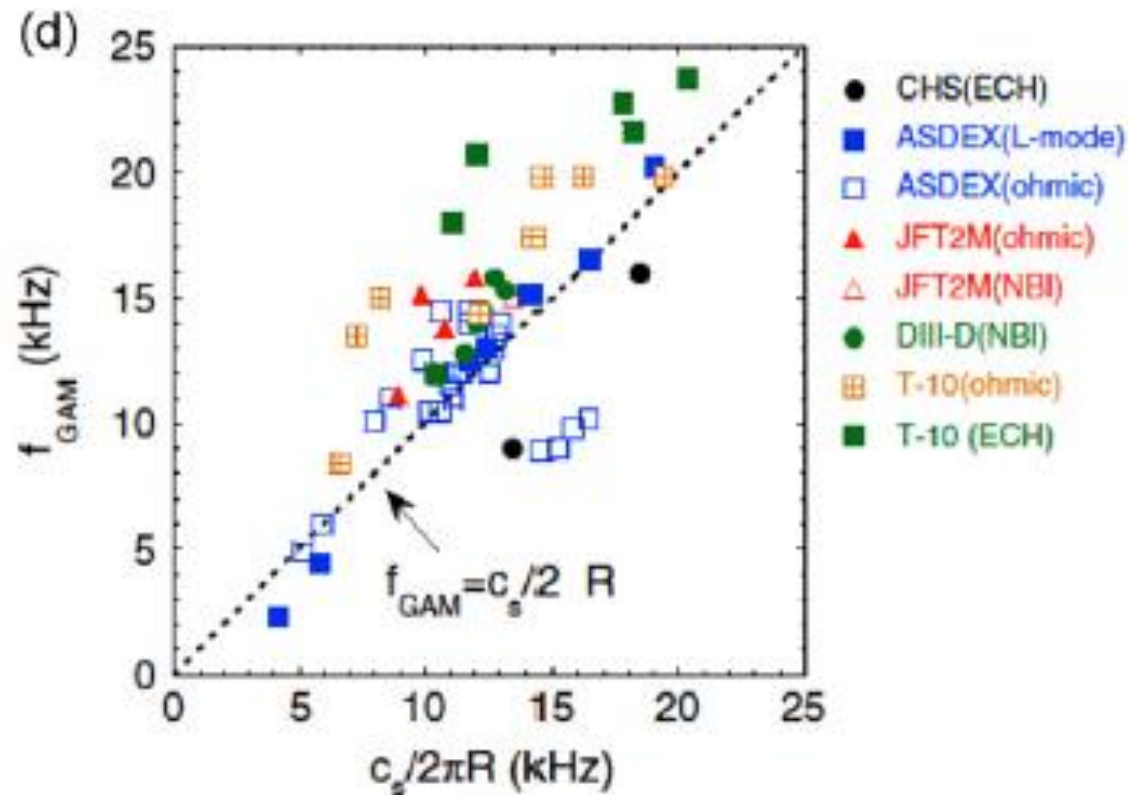
# GAM seen on numerous devices using different measurement techniques

- Seems to be in nearly all machines, if looked for
- See Fig. 11 of Fujisawa, Nuclear Fusion (2009) for legend



# Broad cross-machine agreement of GAM frequency with theory

- Discrepancies have spurred additional theory developments to refine GAM frequency and damping rates (due to geometry, nonlinear effects, ...)



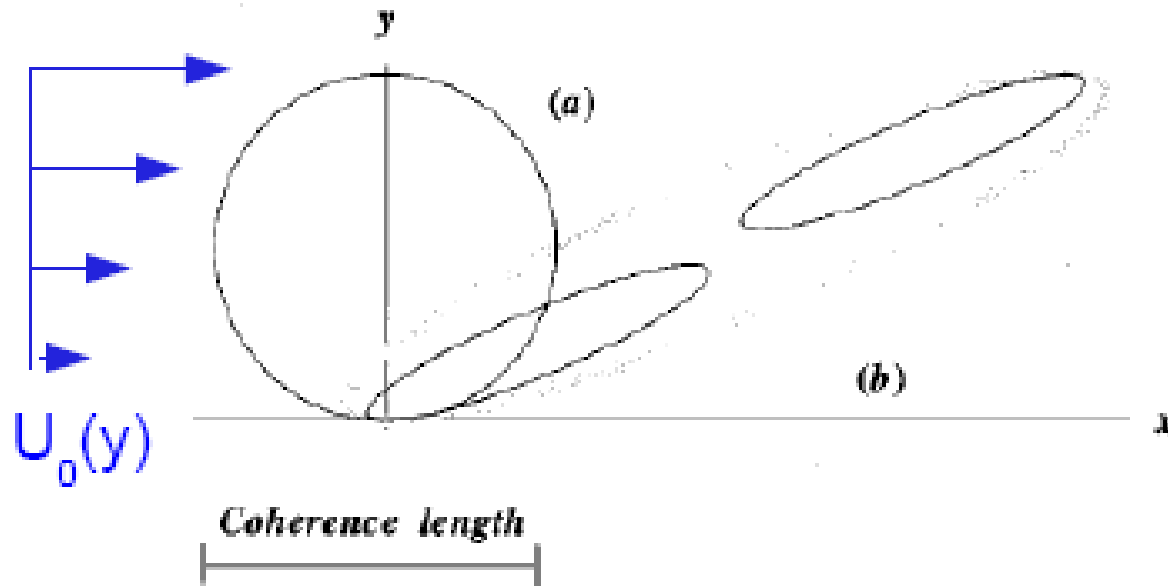
# Suppression of ion scale turbulence in tokamaks

$E \times B$  shear

Reverse magnetic shear

Low aspect ratio + high beta equilibrium

# Equilibrium background ( $E \times B$ ) flows can suppress turbulence



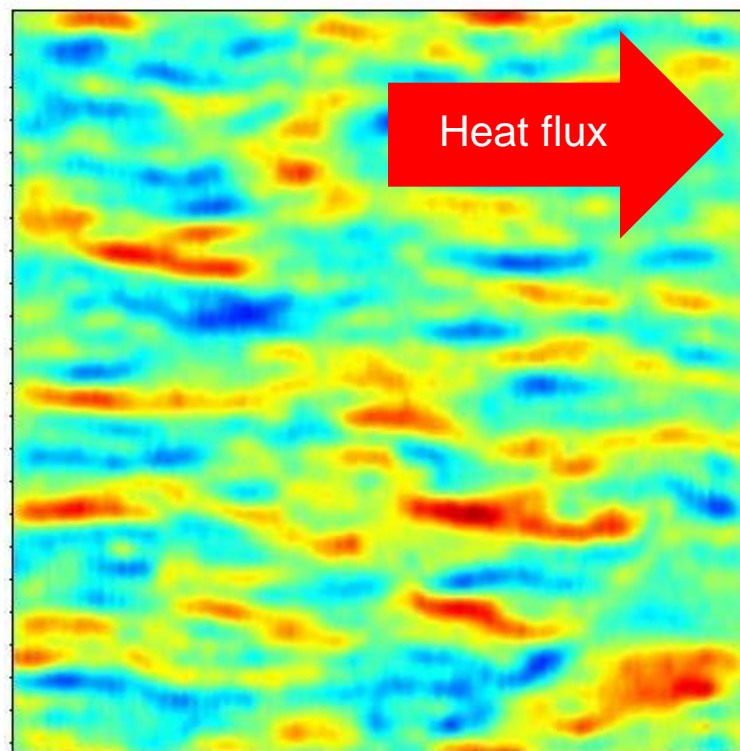
Loosely need:  
 $dU/dy > \tau_c^{-1}$

- Shear flow in neutral (3D) fluids is a source of free-energy, how does it stabilize turbulence in magnetized plasmas?
- Three conditions for sheared flow suppression of turbulence (Terry, RMP 2000):
  - Shear flow should be stable ( $\rightarrow$  Kelvin-Helmholtz threshold different in 2D)
  - Turbulence must reside in region of shear flow for longer than an eddy-turnover time/decorrelation time ( $\rightarrow$  tokamak is a periodic system)
  - Dynamics should be 2D ( $\rightarrow$  strong guide magnetic field)

# Large scale sheared flows can tear apart turbulent eddies, reduce turbulence → improve confinement

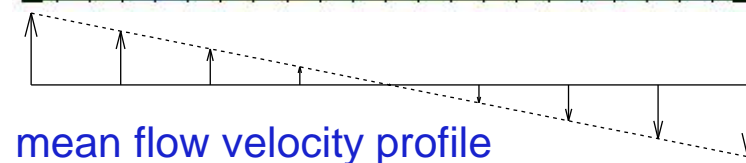
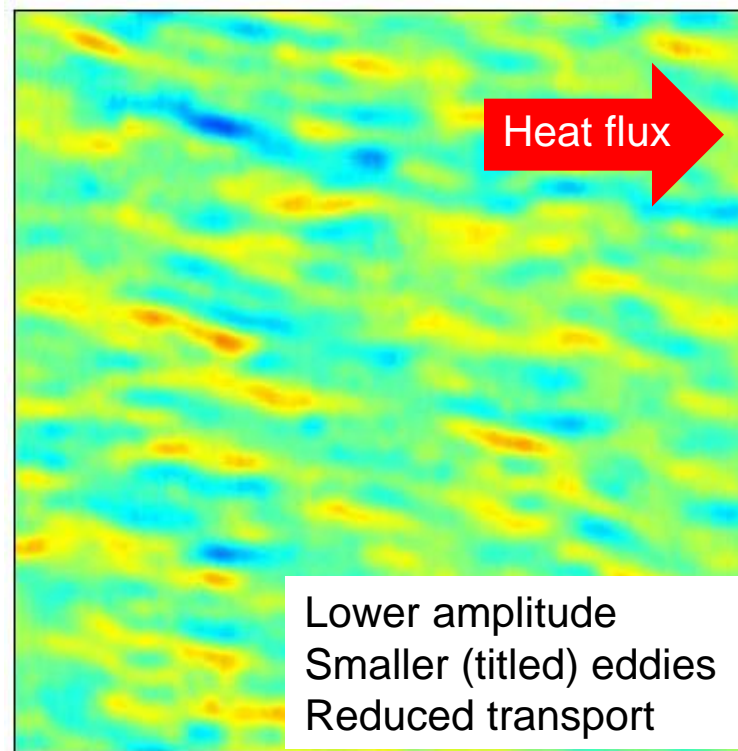
Simulations for NSTX (PPPL) – a low aspect ratio tokamak

Snapshot of density without flow shear



← 100 ion radii  
6,000 electron radii →  
~50 cm

Snapshot of density with flow shear



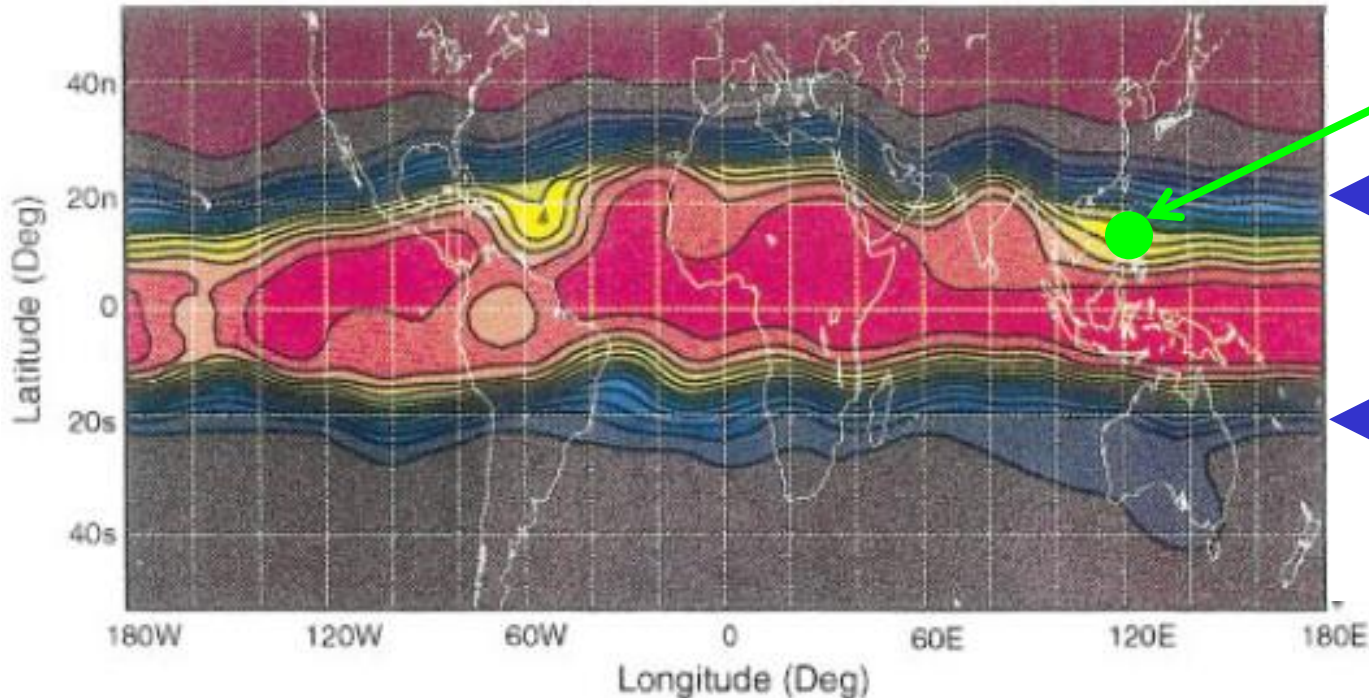


# There are also examples of turbulence suppression via sheared flows in neutral fluids

- Thin (quasi-2D) atmosphere in axisymmetric geometry of rotating planets similar to tokamak plasma turbulence
- Stratospheric ash from Mt. Pinatubo eruption (1991) spread rapidly around equator, **but confined in latitude by flow shear**



Aerosol concentration

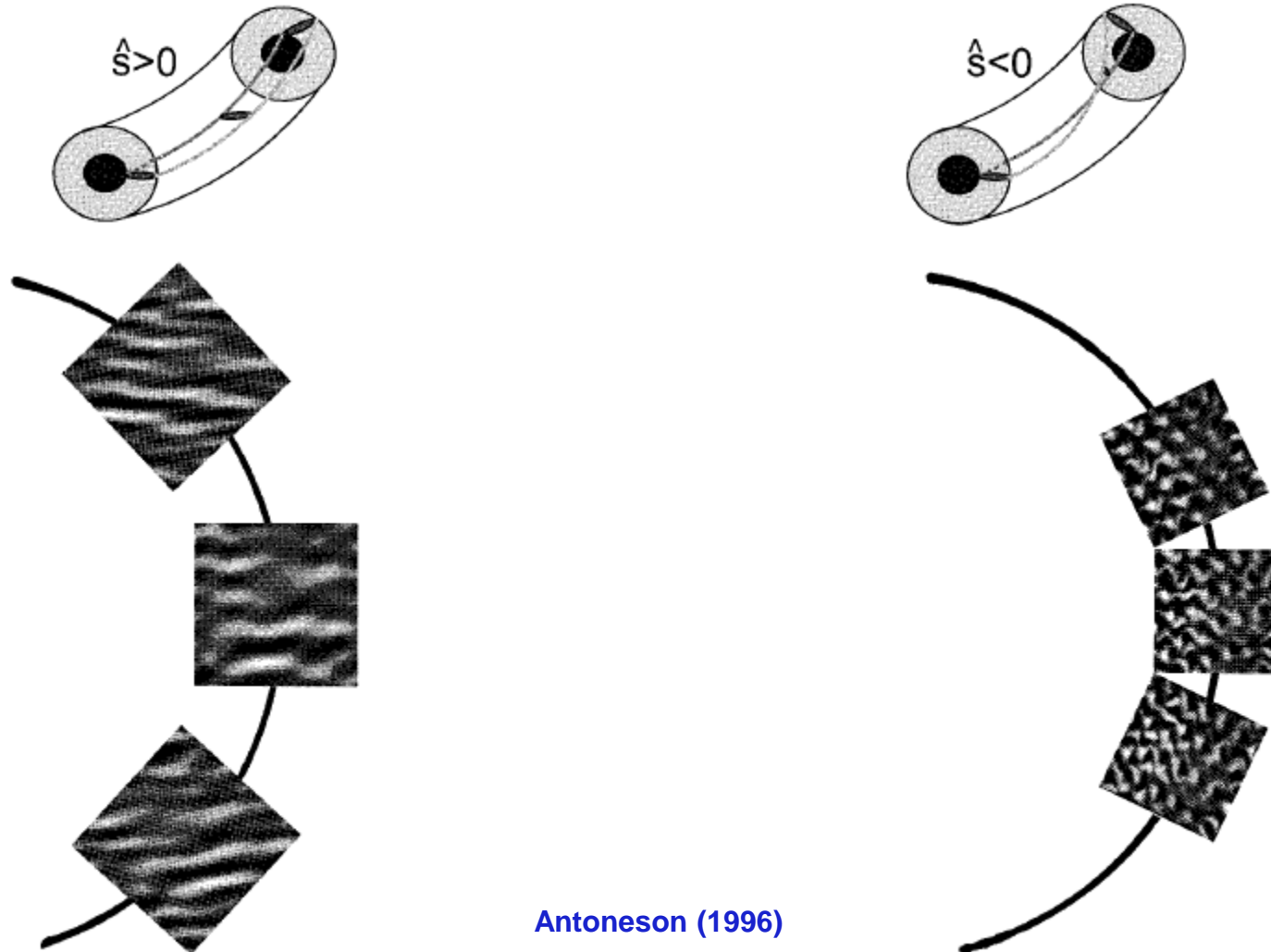


Large shear in stratospheric equatorial jet

(Trepte, 1993;  
P.W. Terry, 2000)

# Negative magnetic shear (rate of change in field line pitch/helicity) can minimize ITG turbulence

- E.g., magnetic shear influences stability by twisting radially-elongated instability to better align (or misalign) with bad curvature drive
- Negative magnetic shear can minimize radial extent, growth and resulting transport

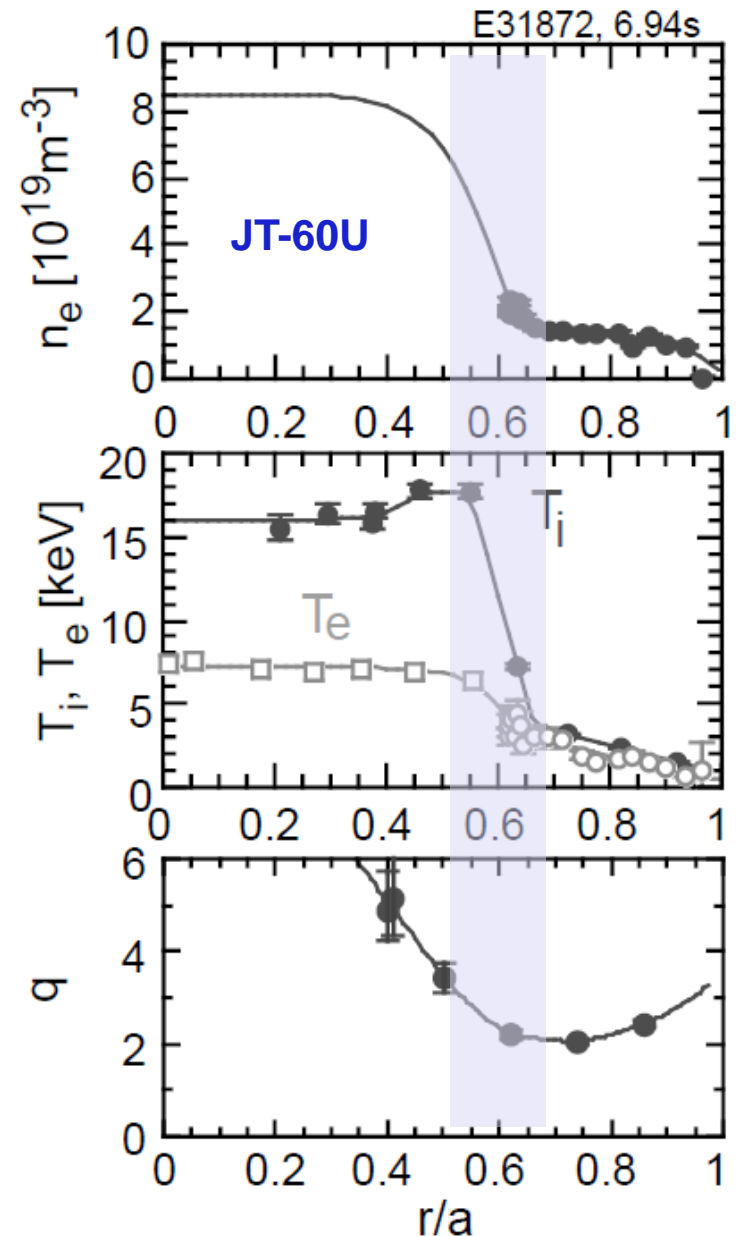


Antoneson (1996)

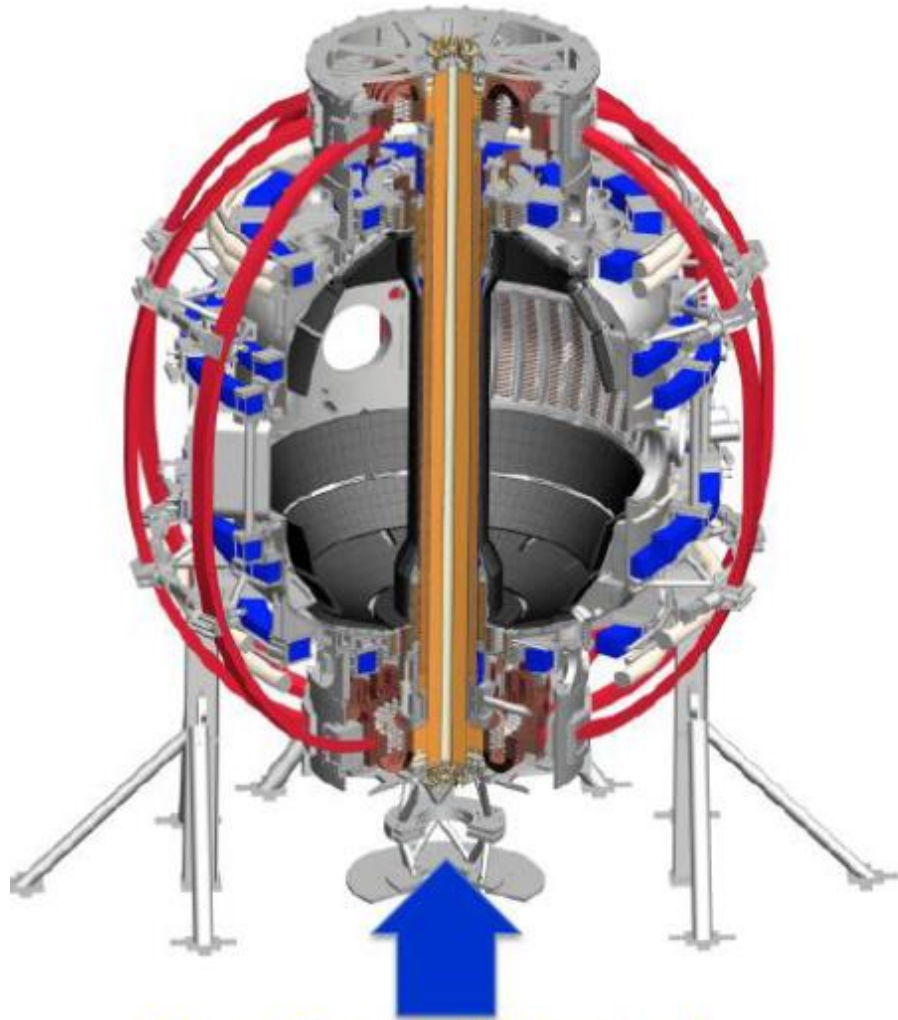
# Reverse magnetic shear can lead to internal transport barriers (ITBs)

- ITBs established on numerous devices
- Used to achieve “equivalent”  $Q_{DT,eq} \sim 1.25$  in JT-60U (in D-D plasma)
- $\chi_i \sim \chi_{i,NC}$  in ITB region  
**(complete suppression of ion scale turbulence)**
  - What sets anomalous electron loss?

*Ishida, NF (1999)*

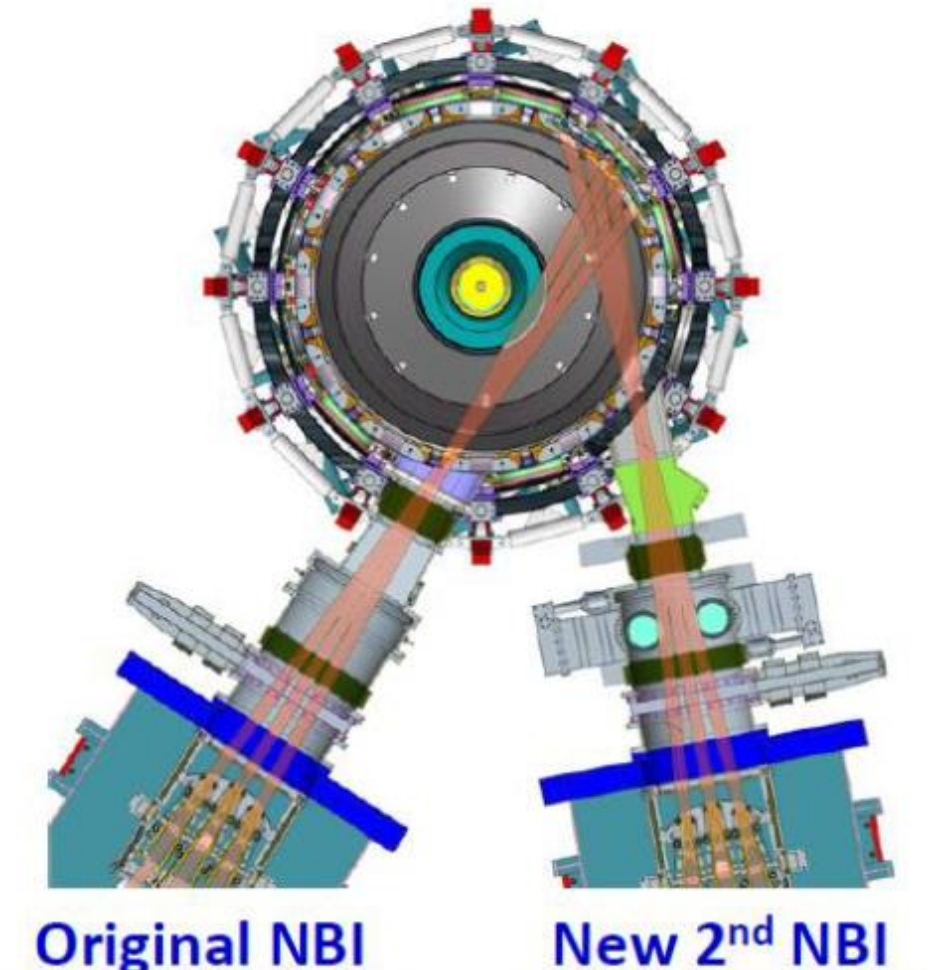


Low aspect ratio “spherical” tokamaks, like NSTX-U at PPPL,  
access very high  $\beta = p/B^2/2\mu_0 \rightarrow$  suppresses ITG



**New Central Magnet**

1 Tesla at plasma center,  $I_p = 2\text{MA}$ , 5s



**Original NBI**

( $R_{\text{TAN}} = 50, 60, 70\text{cm}$ )  
5MW, 5s, 80keV

**New 2<sup>nd</sup> NBI**

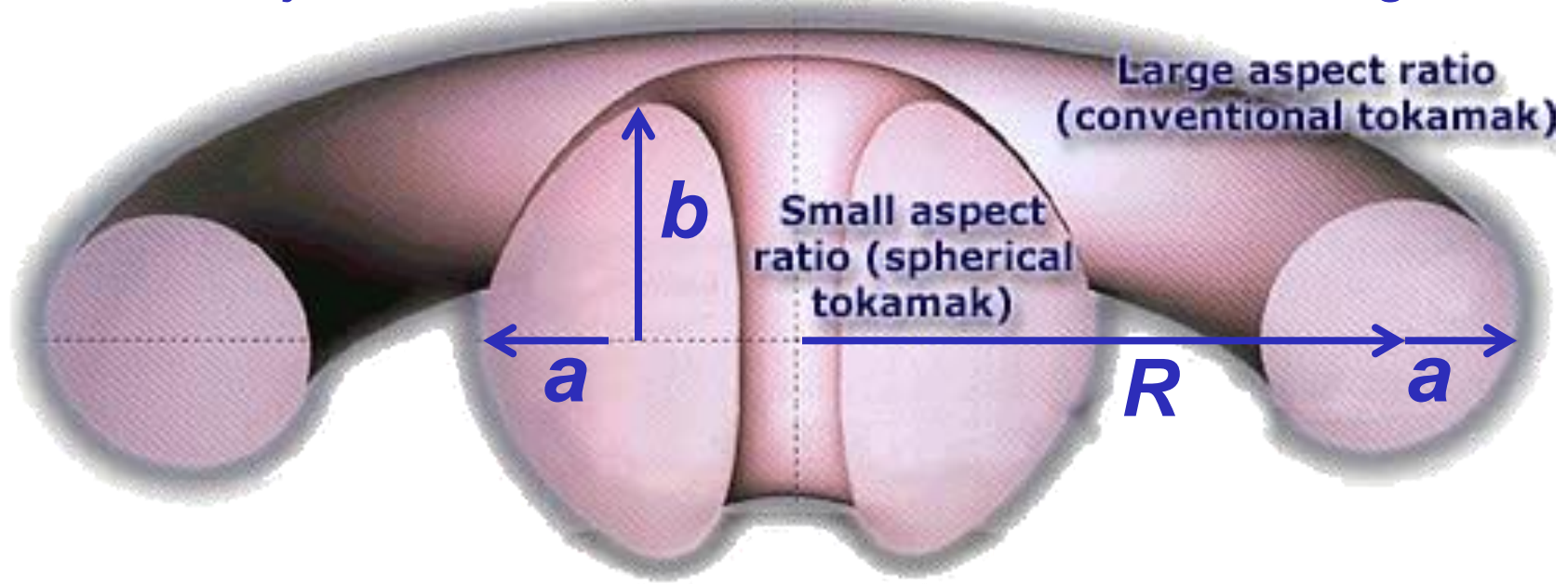
( $R_{\text{TAN}} = 110, 120, 130\text{cm}$ )  
5MW, 5s, 80keV

**Aspect ratio is an important free parameter,  
can try to make smaller reactors (i.e. cheaper)**

**Aspect ratio  $A = R / a$**

**Elongation  $\kappa = b / a$**

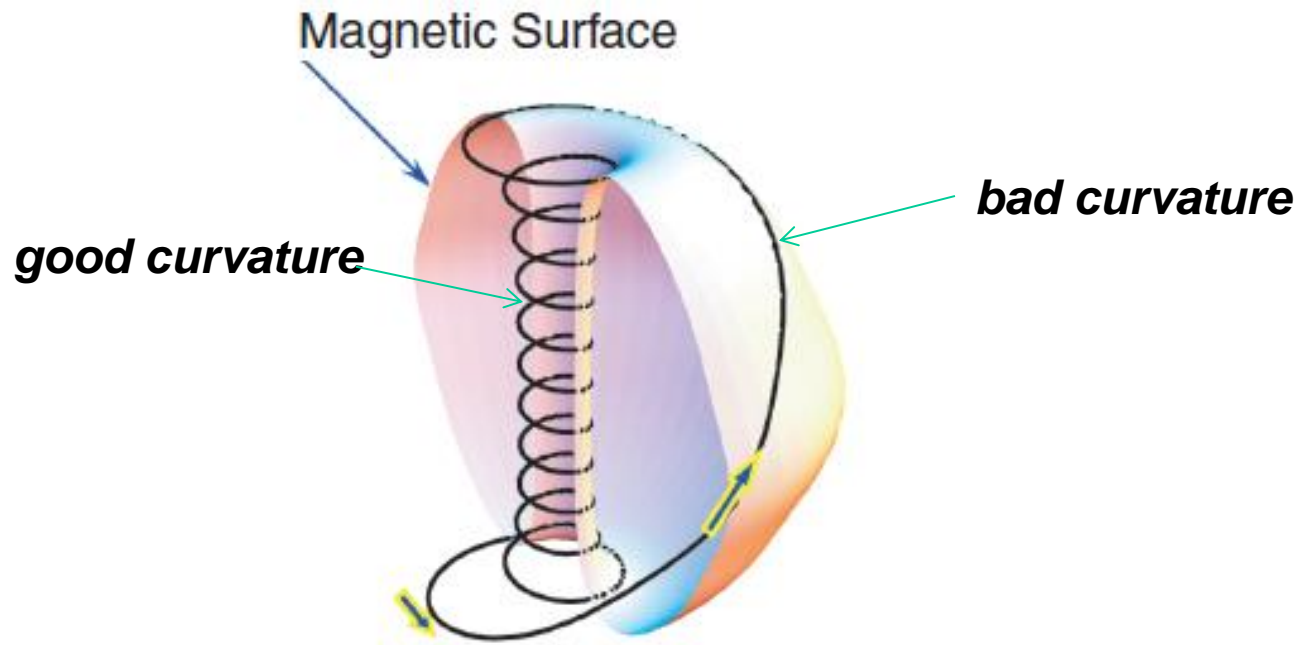
**$R =$  major radius,  $a =$  minor radius,  $b =$  vertical  $\frac{1}{2}$  height**



**But smaller  $R =$  larger curvature,  $\nabla B (\sim 1/R)$  -- isn't this terrible for "bad curvature" driven instabilities?!?!?**

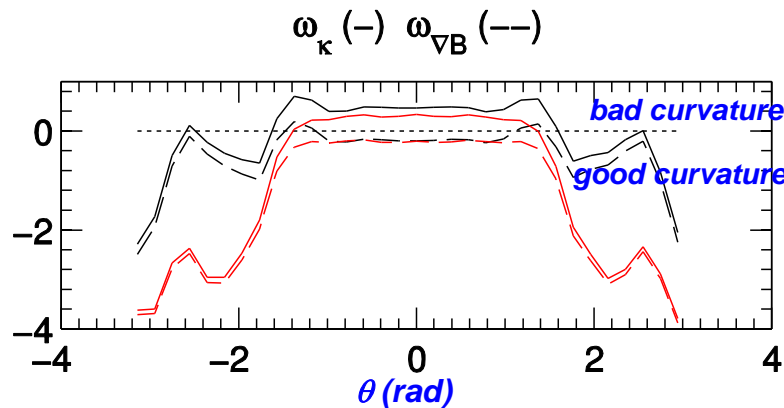
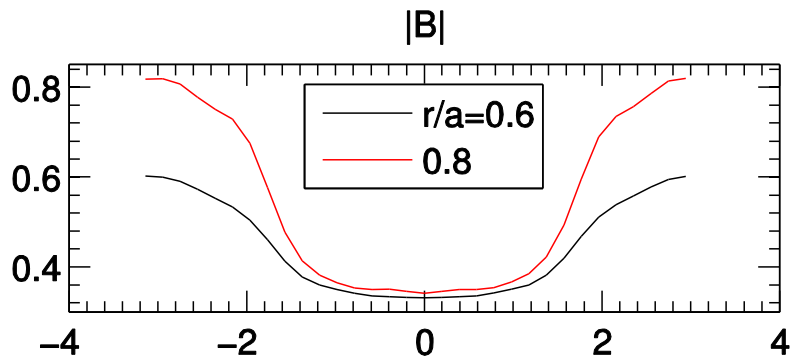
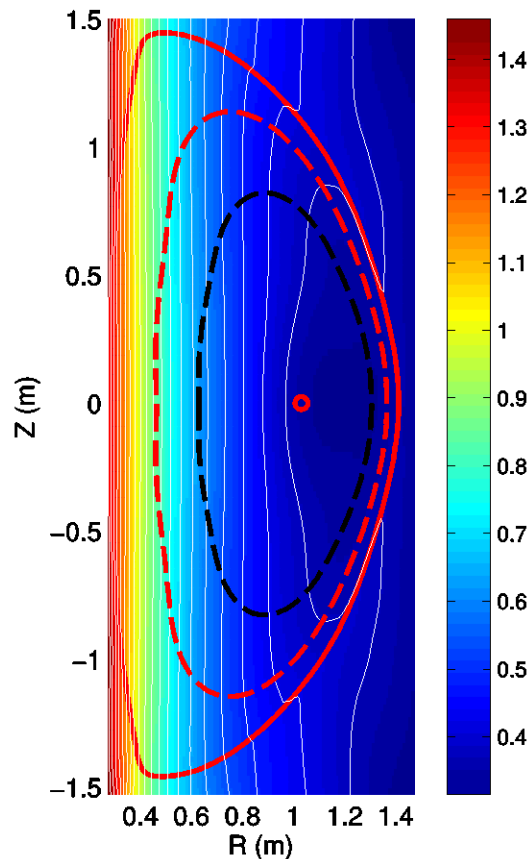
# Many elements of ST are stabilizing to toroidal, electrostatic ITG/TEM drift waves

- Short connection length → **smaller average bad curvature**



# Many elements of ST are stabilizing to toroidal, electrostatic ITG/TEM drift waves

- Short connection length → **smaller average bad curvature**
- Quasi-isodynamic ( $\sim$ constant B) at high  $\beta$  → **grad-B drifts stabilizing [Peng & Strickler, NF 1986]**

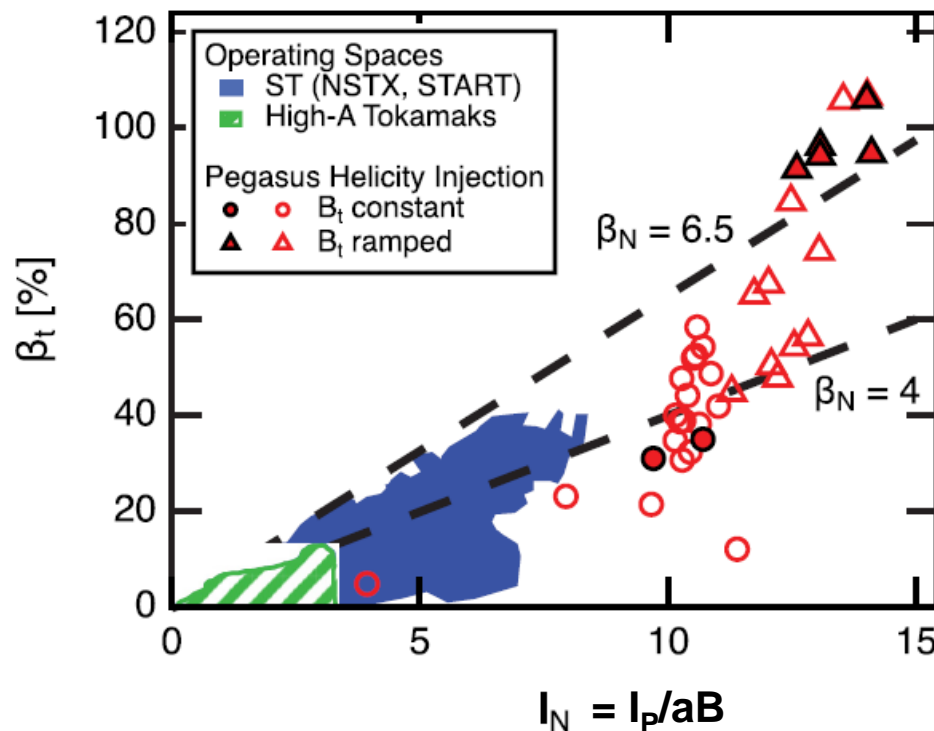


$$\vec{v}_\kappa = mv_\parallel^2 \frac{\hat{b} \times \vec{\kappa}}{qB}$$

$$\vec{v}_{\nabla B} = \frac{mv_\perp^2}{2} \frac{\hat{b} \times \nabla B/B}{qB}$$

# Many elements of ST are stabilizing to toroidal, electrostatic ITG/TEM drift waves

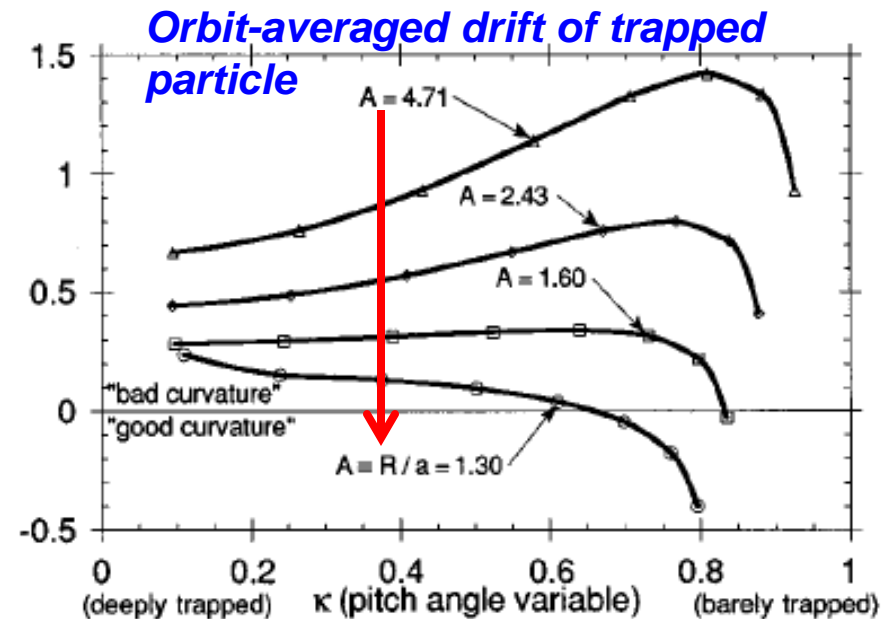
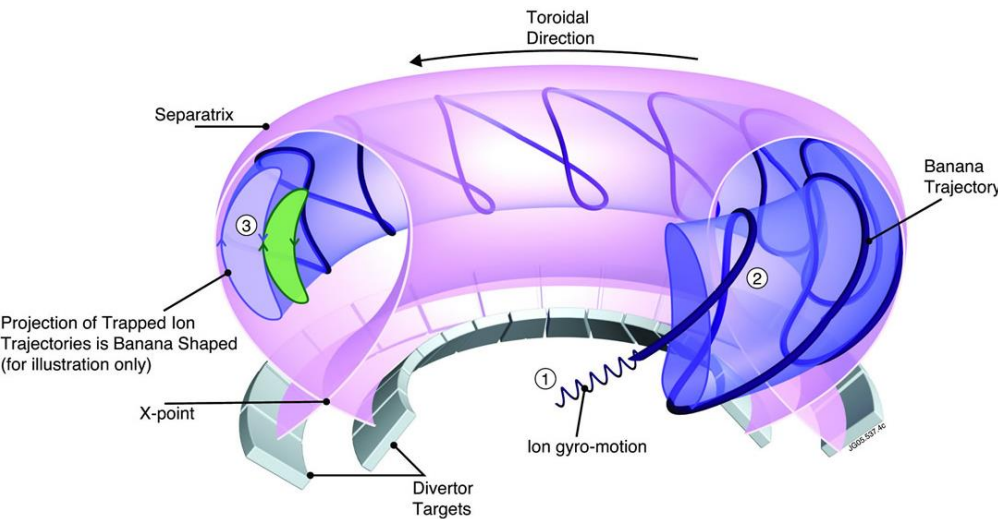
- Short connection length → **smaller average bad curvature**
- Quasi-isodynamic ( $\sim$ constant B) at high  $\beta$  → **grad-B drifts stabilizing [Peng & Strickler, NF 1986]**
- **These same features stabilize macroinstabilities (MHD), allowing for very high  $\beta$  equilibrium:  $\sim$ 40% on NSTX,  $\sim$ 100% on Pegasus (U-Wisc)**





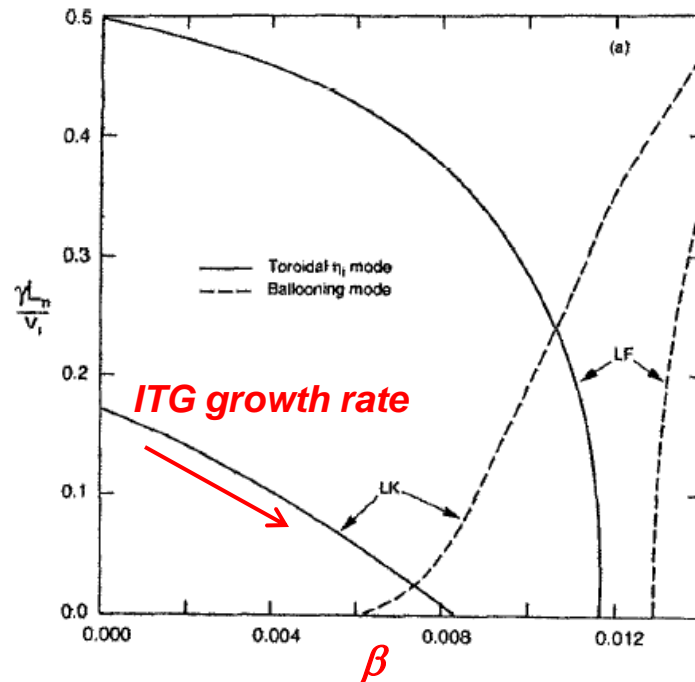
# Many elements of ST are stabilizing to toroidal, electrostatic ITG/TEM drift waves

- Short connection length → **smaller average bad curvature**
- Quasi-isodynamic ( $\sim$ constant B) at high  $\beta$  → **grad-B drifts stabilizing [Peng & Strickler, NF 1986]**
- Large fraction of trapped electrons, BUT precession weaker at low A → **reduced TEM drive [Rewoldt, Phys. Plasmas 1996]**



# Many elements of ST are stabilizing to toroidal, electrostatic ITG/TEM drift waves

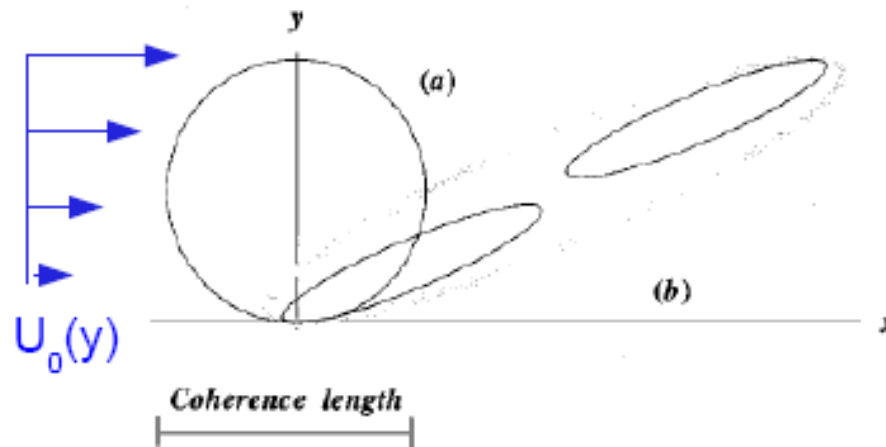
- Short connection length → **smaller average bad curvature**
- Quasi-isodynamic ( $\sim$ constant B) at high  $\beta$  → **grad-B drifts stabilizing [Peng & Strickler, NF 1986]**
- Large fraction of trapped electrons, BUT precession weaker at low A → **reduced TEM drive [Rewoldt, Phys. Plasmas 1996]**
- Strong coupling to  $\delta B_{\perp} \sim \delta A_{\parallel}$  at high  $\beta$  → **stabilizing to ES-ITG**



Kim, Horton, Dong, PoFB (1993)

# Many elements of ST are stabilizing to toroidal, electrostatic ITG/TEM drift waves

- Short connection length → **smaller average bad curvature**
- Quasi-isodynamic ( $\sim$ constant B) at high  $\beta$  → **grad-B drifts stabilizing [Peng & Strickler, NF 1986]**
- Large fraction of trapped electrons, BUT precession weaker at low A → **reduced TEM drive [Rewoldt, Phys. Plasmas 1996]**
- Strong coupling to  $\delta B_{\perp} \sim \delta A_{\parallel}$  at high  $\beta$  → **stabilizing to ES-ITG**
- Small inertia ( $nmR^2$ ) with uni-directional NBI heating gives strong toroidal flow & flow shear →  **$E \times B$  shear stabilization ( $dv_{\perp}/dr$ )**



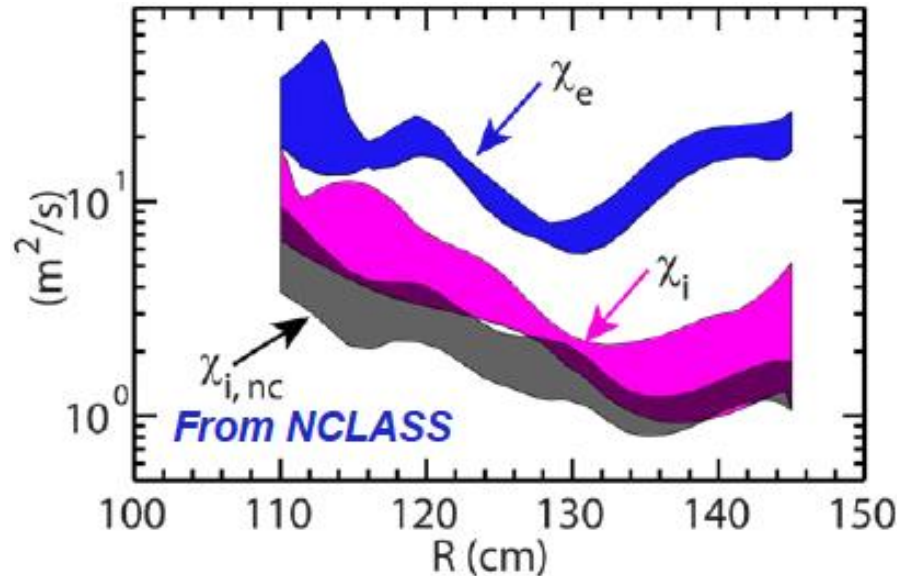
*Biglari, Diamond, Terry, PoFB  
(1990)*

# Many elements of ST are stabilizing to toroidal, electrostatic ITG/TEM drift waves

- Short connection length → **smaller average bad curvature**
  - Quasi-isodynamic ( $\sim$ constant B) at high  $\beta$  → **grad-B drifts stabilizing [Peng & Strickler, NF 1986]**
  - Large fraction of trapped electrons, BUT precession weaker at low A → **reduced TEM drive [Rewoldt, Phys. Plasmas 1996]**
  - Strong coupling to  $\delta B_{\perp} \sim \delta A_{\parallel}$  at high  $\beta$  → **stabilizing to ES-ITG**
  - Small inertia ( $nmR^2$ ) with uni-directional NBI heating gives strong toroidal flow & flow shear →  **$E \times B$  shear stabilization ( $dv_{\perp}/dr$ )**
- ⇒ **Not expecting strong ES ITG/TEM instability (much higher thresholds)**

- BUT High beta drives EM instabilities:
  - **microtearing modes (MTM)**  $\sim \beta_e \cdot \nabla T_e$
  - **kinetic ballooning modes/energetic particle modes (KBM/EPM)**  $\sim \alpha_{\text{MHD}} \sim q^2 \nabla P / B^2$  &  $\nabla P_{\text{fast}}$
- Large shear in parallel velocity can drive **Kelvin-Helmholtz-like instability**  $\sim dv_{\parallel}/dr$

# Ion thermal transport in ST H-modes (higher beta) usually very close to collisional (neoclassical) transport theory



- Consistent with ITG/TEM stabilization by equilibrium configuration & strong  $E \times B$  flow shear
  - Impurity transport (intrinsic carbon, injected Ne, ...) also usually well described by neoclassical theory [Delgado-Aparicio, NF 2009 & 2011 ; Scotti, NF 2013]
- **Electron energy transport always anomalous**
  - Toroidal angular momentum transport also anomalous (Kaye, NF 2009)

# Beyond ITG/TEM turbulence

# Electron scale (ETG) turbulence

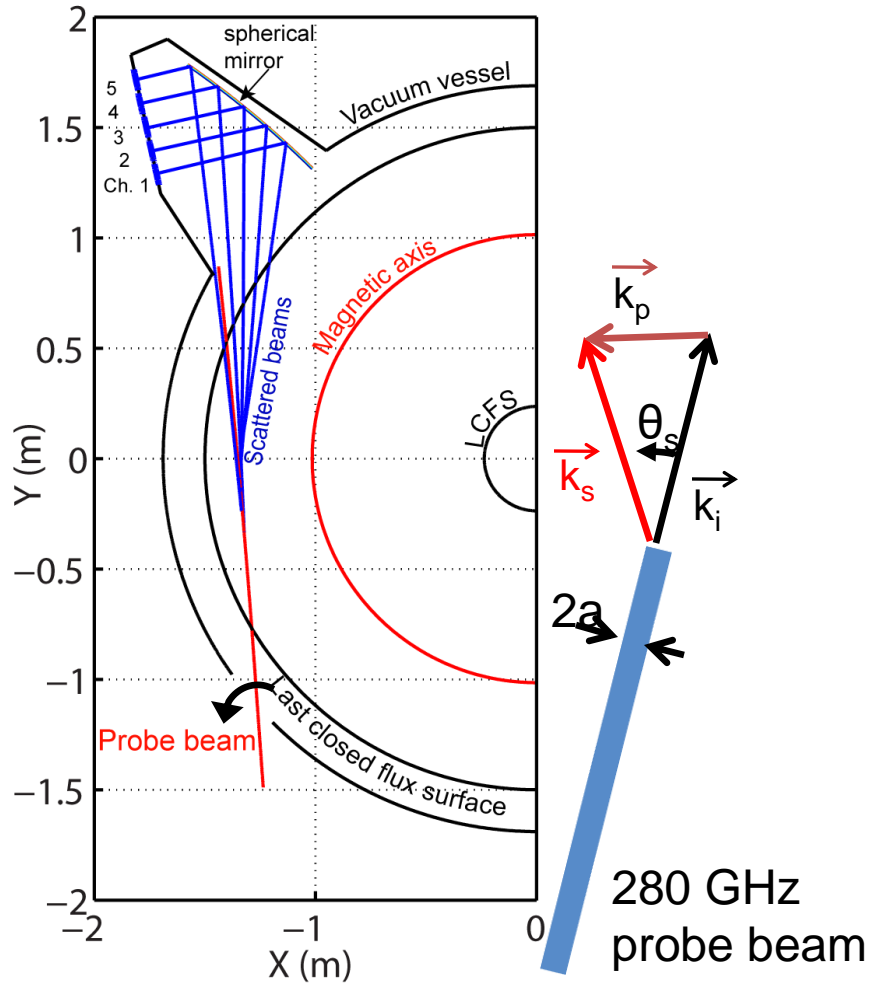
ETG is “isomorphic” to ITG:

replace  $m_i \rightarrow m_e$ ,  $T_i \rightarrow T_e$  ( $\rho_i \rightarrow \rho_e$ ,  $v_{Ti} \rightarrow v_{Te}$ )

$\gamma_{ITG} / (v_{Ti}/L_{Ti})$  vs  $k_{\theta}\rho_i \rightarrow \gamma_{ETG} / (v_{Te}/L_{Te})$  vs  $k_{\theta}\rho_e$

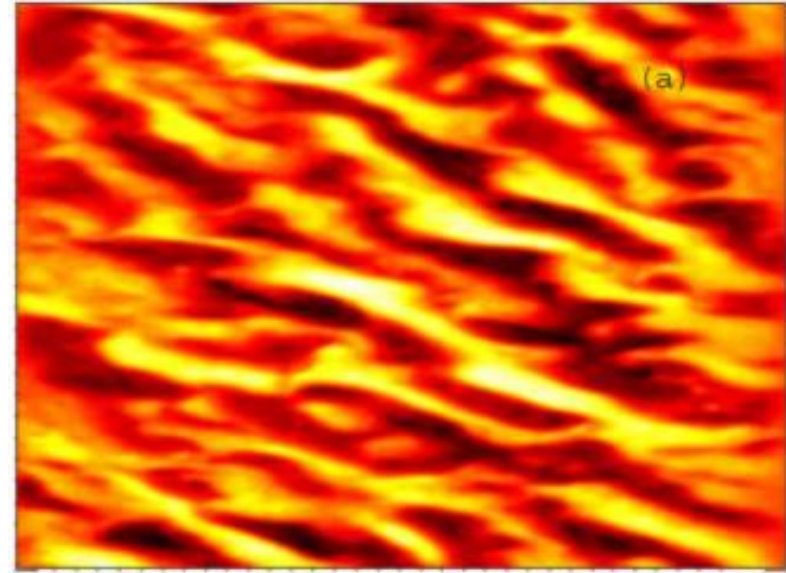
# Microwave scattering used to detect high- $k_{\perp}$ ( $\sim$ mm) fluctuations

## High- $k$ microwave scattering configuration



Mazzucato, PRL (2008)  
Smith, RSI (2008)

## density fluctuations from ETG simulation



6 ion radii  
360 electron radii  
 $\sim$ 2 cm

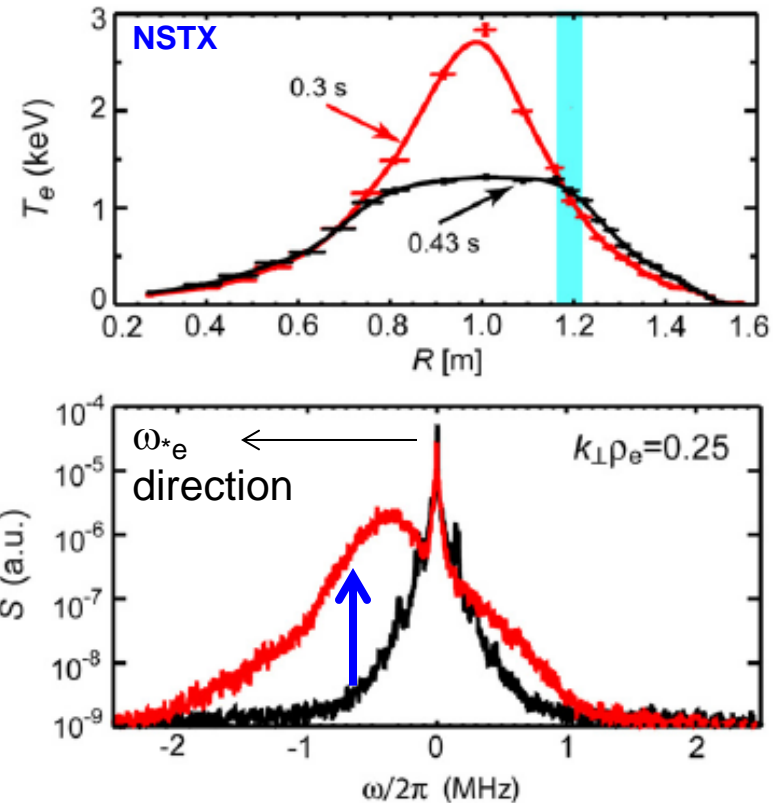
Guttenfelder, PoP (2011)

**NSTX**



# Correlation observed between high-k scattering fluctuations and $\nabla T_e$

- Applying RF heating to increase  $T_e$
  - Fluctuations increase as expected for ETG turbulence ( $R/L_{Te} > R/L_{Te,crit}$ )
- Other trends measured that are consistent with ETG expectations, e.g. reduction of high-k scattering fluctuations with:
1. Strongly reversed magnetic shear (Yuh, PRL 2011)
    - Simulations predict comparable suppression (Peterson, PoP 2012)
  2. Increasing density gradient (Ren, PRL 2011)
    - Simulations predict comparable trend (Ren, PoP 2012, Guttenfelder NF, 2013, Ruiz PoP 2015)
  3. Sufficiently large  $E \times B$  shear (Smith, PRL 2009)
    - Observed in ETG simulations (Roach, PPCF 2009; Guttenfelder, PoP 2011)

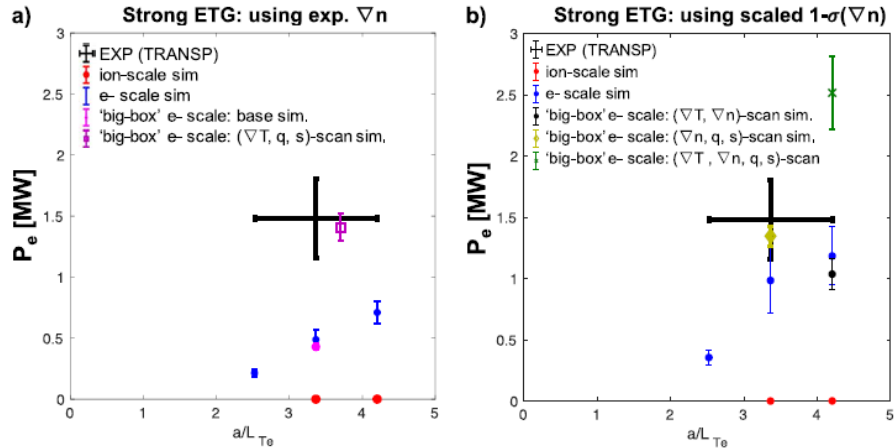


E. Mazzucato et al., NF (2009)

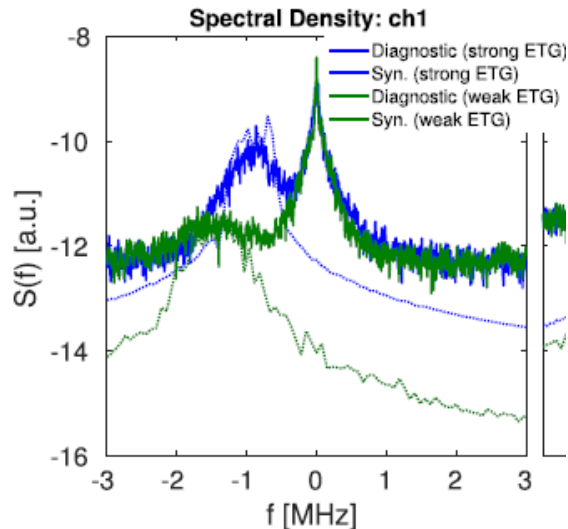
**Many ETG trends observed in NSTX, challenging to correctly predict transport**

# Rigorous validation of NSTX ETG predictions via resolution & sensitivity tests + comparing turbulence measurements via synthetic diagnostic

## Matched experimental fluxes varying inputs within uncertainties

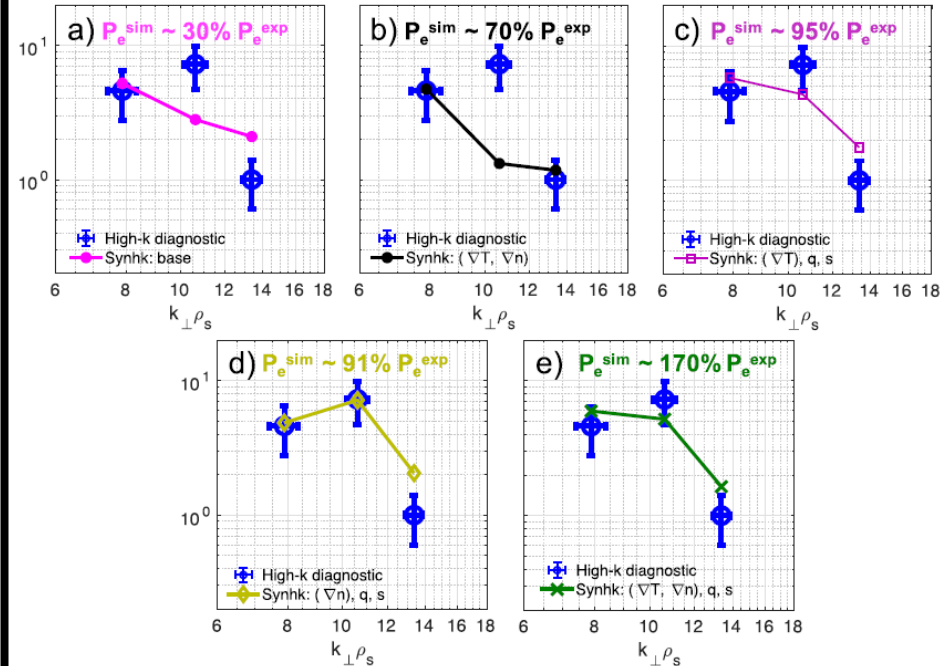


## Matched turbulence frequency spectra using simulation & synthetic diagnostic for high-k microwave scattering



## Matching turbulence wavenumber spectra shape via sim + synthetic diagnostic & varying inputs within uncertainties

Wavenumber spectra shape comparisons for the strong ETG condition



# Electromagnetic (drift wave) turbulence

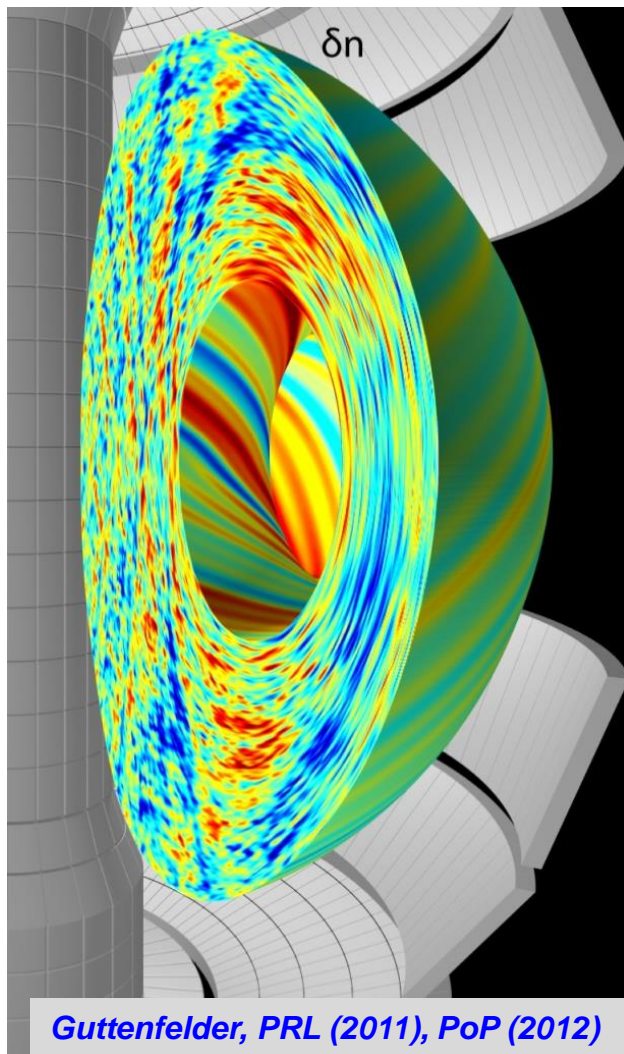
Microtearing mode (MTM) turbulence: small scale (large  $n$ ,  $m$ ) tearing modes driven unstable by  $\nabla T_e$  at sufficient  $\beta_e$

Kinetic ballooning mode (KBM) turbulence: kinetic analog to ideal MHD high- $n$  ballooning modes driven by  $\nabla p_{\text{tot}}$ , expected to set upper limit on achievable pressure gradient

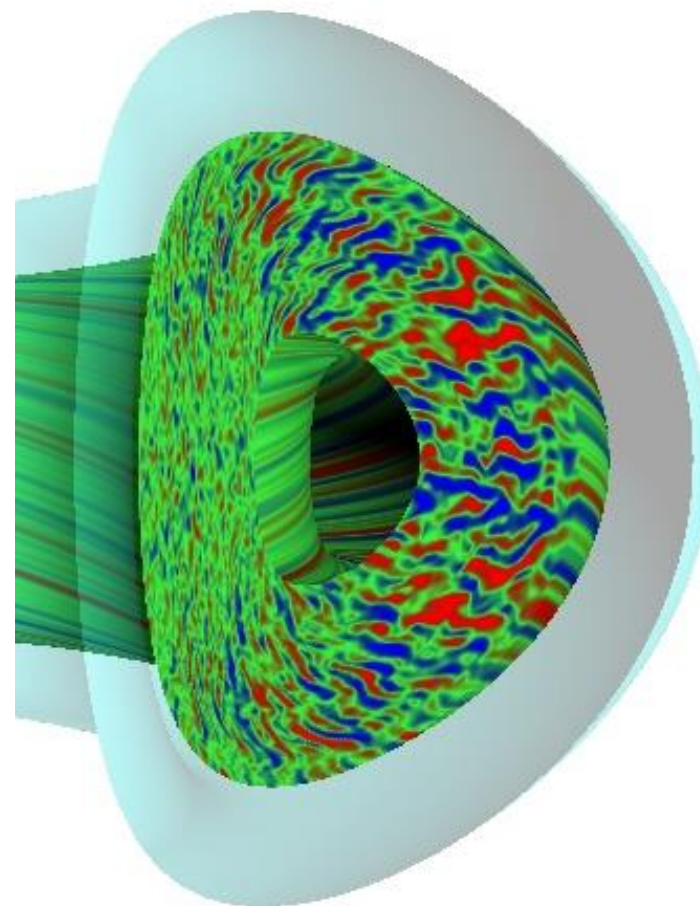
*All high performance tokamak discharges either have transport barriers or operate at high beta (for significant self-driven bootstrap current)  $\rightarrow$  EM turbulence will always be important*

# MTM density fluctuations distinct from ballooning modes like ITG (simulations)

## NSTX MTM turbulence

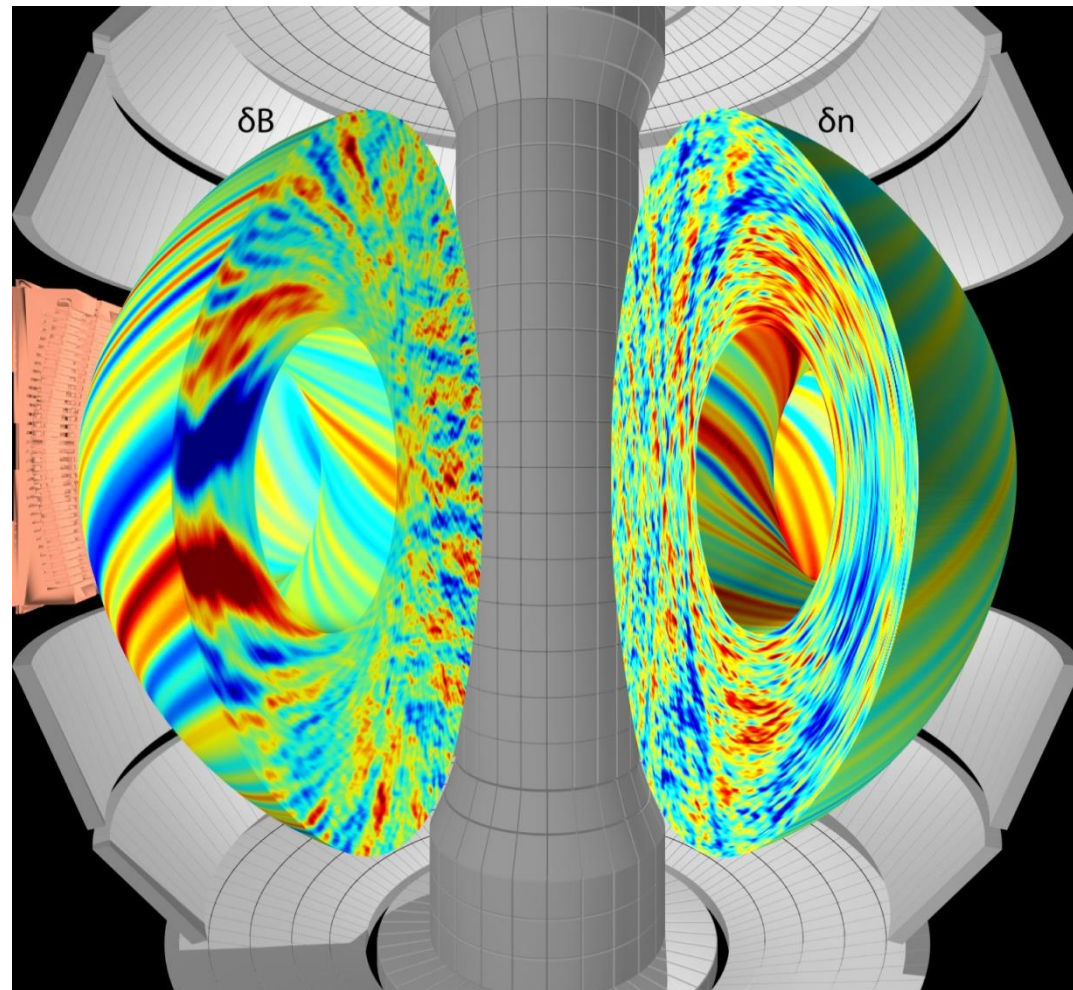


## DIII-D ITG turbulence



# MTM structure distinct from ballooning modes

## Predictions from MTM simulation



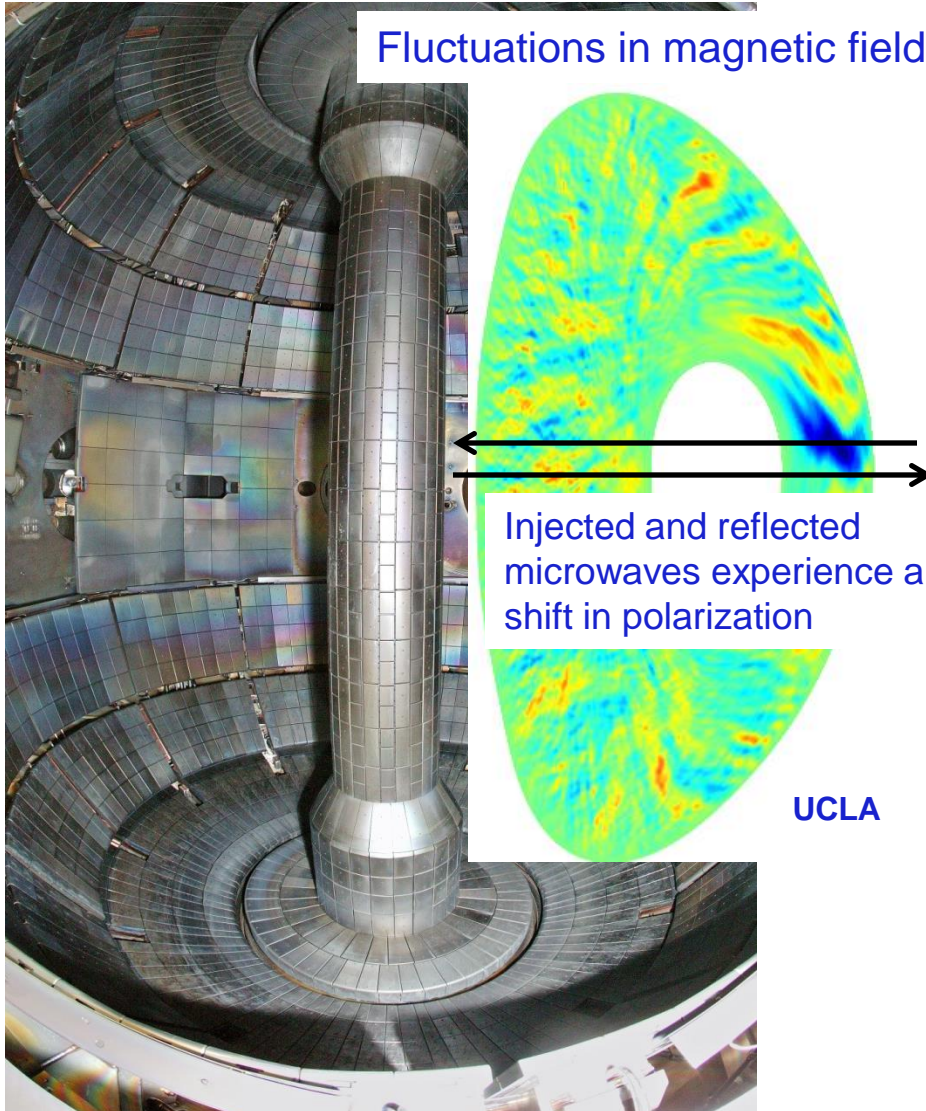
- Narrow density perturbations due to high- $m$  tearing mode around rational surfaces  $q=m/n$ 
  - Potential to validate with beam emission spectroscopy (BES) imaging
- Large amplitude  $\delta B/B \sim 10^{-3}$ 
  - Potential for internal  $\delta B$  measurements

Visualization courtesy F. Scotti (LLNL)

# Very challenging to measure internal magnetic fluctuations

NSTX (PPPL)

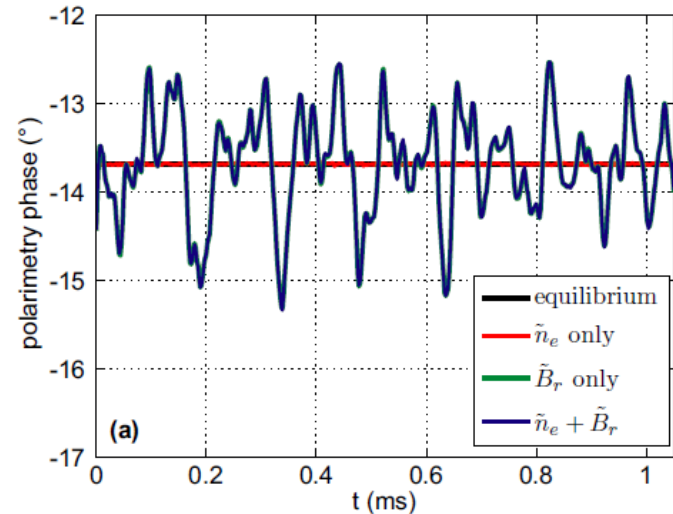
Fluctuations in magnetic field



Injected and reflected microwaves experience a shift in polarization

UCLA

- Synthetic diagnostic calculations predict polarimetry should be sensitive



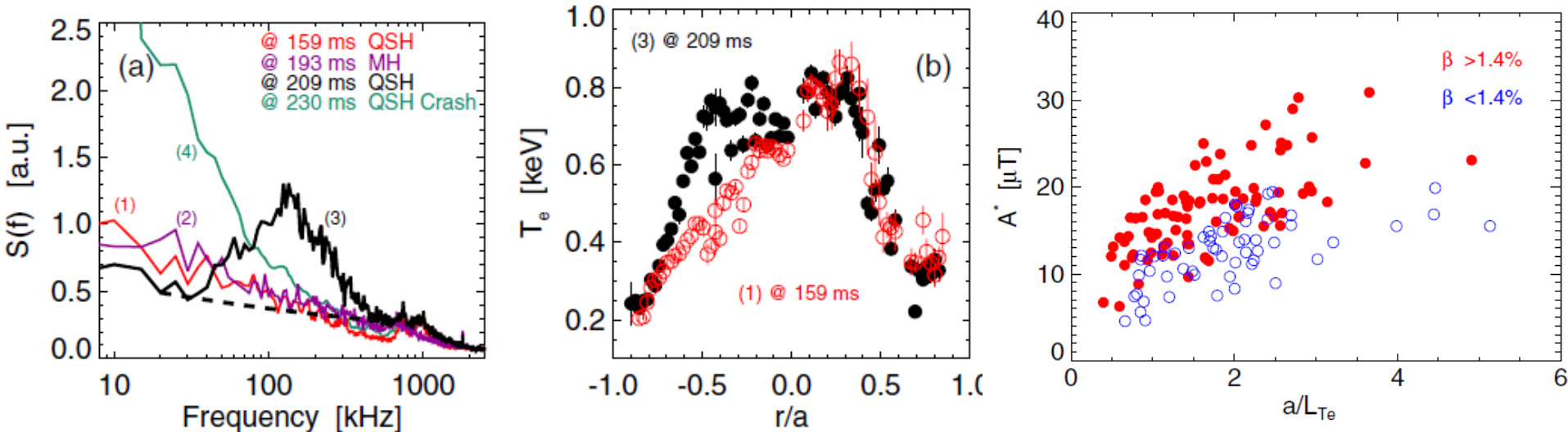
Zhang, PPCF (2013)

Guttenfelder, PRL (2011)

- UCLA collaborators will be installing polarimetry and cross-polarization scattering (CPS) on NSTX-U in 2021-2025 (good time to get involved!)

# Inference of microtearing turbulence via magnetic probes in RFX reversed field pinch (Zuin, PRL 2013)

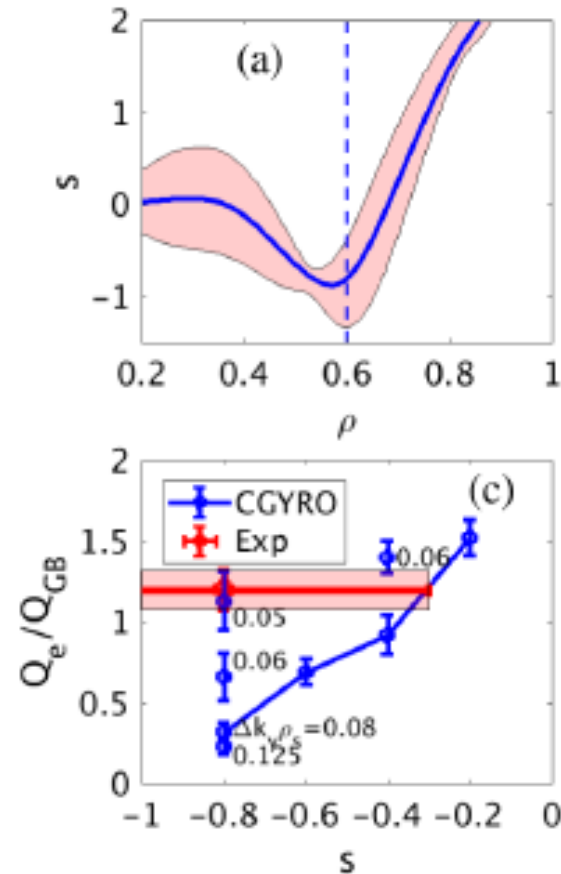
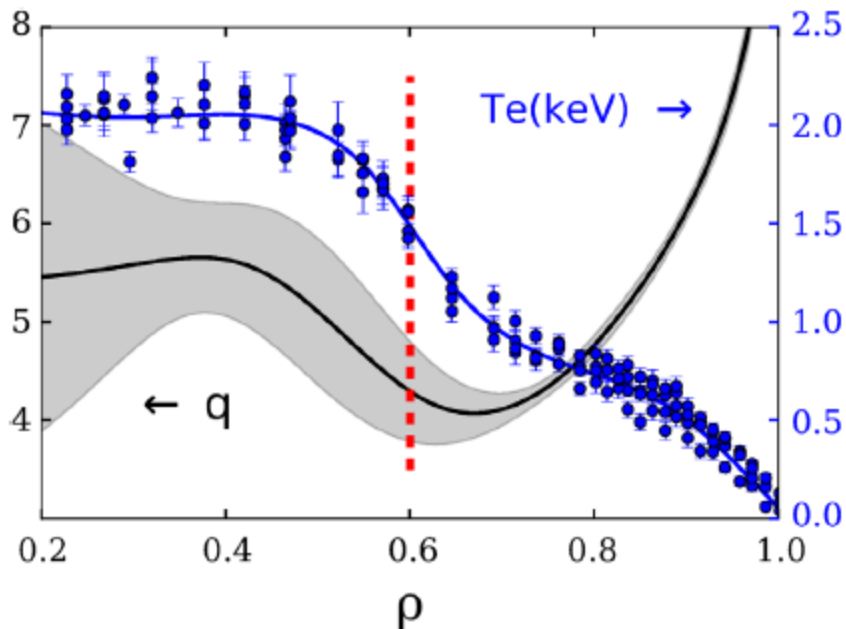
- Used internal array of closely spaced ( $\sim$ wavenumber resolved) high frequency Mirnov coils ( $\sim$ dB/dt) mounted near vacuum vessel wall
- Confinement and  $T_e$  increase during “quasi-single helicity” (QSH) state  $\rightarrow$  broadband  $\delta B$  measured (left figure, #3 curve)
- $\delta B$  amplitude increases with  $a/L_{Te}$  &  $\beta$  (expected for MTM)
- Measured frequency and mode numbers (n,m) align with linear gyrokinetic predictions of MTM



- Additional MTM inferences using novel heavy ion beam probe technique (internal, non-perturbative) in JIPPT-IIU tokamak (Hamada, NF 2015)

# Analysis indicates MTM sets electron transport in the internal transport barrier in DIII-D high- $\beta_{pol}$ discharges

- Large  $\alpha \sim \nabla\beta_{pol}$  gives strong Shafranov shift + negative magnetic shear ( $s < 0$ ) stabilizes ITG/TEM (ion thermal transport is neoclassical)
- MTM turbulence predicted to limit electron thermal transport in region of  $s < 0$



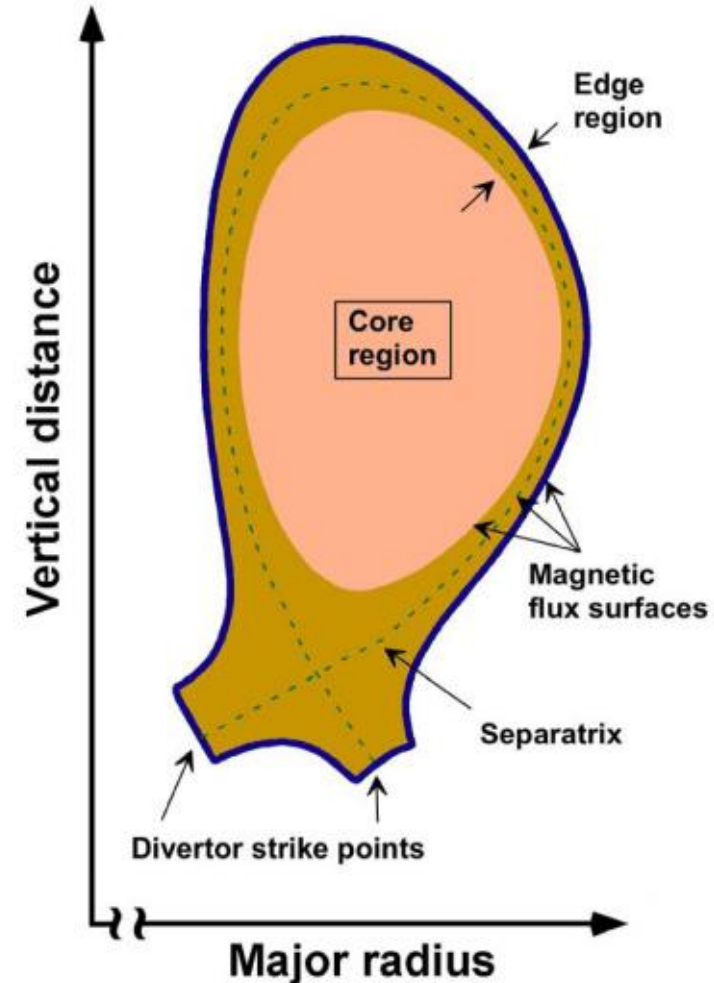
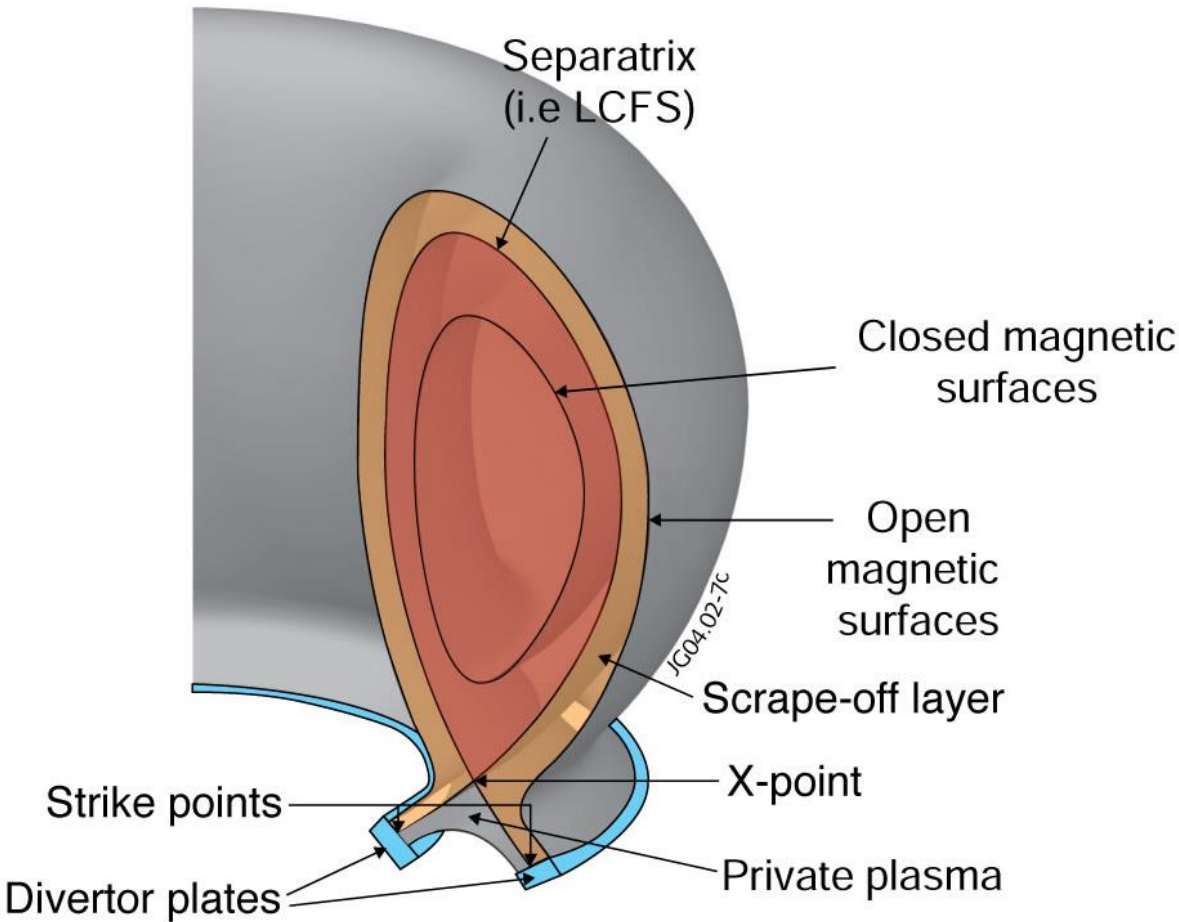
- Significant correlation between interferometer measurements and MTM expectations in other DIII-D discharges [J. Chen, APS 2019]



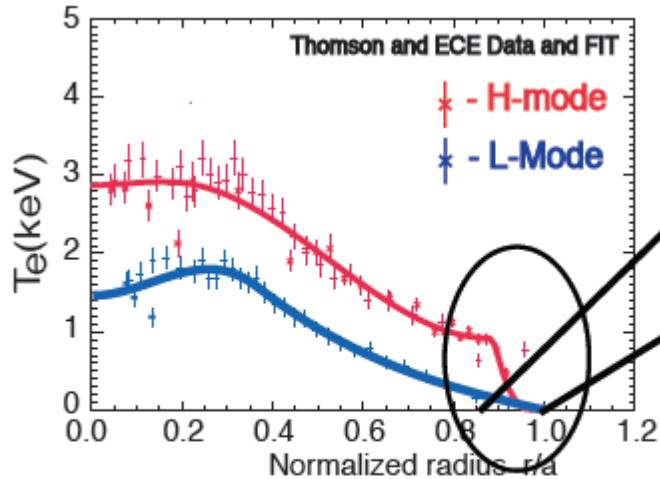
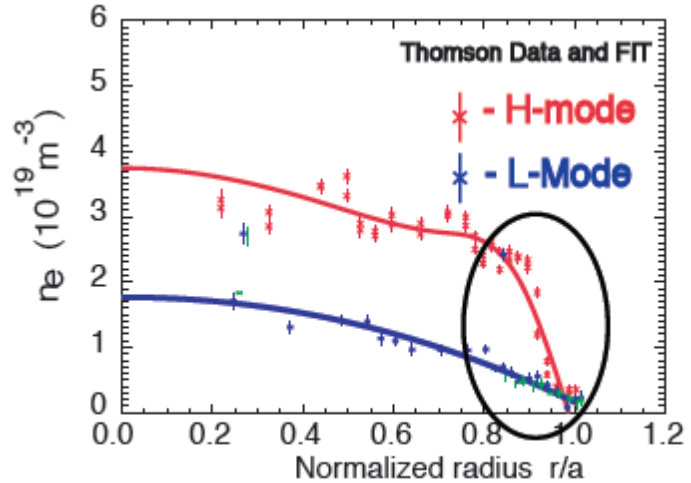
# **EDGE TURBULENCE L-H TRANSITION**

# Moving outwards from the hot core

- Especially **core**, **edge** (just inside separatrix), and **scrape-off layer** (SOL, just outside separatrix)

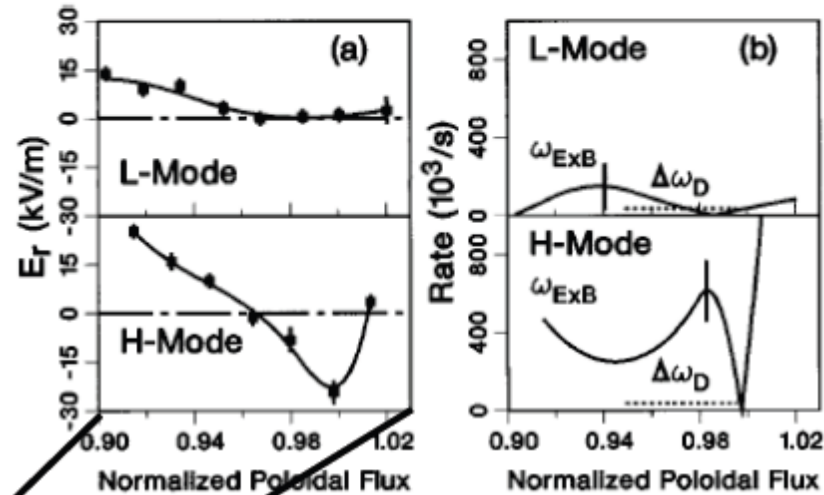


# Spontaneous “H-mode” edge transport barrier can form with sufficient heating power → improved confinement



Data from DIII-D

(from Carter, 2013)

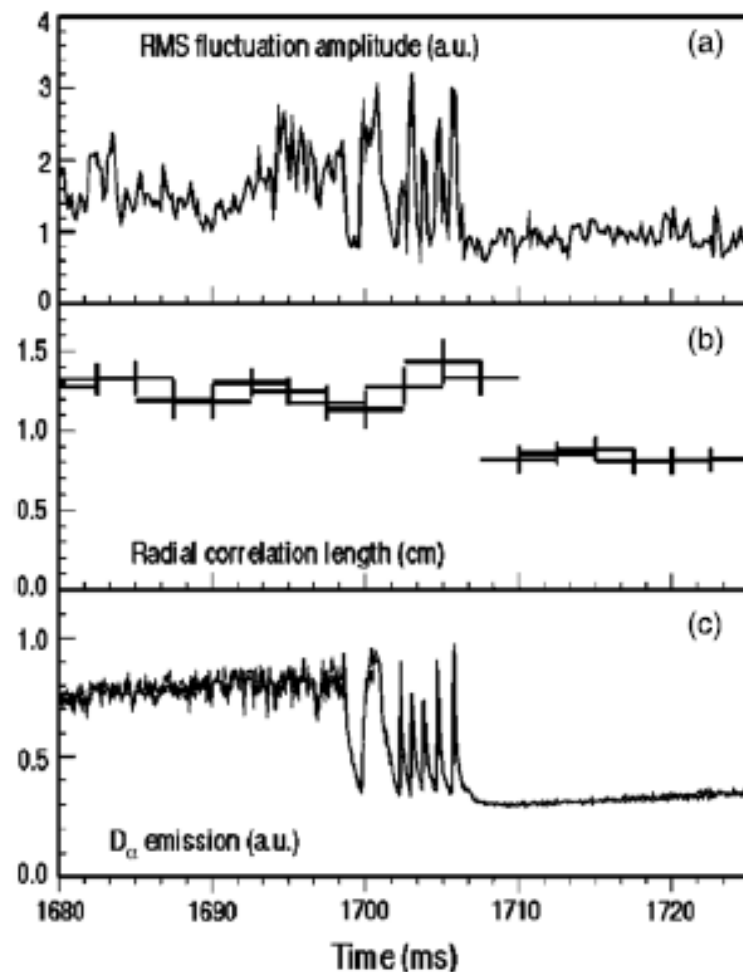


Burrell 1997

- Correlated with strong shear in equilibrium radial electric field ( $E_r$ )
- Suppression of turbulence predicted when equilibrium shearing rate ( $\omega_{E \times B}$ ) > turbulence decorrelation rate ( $\Delta\omega_D$ ) [Biglari, 1990; Hahm, 1994]

# Transition from L→H correlated with drop in turbulence amplitude, reduction in radial correlation length

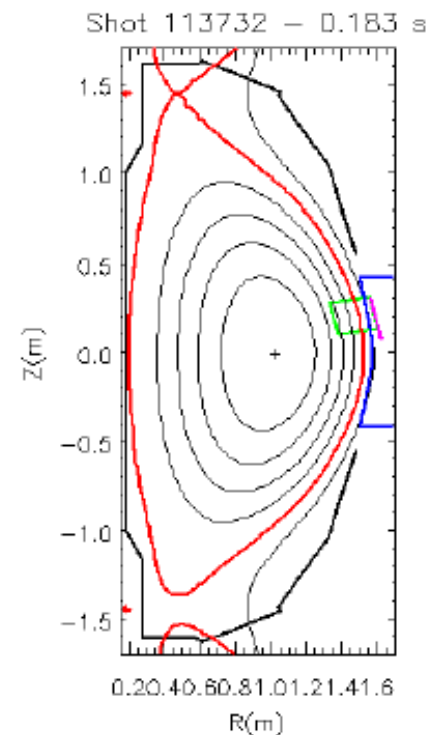
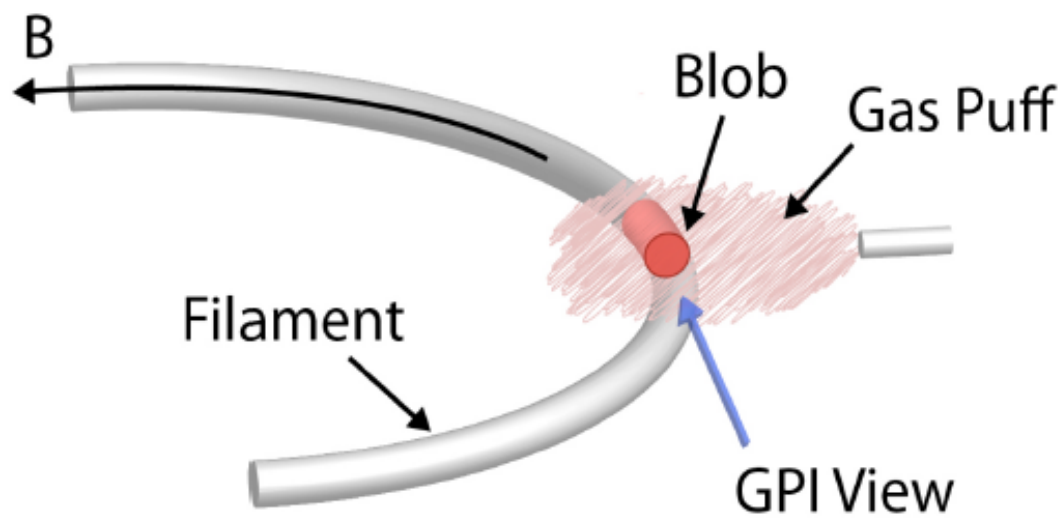
- Consistent with  $E \times B$  shear suppression
- Understanding what *initiates* the transition and the dynamics involved is still being developed
- Practically important for understanding how much power required to reach H-mode ( $\rightarrow$  *almost all reactor designs assume H-mode*)



Burrell, PoP (1997)  
Coda, Phys. Lett. A (2000)

# Edge Turbulence Measurements in NSTX

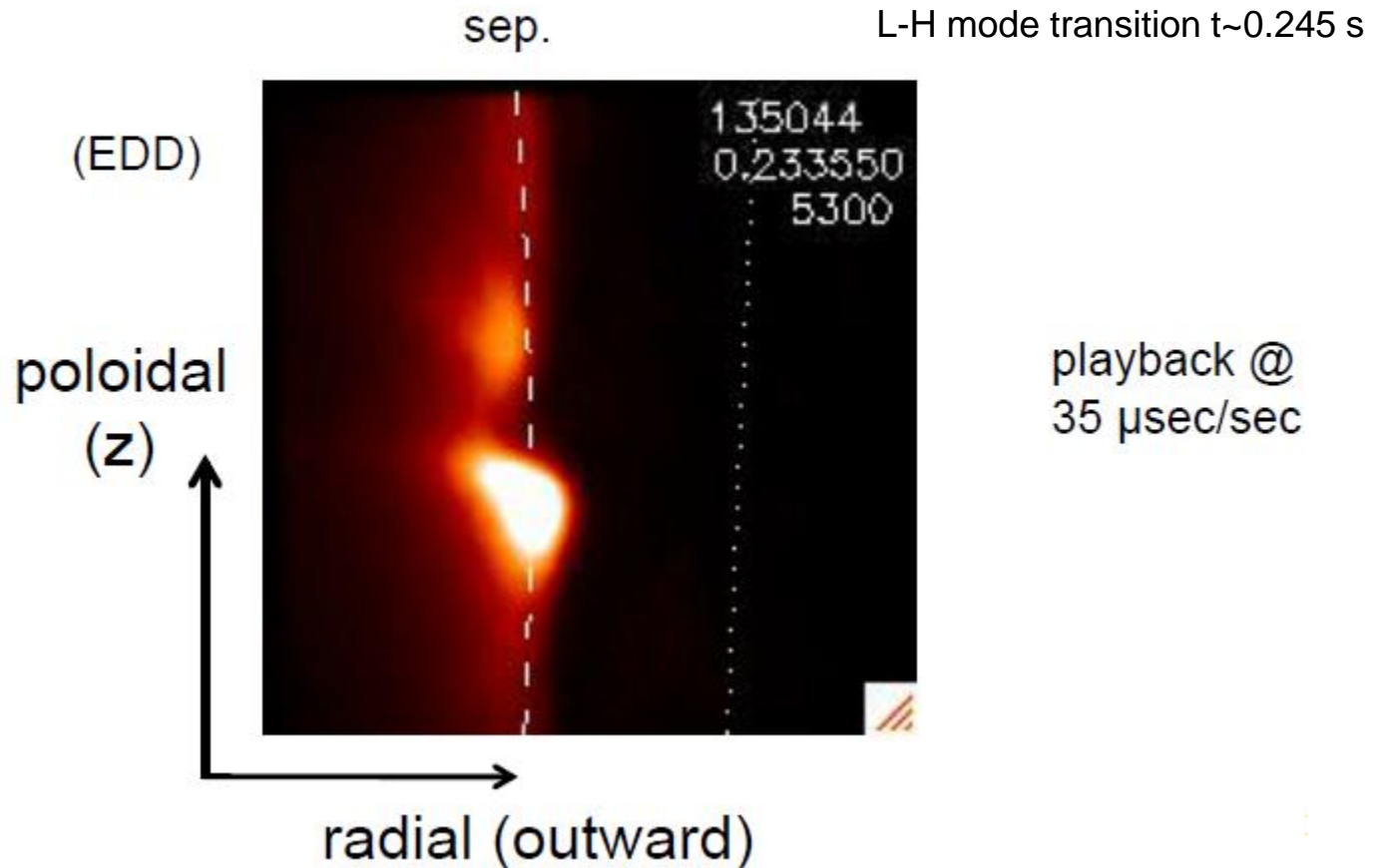
- High speed cameras make images of edge turbulence
- 3-D 'filaments' localized to 2-D by gas puff imaging (GPI)



Zweben et al, Nuclear Fusion 44 (2004), R. Maqueda et al, Nucl. Fusion 50 (2010)

# Lots of videos via Stewart Zweben: <http://w3.pppl.gov/~szweben/>

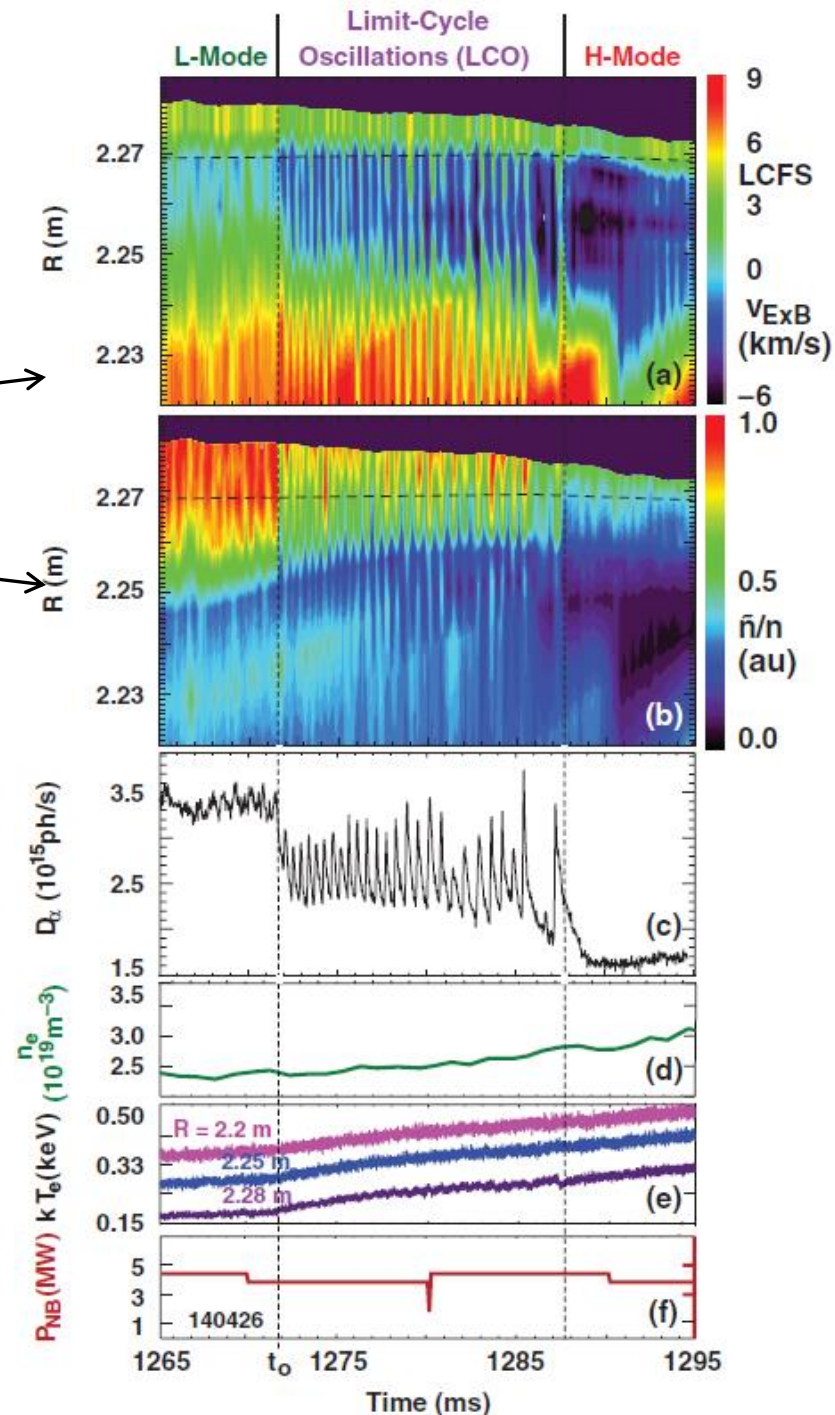
- This movie 285,000 frames/sec for ~ 1.4 msec
- Viewing area ~ 25 cm radially x 25 cm poloidally



# Multiple doppler backscattering diagnostics provide $\delta n$ , $\delta v_{E \times B}$ at multiple radii simultaneously (DIII-D)

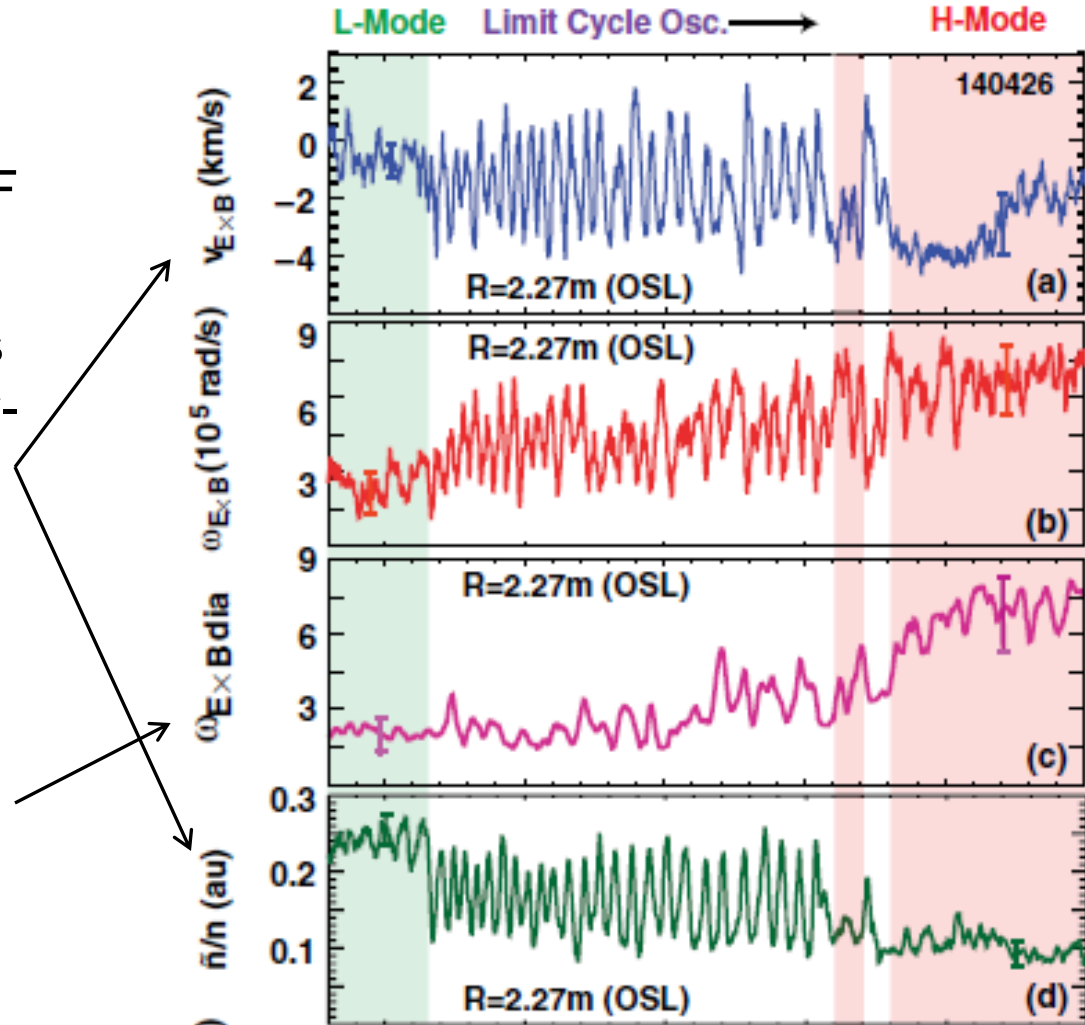
- During dithering L-H phase (identified by  $D_\alpha$  signal),  $\delta v_{E \times B}$  and  $\delta n$  start to oscillate
- Equilibrium  $n_e$ ,  $T_e$  begin to increase
- Eventually strong equilibrium flow shear locks in, fluctuations drop permanently, and pedestal finishes forming

DIII-D, Schmitz, PRL (2012)



# Dynamics consistent with two-predator – prey model (Kim, PRL 2003)

- In L-mode, increasing turbulence drives stronger ZF
- Eventually starts to suppress turbulence, leads to predator-prey limit cycle oscillation between ZF and turbulence
- As confinement (and gradients) increases, equilibrium  $E_r$  driven by  $\nabla \Pi$  increases, until it is strong enough to maintain suppression



DIII-D, Schmitz, PRL (2012)

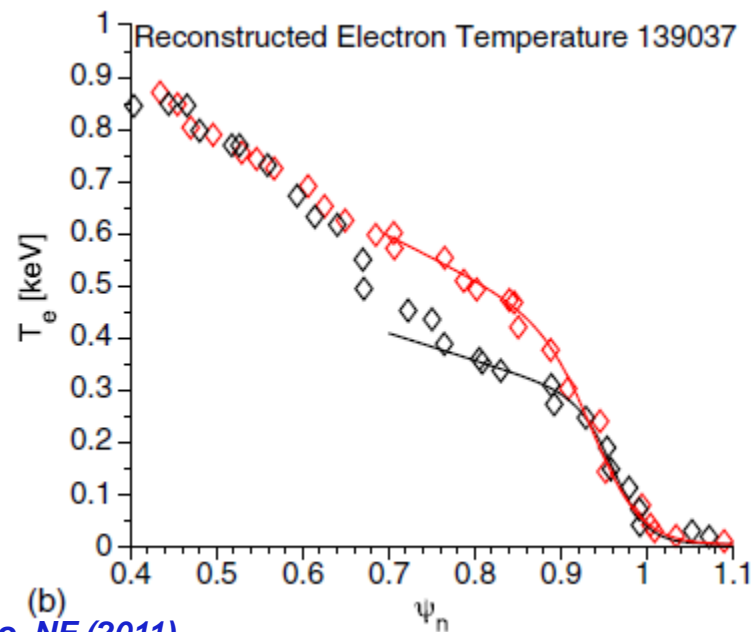
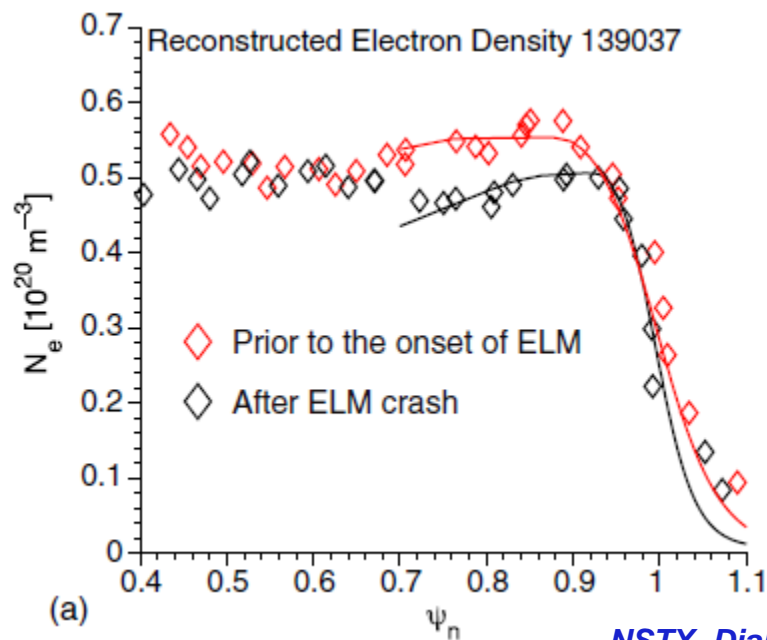
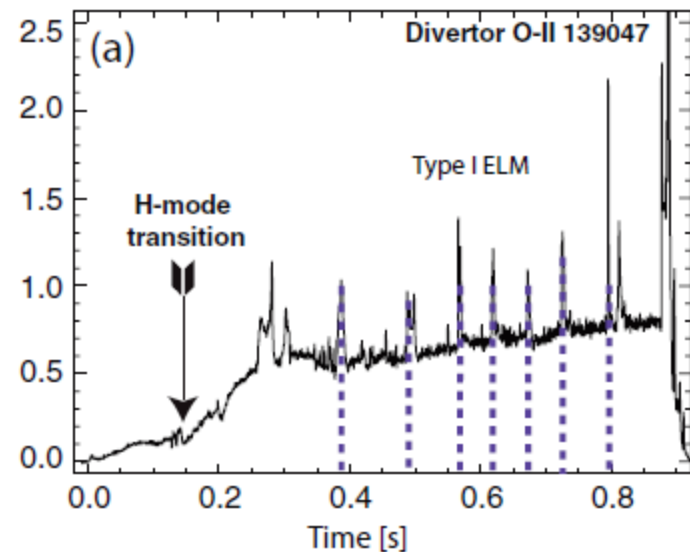


# **EDGE TURBULENCE**

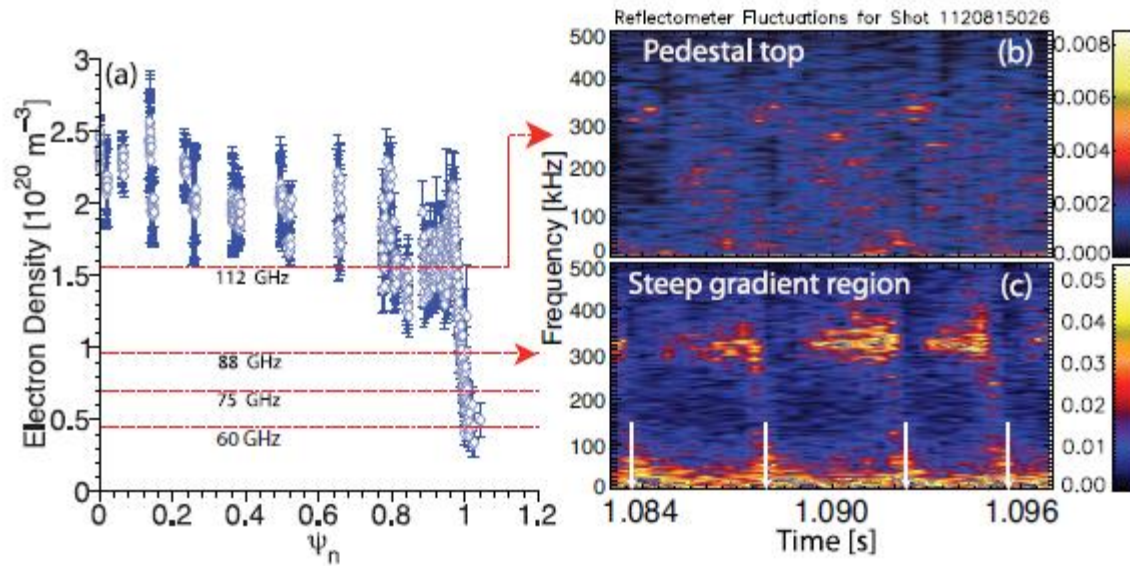
## **H-mode pedestal**

# In fully-developed H-modes, periodic MHD instabilities (Edge Localized Modes, ELMs) often occur

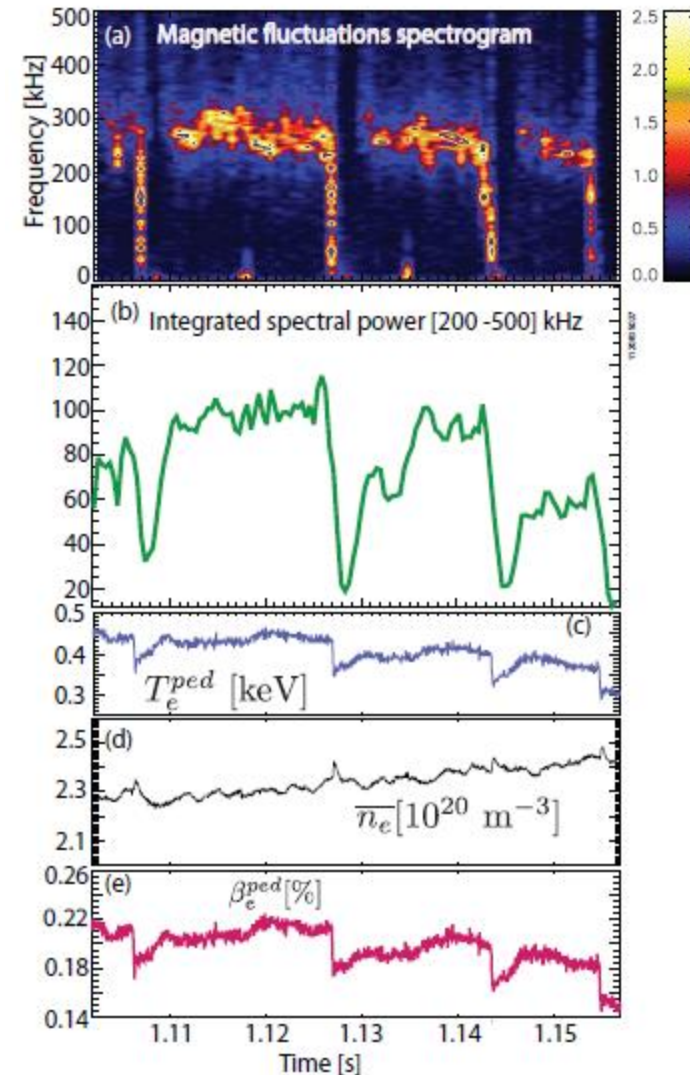
- Rapidly expels energy (see GPI videos)
- Profiles drop after ELM, recover between ELMs
- General question of what transport mechanism limits H-mode pedestal & post-ELM recovery



# Local density and magnetic fluctuations measured inter-ELM - possible importance of EM turbulence

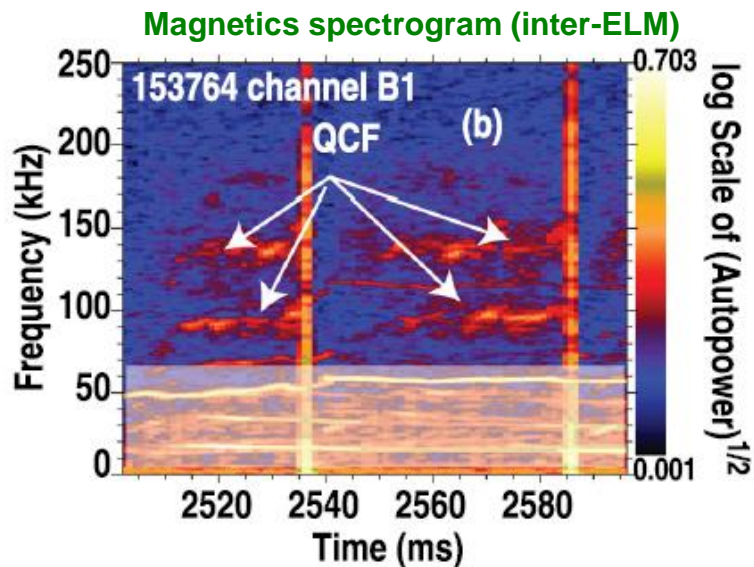


- Density from reflectometry (& Gas Puff Imaging)
- Magnetic probes inserted 2 cm from separatrix (measures same  $k_\theta$  as density)
- Evidence for importance of EM turbulence?
  - Leading theory posits KBM (EM drift wave) as a key contributor setting H-mode pedestal (Snyder, NF, 2011)
  - Recent analysis indicates magnetic signatures consistent with MTM



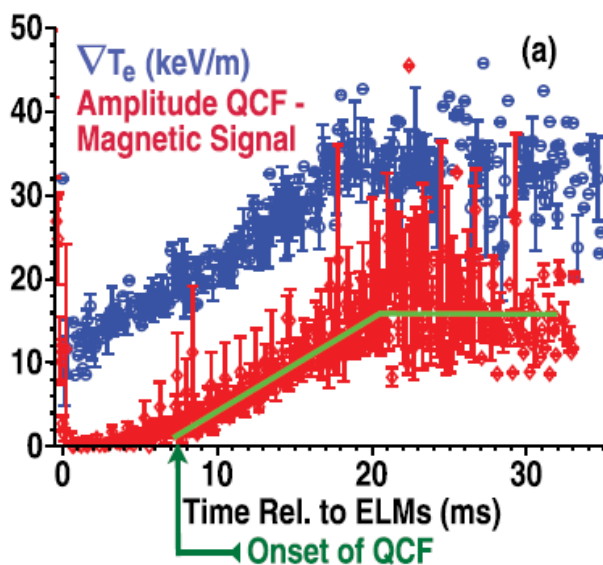
Alcator C-Mod, Diallo, PRL (2014)

# Ensemble of inter-ELM measurements (DIII-D) indicate magnetic amplitude correlated with recovery of $\nabla T_e$

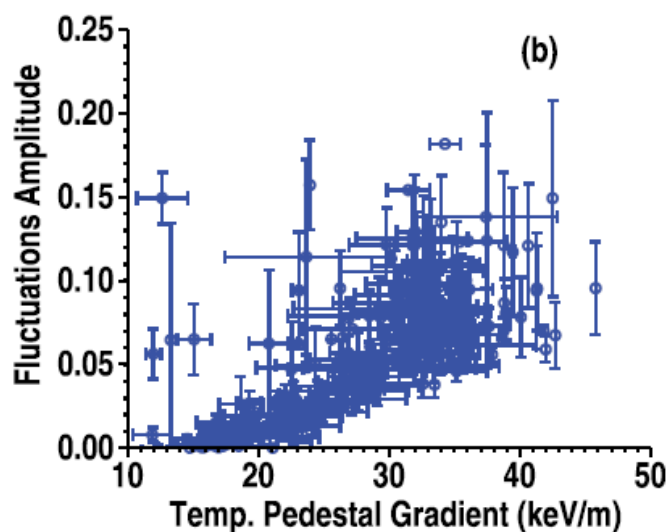


- $\delta B \sim \nabla T_e$  more consistent with MTM expectations
  - MTM specifically driven by  $\nabla T_e$  (to regulate electron heat flux)
  - KBM is driven by  $\nabla P_{\text{tot}}$

Ensemble evolution of inter-ELM  $\delta B$  &  $\nabla T_e$



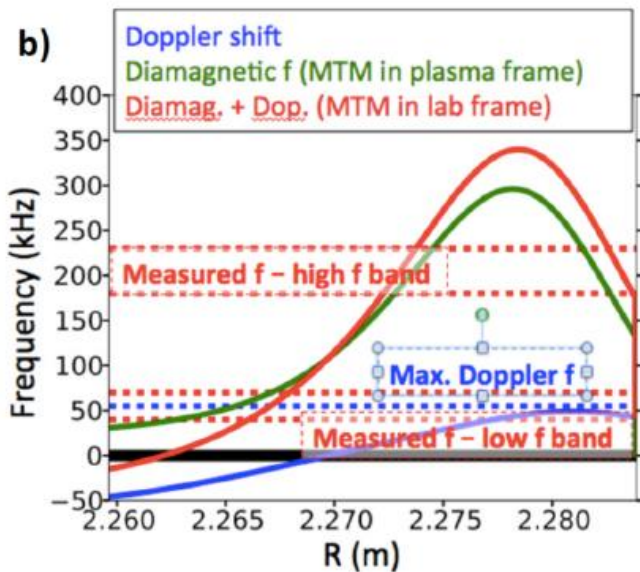
$\delta B$  vs  $\nabla T_e$  (from inter-ELM ensemble)



# Recent gyrokinetic analysis indicates these magnetic signatures are consistent with MTM

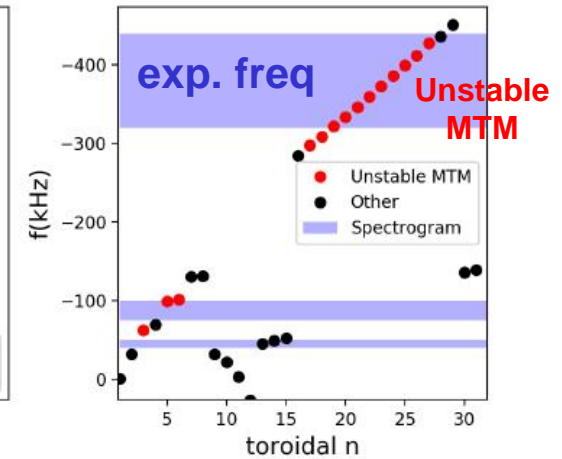
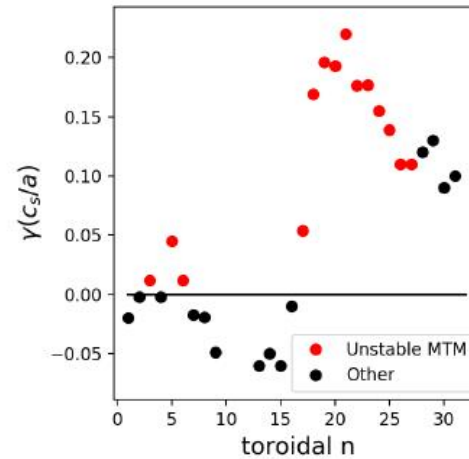
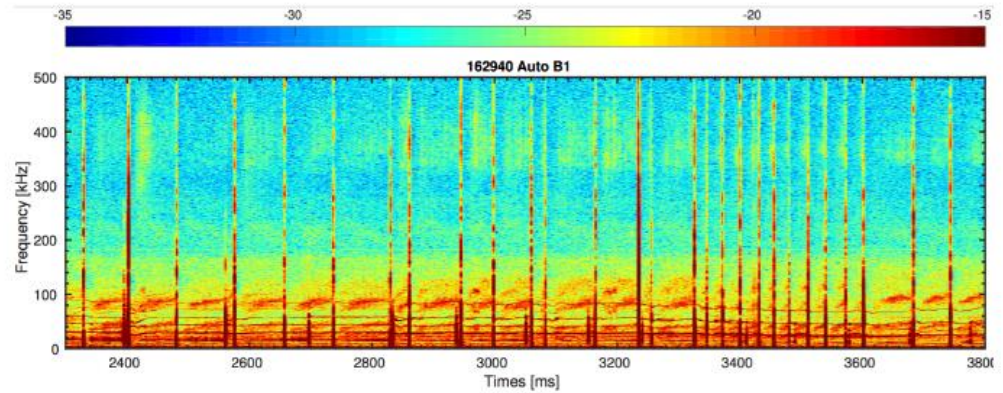
- Similar frequencies as MTM ( $\omega_{\text{MTM,lab}} \sim \omega_{*e} + \omega_{\text{Doppler}}$ )
- Selective appearance of toroidal mode numbers correlated with overlap of corresponding rational surfaces ( $q_{\text{rat}} = m/n$ ) with maximum  $\omega_{*e}$
- Nonlinear transport predicted to be significant [Hatch, NF 2017, 2019, & 2020]

Frequency vs. radius (from magnetics observation and MTM prediction)



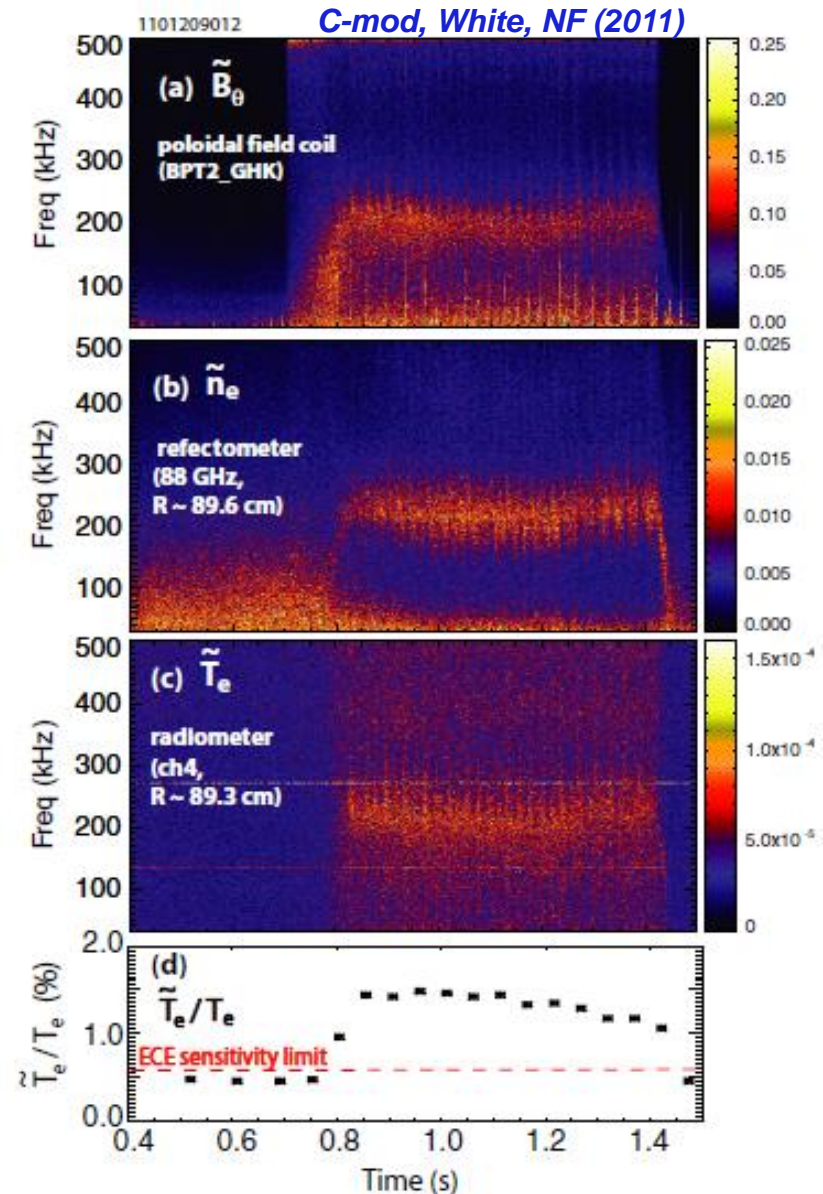
Kotschenreuther, NF (2019)  
Hatch, NF (2020)

Magnetics spectrogram (DIII-D 162940)



# Various fluctuations observed in ELM free pedestal regions – Weakly Coherent Mode in C-mod I-mode

- I-mode in C-mod similar to H-mode except temperature pedestal only
- Evidence for weakly coherent density, temperature & magnetic fluctuations associated with increased particle transport preventing density pedestal
- Other examples exist in ELM-free H-modes (EHO in DIII-D; QCM in C-Mod EDA H-mode)
- **Is this turbulence?**



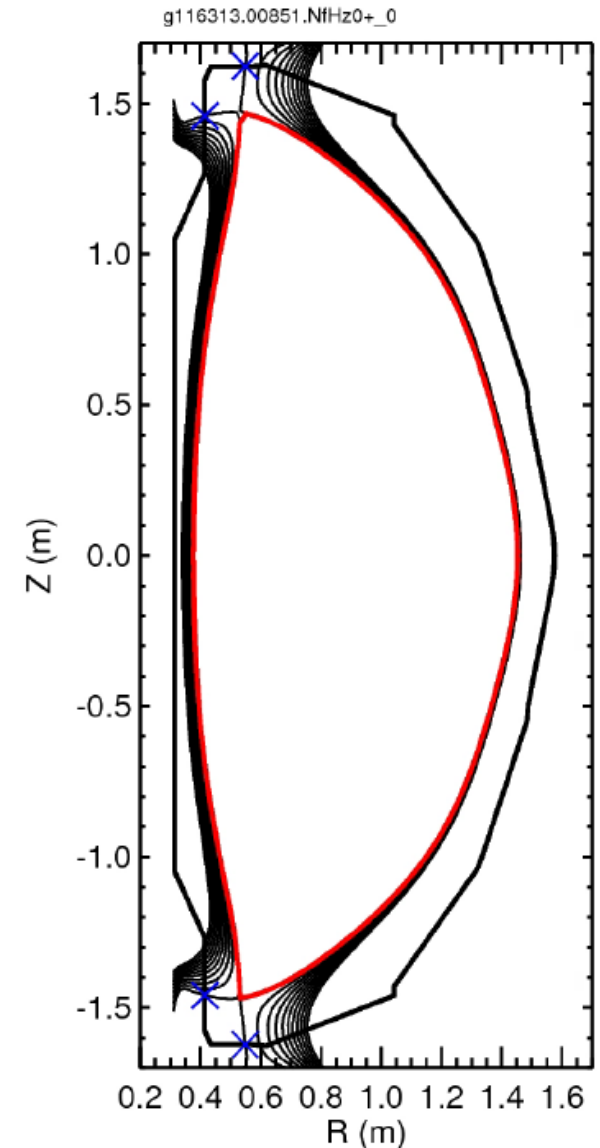
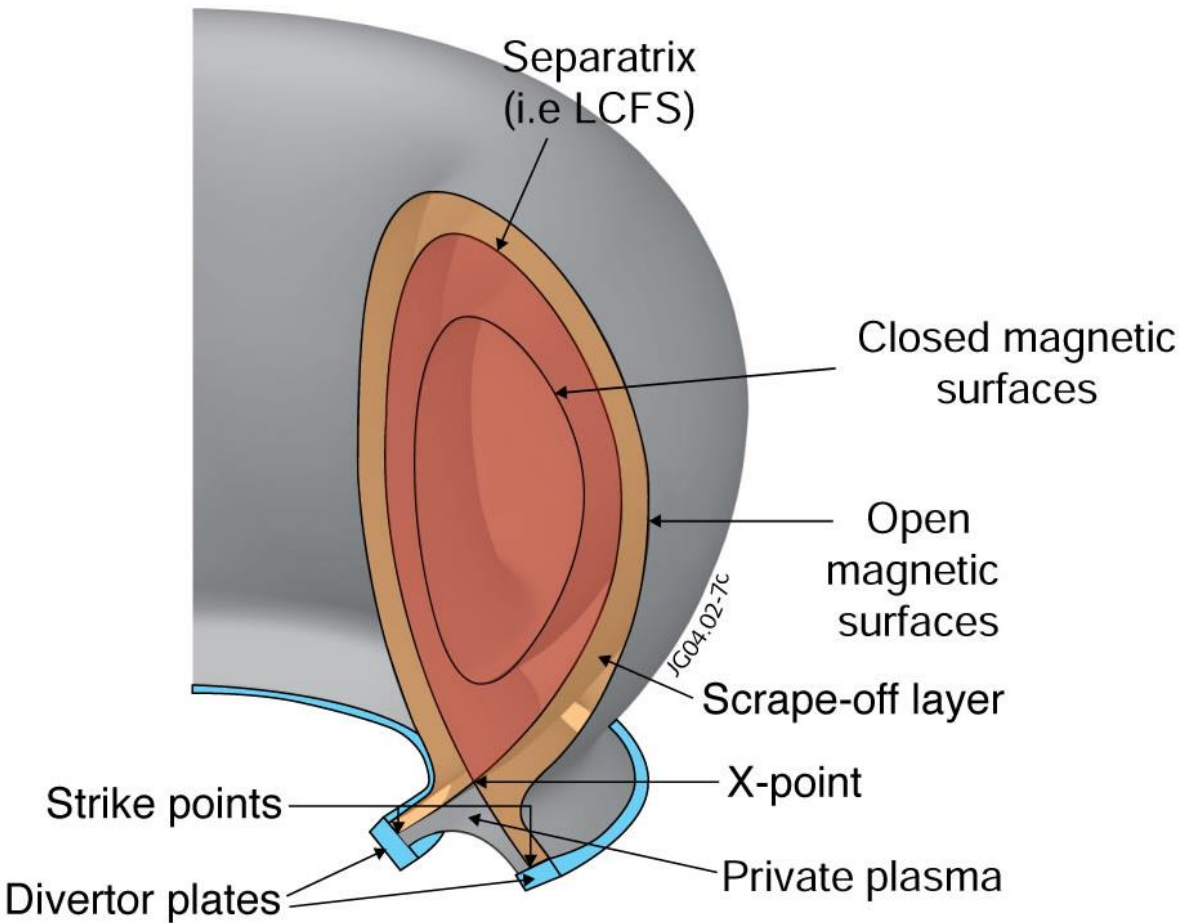
# **SCRAPE OFF LAYER TURBULENCE**

- Concept of “turbulence” in open field lines starts to change a bit
- Often get blobby, strongly intermittent behavior



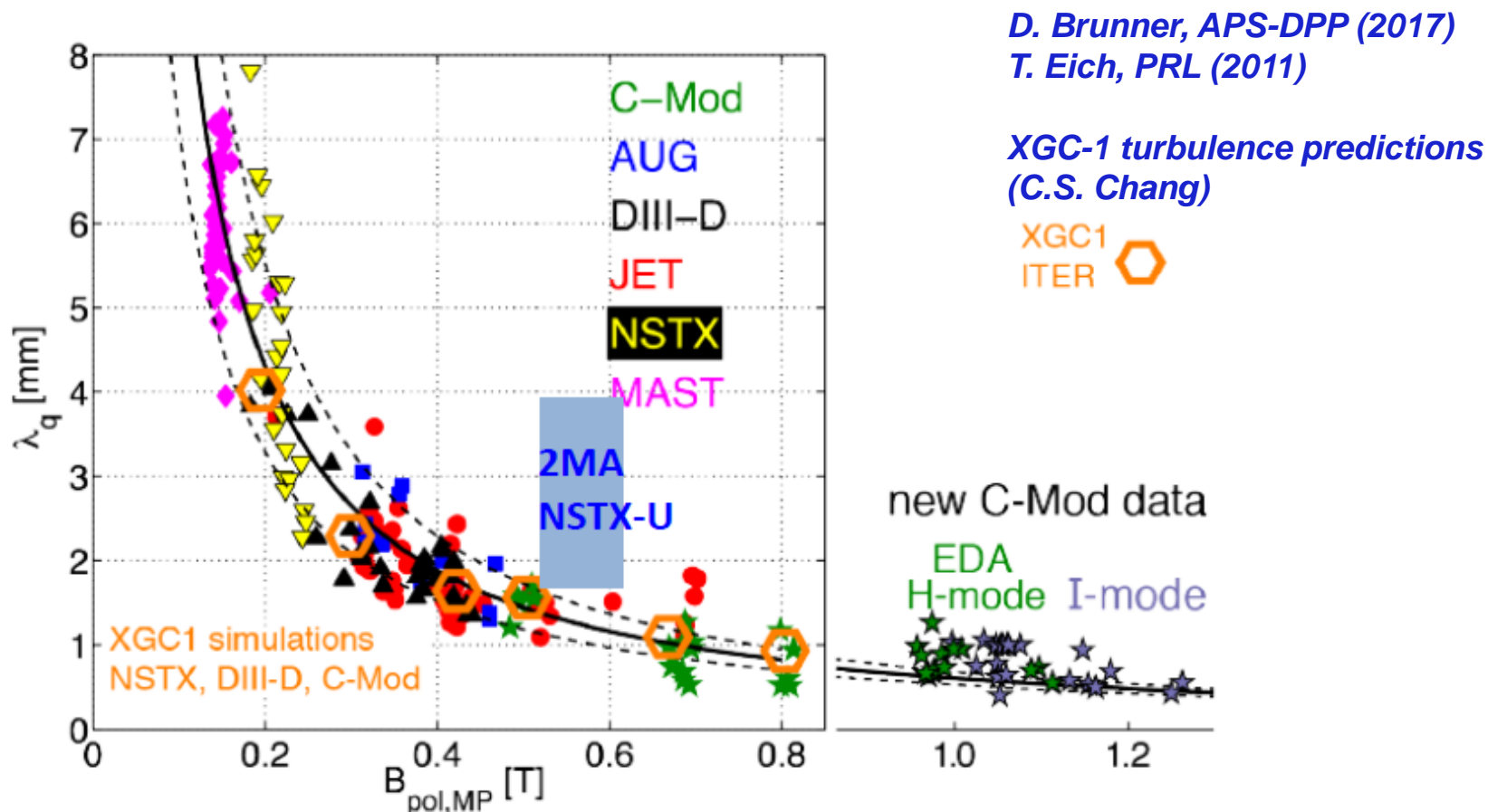
# Going to refer to different spatial regions in the tokamaks

- Especially **core**, **edge** (just inside separatrix), and **scrape-off layer** (SOL, just outside separatrix)



# Understanding scrape-off-layer (SOL) heat-flux width extremely important under reactor conditions

- Narrow SOL heat flux width  $\lambda_q$  leads to huge ( $>10 \text{ MW/m}^2$ ) heat flux density on the divertor plasma facing components (PFCs)  $\rightarrow$  significant concern for sputtering and erosion
- Empirical scaling ( $\lambda_q \sim 1/B_{\text{pol,MP}}$ ) very unfavorable for reactors
- **Recent turbulence simulations suggest a possible break from this scaling**



# Many options being considered for divertor/SOL magnetic geometry

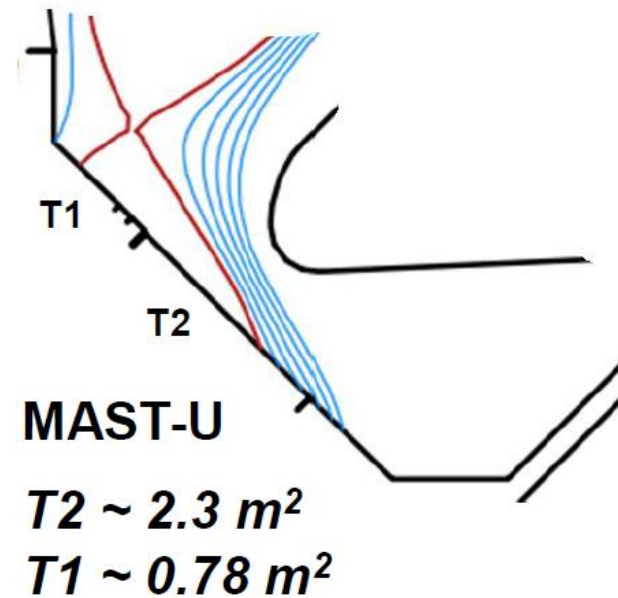
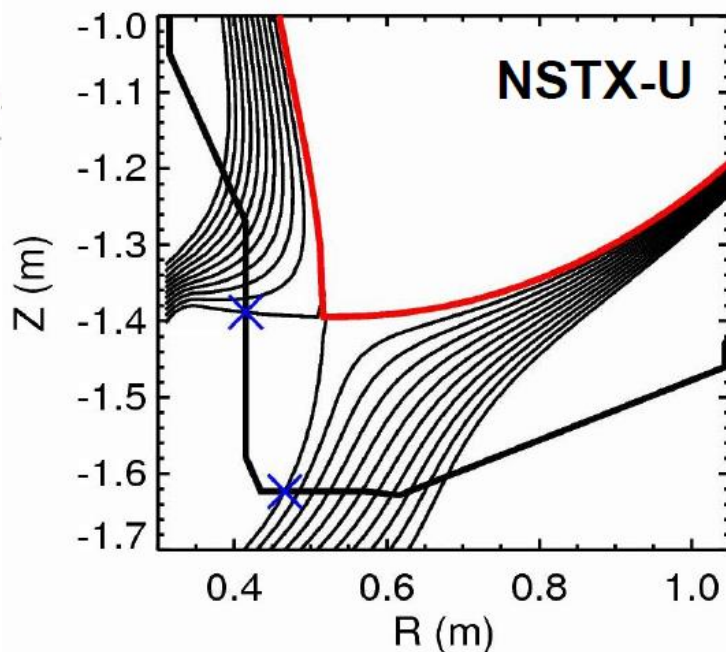
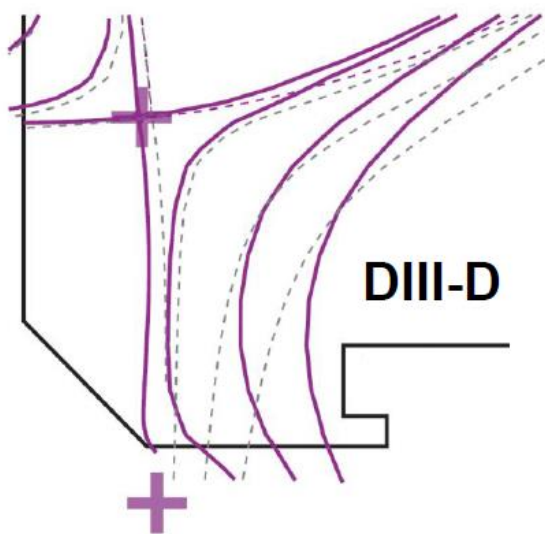
- Requires additional complexity in poloidal field coils and controllability
- Generally will also required impurity seeding in core/edge plasma to radiate much of the power
- **Spreading (from turbulence) could reduce heat flux density**

## X divertor

## Snowflake divertor

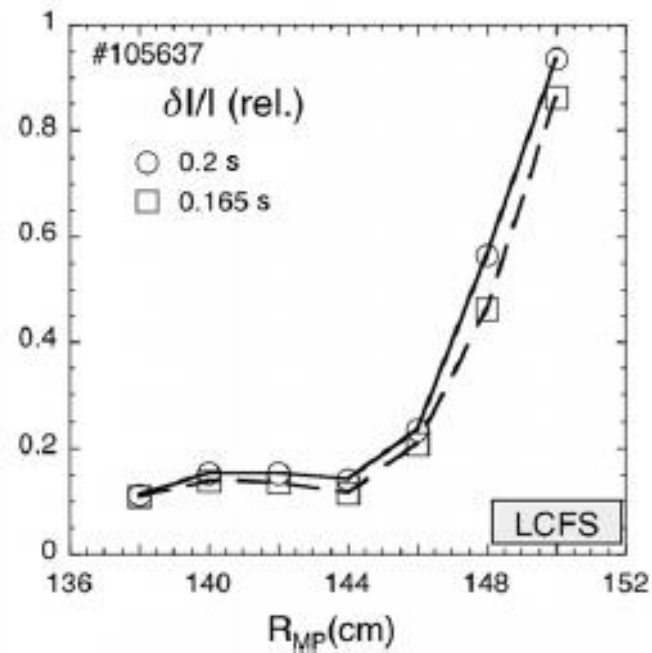
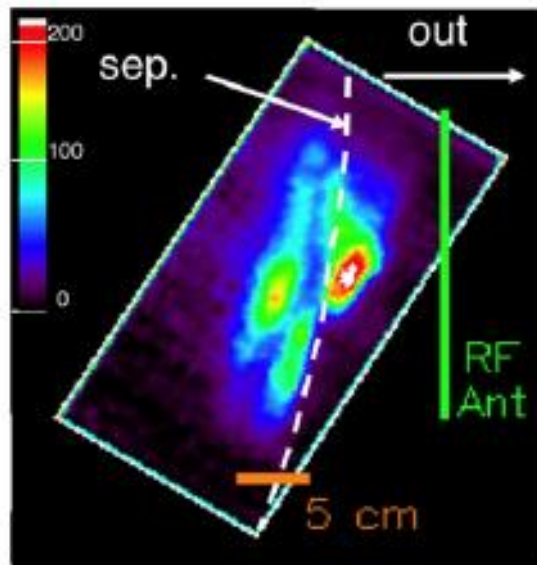
## Super-X divertor

### X Divertor



# Outside separatrix, blobs can be ejected and self-propagate to vessel wall (NSTX GPI)

- Plasma is much less dense farther out in scrape-off layer
- Relative intensity of blob becomes large ( $\delta I/I$ )
- Measurements are generally intermittent (large skewness, kurtosis)

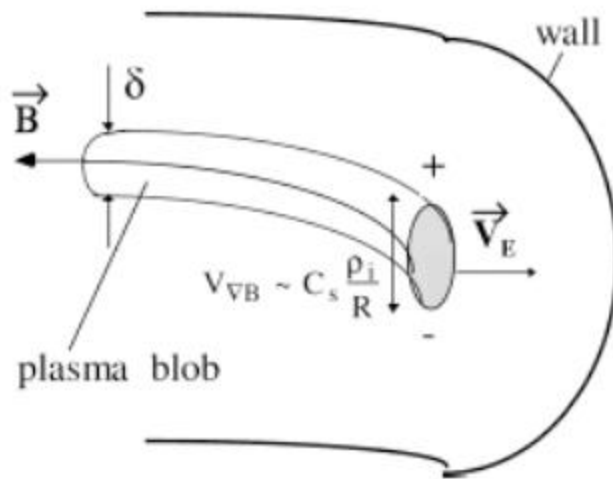


Many characterizations of blob size, velocity, trajectory, etc... [Zweben; Lampert; others...]

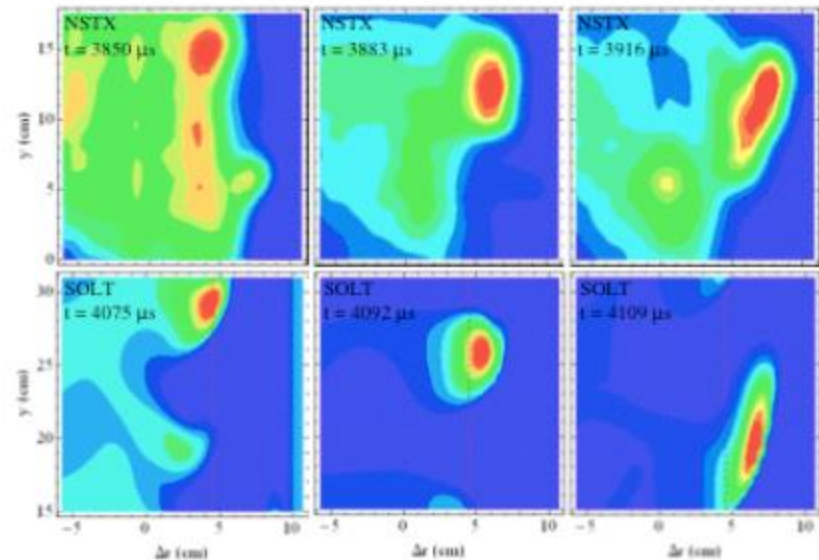
# Theories and simulations exist that predict blob characteristics: size, density, velocity

- Simulations further out in edge become progressively more challenging, more effects to deal with (neutrals, open field lines to conducting walls, dust, ...)

simple 'blob' model (Krash. 2001)

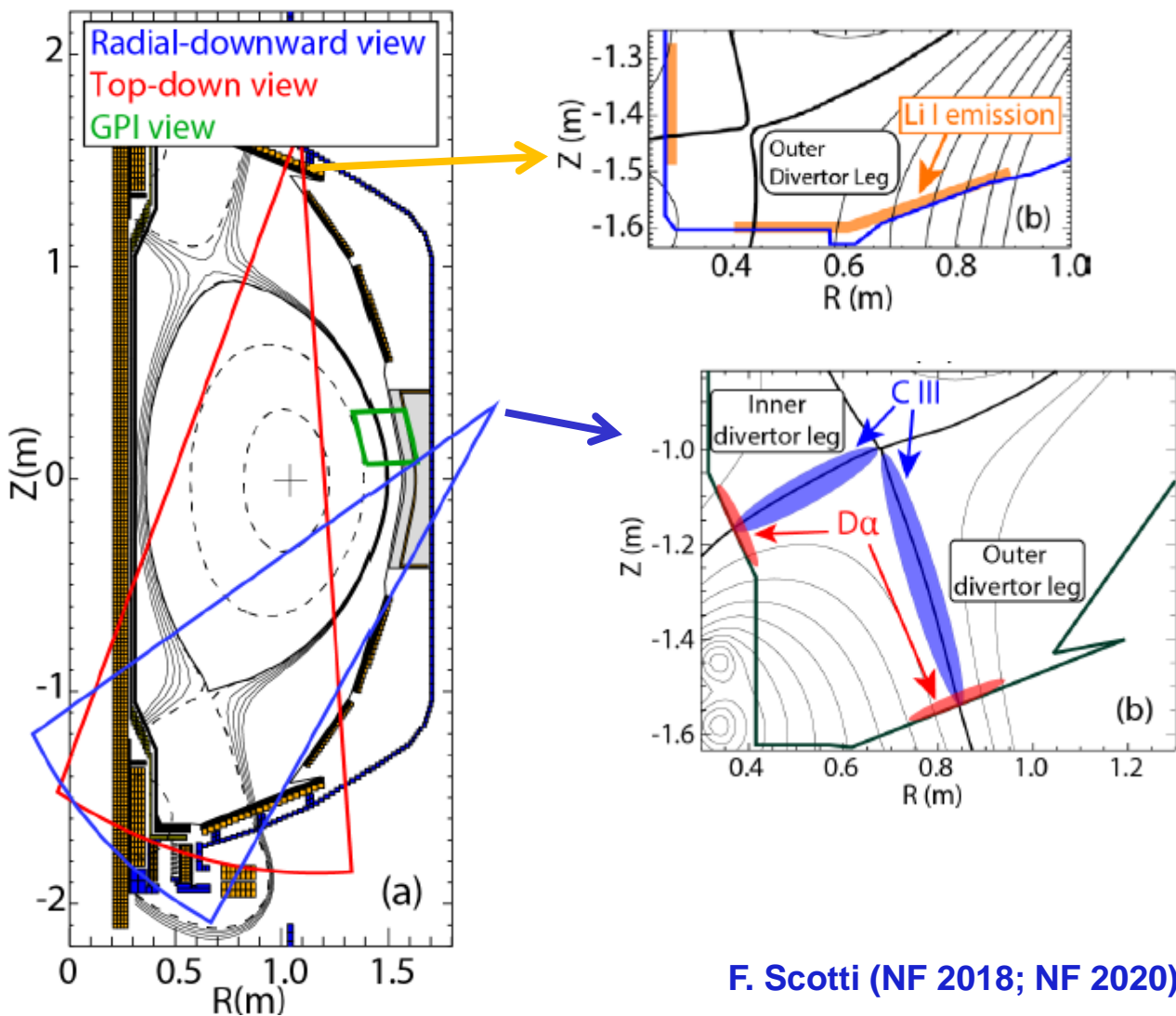


2D turbulence model (D'Ippolito 2008)

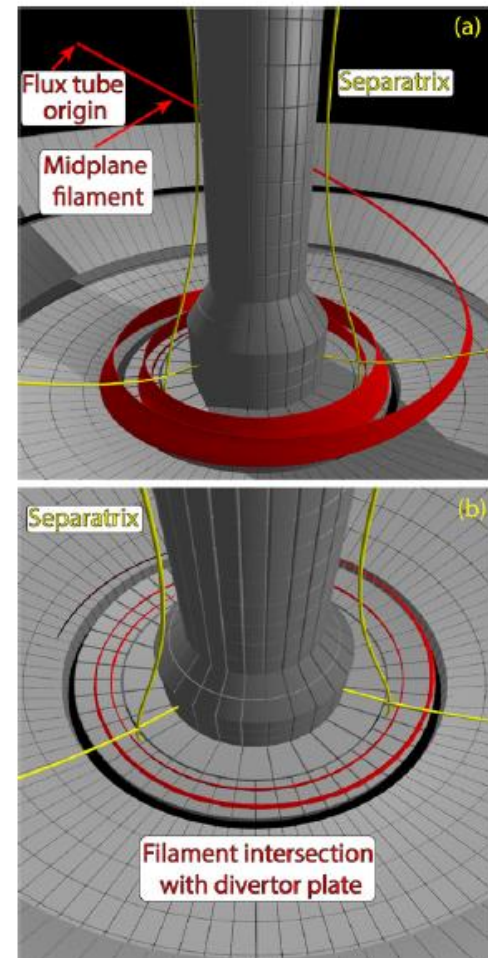


# NSTX measurements investigate blob correlation along open field lines from upstream midplane, through divertor region, to divertor floor

- GPI for upstream separatrix turbulence near midplane (bad curvature drive)
- $C^{2+}$  emission to measure fluctuations in cool divertor region
- Neutral Li I emission to measure fluctuations very surface (~few mm off divertor floor in NSTX)

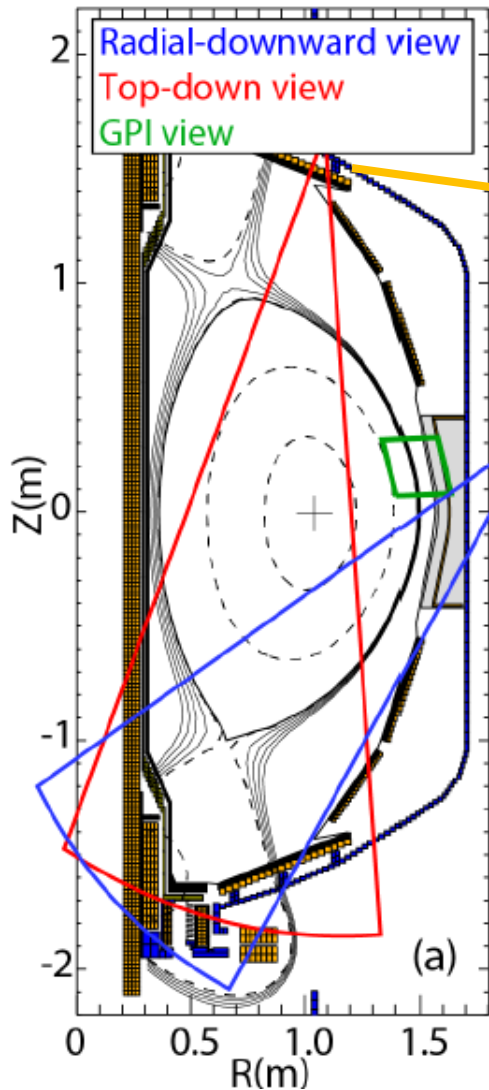


## Projection of a field-aligned filament



# NSTX measurements investigate blob correlation along open field lines from upstream midplane, through divertor region, to divertor floor

- GPI for upstream separatrix turbulence near midplane (bad curvature drive)
- $C^{2+}$  emission to measure fluctuations in cool divertor region
- Neutral Li I emission to measure fluctuations very surface (~few mm off divertor floor in NSTX)



**C<sup>2+</sup> divertor leg image**

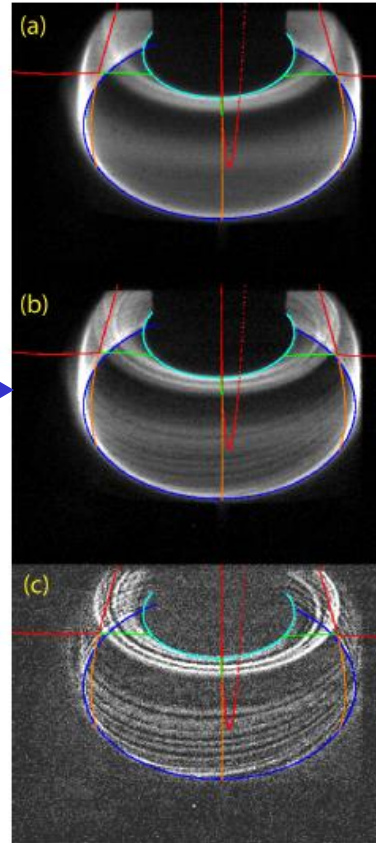


Figure 6: (a) Lower divertor C III emission averaged over 1 ms; (b) raw frame acquired at 100 kHz and with 9.3  $\mu s$  exposure; (c) raw frame after high pass filtering (c). Projection of the separatrix (red), inner (green) and outer (orange) divertor legs, inner (cyan) and outer (blue) strike points from EFIT02 and plot from

F. Scotti (NF 2018; NF 2020)

**Li I divertor floor image**

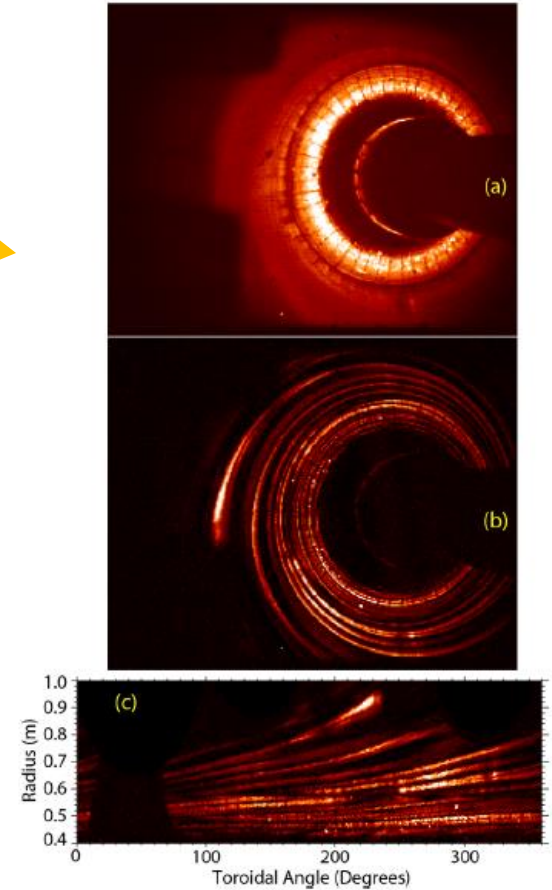
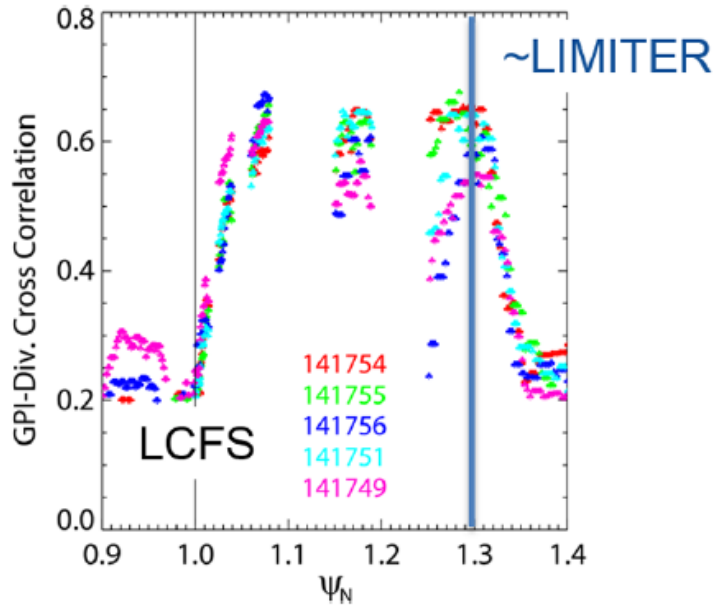


Figure 4. Images of the lower divertor in neutral lithium emission: (a) average over 1 ms, (b) single frame (9  $\mu s$ ) after moving minimum subtraction, (c) image in (b) plotted as a function of toroidal angle and divertor radius.

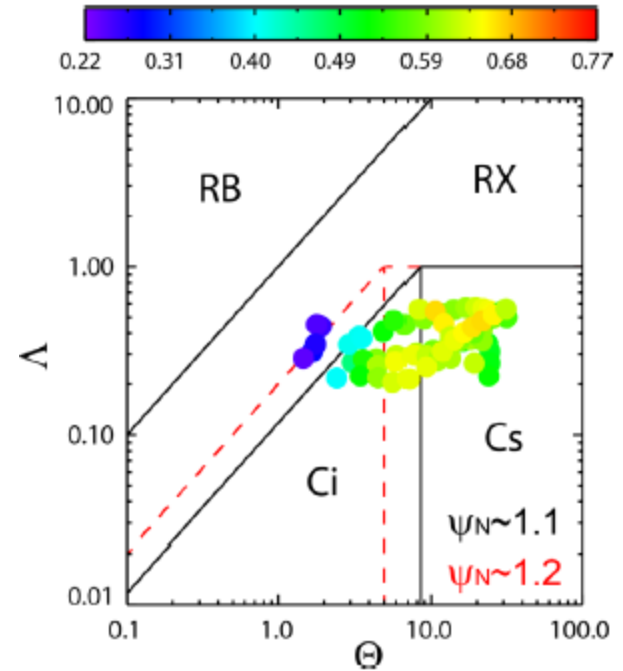
# Upstream (midplane) blob filaments seen to propagate down to divertor far away from X-point, but can also exist in isolation, driven independently near X-point

- Correlation between upstream midplane (GPI) and divertor floor (Li I)
- Becomes weaker near separatrix, where strong variation in local magnetic shear can decorrelate upstream & downstream turbulence



**Figure 17.** Maximum value of cross correlation between GPI and divertor imaging for each divertor radius, plotted as a function of  $\psi_N$  for 5 different discharges.

- Comparison to predictions of different blob dynamic regimes [D'Ippolito, 2011]
  - RB: resistive ballooning (disconnected)
  - RX: Resistive X-point (disconnected)
  - Ci: Ideal interchange (connected)
  - Cs: Sheath connected (connected)



These regimes can be identified in a blob regime diagram as a function of a collisionality parameter  $\Lambda$  and a blob size parameter  $\Theta$ . The collisionality parameter  $\Lambda$  is defined as  $\frac{\nu_{ei} L_{\parallel}}{\Omega_e \rho_s}$ . The blob size parameter  $\Theta$  is defined as  $\delta^{5/2}$  where the dimensionless blob size  $\delta$  is obtained normalizing the blob size  $\delta_b$  by the characteristic blob scale  $\delta_* = \rho_s \left( \frac{L_{\parallel}^2}{\rho_s R} \right)^{1/5}$ . In these equations,  $L_{\parallel}$  is the midplane to target connection length,  $\nu_{ei}$  is the electron-ion collision frequency,  $\rho_s$  is the sound Larmor radius,  $R$  is the major radius, and  $\Omega_e$  is the electron gyrofrequency.



## SUMMARY

- Many experiments and diagnostics developed to measure fluctuation amplitudes, spectra, cross-phases, transport, etc... in various regions of magnetically confined plasmas
- Have seen progress in comparing theory/simulation & measurements, with agreement improving from order-of-magnitude to factor of 2-3 or better in limited cases (at least in core plasma)
- Improves confidence (in some regimes) in our physics understanding, which improves our predictive ability (not really addressed here)
- Plenty more to do (pedestals, open field lines, 3D systems)